

Politechnika Śląska  
Wydział Automatyki, Elektroniki i Informatyki

Krzysztof Kotowski

ANALIZA SYGNAŁU EEG DLA POTRZEB  
ROZPOZNAWANIA EMOCJI

Rozprawa doktorska pod kierunkiem  
prof. dr hab. inż. Katarzyny Stąpor

Dyscyplina główna: Informatyka

Gliwice, 2022



Silesian University of Technology  
Faculty of Automatic Control, Electronics and Computer  
Science

Krzysztof Kotowski

ANALYSIS OF EEG SIGNALS FOR EMOTION  
RECOGNITION

Doctoral thesis under the supervision of  
prof. dr hab. inż. Katarzyna Stapor

Main discipline: Computer science

Gliwice, 2022



## **ACKNOWLEDGEMENTS**

This thesis is a culmination and an outcome of my hard work over 5 years of studying at the Silesian University of Technology. During this time, I had a chance to cooperate with many great people that helped me become a better researcher, including my supervisor, coauthors, coworkers, and friends. I would like to greatly thank my parents for creating an environment in which I could develop and achieve my goals. The special award goes to my sister Anna for her support, helpfulness, and memes. The last and deepest gratitude goes to my wife Aleksandra who helped me get through the hardest moments.

I dedicate this work to my son Julian.

# TABLE OF CONTENTS

ACKNOWLEDGEMENTS.....	iii
LIST OF FIGURES.....	v
LIST OF TABLES.....	viii
LIST OF ABBREVIATIONS.....	ix
1 INTRODUCTION.....	1
1.1 Purpose and goals.....	2
1.2 Thesis formulation.....	4
1.3 Original contribution.....	5
1.4 Relevant publications.....	5
1.5 Structure of the dissertation.....	8
2 THEORETICAL BASIS.....	10
2.1 Measuring brain activity.....	10
2.2 Functional brain areas.....	13
2.2.1 Emotion-related brain areas.....	14
2.3 EEG measurements.....	16
2.3.1 Event-related potentials.....	23
2.4 Psychological models of emotion.....	26
2.4.1 Affective stimuli.....	30
2.4.2 EEG correlates of emotion.....	33
2.5 ERP correlates of emotional face processing.....	35
3 NEW METHODS OF ERP EXTRACTION FOR EMOTIONAL FACE PROCESSING.....	40
3.1 Adaptation of Emotiv EPOC+.....	41
3.1.1 Emotional face processing experiment.....	42
3.1.2 Stimuli marking circuit.....	43
3.1.3 ERP extraction and results.....	45
3.2 Improved robust weighted averaging.....	49
3.2.1 Methods.....	49
3.2.2 Simulation study.....	53
3.2.3 Validation on emotional face processing experiment.....	57
3.3 Semi-automatic ocular artifacts filtration.....	60
3.3.1 Materials.....	60
3.3.2 Methods.....	62
3.3.3 Simulation study and comparison with other methods.....	67
3.3.4 ERP extraction and results on real-life data.....	71
4 GENERAL DISCUSSION AND CONCLUSIONS.....	77
5 BIBLIOGRAPHY.....	81

## LIST OF FIGURES

Proper permissions were obtained for figures published in copyrighted sources. If there is no source given, the figure was prepared by the author of this dissertation.

Figure 2-1. Main brain lobes and examples of functional areas of the brain (source: <a href="http://tinyurl.com/brainareas">tinyurl.com/brainareas</a> ).....	13
Figure 2-2. On the left: the BrainProducts actiCAP EEG cap with 64 electrodes (source: [25]). On the right: the Emotiv EPOC+ wireless headset with 14 electrodes (source: <a href="http://flic.kr/p/diA5hh">flic.kr/p/diA5hh</a> ).....	16
Figure 2-3. Modified combinatorial nomenclature for the 10-10 system of EEG electrode placement (source: [64]).....	18
Figure 2-4. A recording of resting-state brain activity from Emotiv EPOC+.....	19
Figure 2-5. An example of a power spectral density plot for all electrodes of a selected participant from the study [20].....	20
Figure 2-6 On the left: the example of an ERP waveform with marked peaks. On the right: components (C1, C2, C3) underlying this ERP waveform (example adapted from: [25]).....	24
Figure 2-7. The prevalence of ERP research. A) The number of articles on the topic of ERPs per year. B) The number of ERP articles related to different topics (source: [91]).....	24
Figure 2-8. Facial expressions of 6 basic Ekman's emotions. Top row: anger, fear, disgust. Bottom row: surprise, happiness, sadness (source: [100]). .	27
Figure 2-9. Plutchik's wheel of emotions (source: Wikimedia Commons) .....	28
Figure 2-10. The circumplex model of emotions with primary and secondary emotions marked (source: [110]).....	29
Figure 2-11. My proposed mapping from the valence-arousal-approach/avoidance model to 9 discrete emotions from the CAP-D dataset (source: [24]).....	30
Figure 3-1. The simplified diagram of my new proposed stimuli marking circuit (source: [15]).....	43
Figure 3-2. On the left: the original 8 epochs (dotted lines) and their average (solid line). On the right: the same 8 epochs corrected using our stimuli marking circuit (source: [15]).....	45
Figure 3-3. The block diagram of the ERP extraction pipeline (source: [15]). ..	47
Figure 3-4. An averaged ERP waveform for emotional and neutral faces for the selected participant at the electrode O1 (source: [15]).....	48

Figure 3-5. 200 raw generated epochs and their average (the deterministic component) at the POz electrode (source: [21]).....	54
Figure 3-6. 260 distorted generated epochs at the POz electrode and their average (source: [21]). .....	54
Figure 3-7. The notched boxplot of bootstrap RMSE for different averaging schemes for the raw simulated dataset and its bandpass filtered version (source: [21]). .....	56
Figure 3-8. The notched boxplot of bootstrap MAX for different averaging schemes for the raw simulated dataset and its bandpass filtered version (source: [11]). .....	56
Figure 3-9. A weighted ERP image of the generated dataset calculated using the new corWACFM method (source: [11]). .....	57
Figure 3-10. The epochs from the real-life data for the electrode P8 and their average (source: [11]). .....	58
Figure 3-11. Comparison of the averaged ERP waveforms for the real-life dataset using different averaging schemes (source: [11]). .....	59
Figure 3-12. The diagram of a research-grade hardware setup used in N250 experiments (source: [22]).....	62
Figure 3-13. EEG signal decomposition and filtration using ICA (source: [197]). .....	63
Figure 3-14. The initial EEG preprocessing procedures (source: [22]). .....	64
Figure 3-15. A topographic map (on the left) of the blink-related independent component for participant 15 and its amplitude in consecutive EEG segments (on the right). The amplitude is given in arbitrary units (source: [22]). .....	66
Figure 3-16. The averaged blink-evoked EEG signals before (red plot) and after (black plot) ocular artifacts filtration for selected participants. The $N_{ave}$ is the number of detected blinks (source: [22]). .....	66
Figure 3-17. The proposed method of ocular artifacts removal and ERP epochs extraction (source: [22]). .....	67
Figure 3-18. The comparison of pure, contaminated, and filtered signals for electrode Fp1 for sample 12 with the smallest RMSE after filtration (source: [22]). .....	69
Figure 3-19. Distributions of RMSE values across all samples in the simulated dataset (source: [22]). .....	70
Figure 3-20. Distributions of $\Delta$ SNR values across all samples in the simulated dataset (source: [22]). .....	71

Figure 3-21. Grand-average ERPs for the first (on the left) and the second half (on the right) of the experiment using the proposed filtering with ocular artifact filtration..... 72

Figure 3-22. Grand-average ERPs for the first 1/3 (on the left) and the second 1/3 (on the right) of trials using the proposed filtering with ocular artifact filtration..... 73

Figure 3-23. Strip plots of linked N250 amplitudes between the first 1/3 and the second 1/3 of trials for different types of faces. .... 74

## LIST OF TABLES

Proper permissions were obtained for tables published previously in copyrighted sources. If there is no source given, the table was prepared by the author of this dissertation.

Table 2-1. Characteristics of techniques for brain activity measurement. ....	12
Table 2-2. Basic technical characteristics of low-cost and research-grade EEG systems. ....	17
Table 2-3. Practical applications of EEG in different domains (an extended and updated version of Table 2 from [25]). ....	20
Table 2-4. Public datasets for EEG analysis ordered from the newest to the oldest (an extended and updated version of Table 1 from [25]). ....	21
Table 2-5. The affective picture sets ordered from the newest to the oldest (the extended and updated version of Table 2 from [24]). ....	31
Table 2-6. Public EEG datasets for emotion recognition ordered from the newest to the oldest (the extended and updated version of Table 2.1 from [28]). .	32
Table 2-7. Short descriptions of ERP components related to emotional face processing. The bold-faced components are of particular interest to my dissertation. ....	36
Table 3-1. The order of phases and steps in a typical ERP study. The underlined steps are included in the main contributions of this dissertation. ....	40
Table 3-2. The proposed corWACFM algorithm for robust weighted averaging of ERP epochs. The proposed improvements to the original WACFM are underlined. ....	52
Table 3-3. The average effect of ocular artifact filtering on the RMSE for different channels in the simulated data. The boldfaced font denotes smaller RMSE. The p-values from two-sided signed-rank Wilcoxon are underlined if $p < 0.01$ (source: [22]). ....	69
Table 3-4. Changepoint locations (chp) detected by the <i>segmented</i> method with corresponding RSS and SD of the N250 amplitude series without and with the proposed ocular artifact filtration (source: [22]). ....	75

## LIST OF ABBREVIATIONS

AGI	Artificial general intelligence
AI	Artificial intelligence
BCI	Brain-computer interface
corWACFM	WACFM with correlation-based epochs weighting
ECoG	Electrocorticography
CAR	Common average reference
CWT	Continuous wavelet transform
EEG	Electroencephalography
EOG	Electrooculography
EPN	Early posterior negativity
ERP	Event-related potential
fMRI	Functional magnetic resonance imaging
fNIRS	Functional near-infrared spectroscopy
ICA	Independent components analysis
LFP	Local field potential
LPP	Late positive potential
MEA	Multi-electrode array
MEG	Magnetoencephalography
OSF	Open Science Framework
PAD	Pleasure-Arousal-Dominance emotion model
PET	Positron emission tomography
RMSE	Root mean square error
RSS	Residual sum of squares
SNR	Signal-to-noise ratio
WACFM	Weighted averaging based on criterion minimization

# 1 INTRODUCTION

The brain is still the least understood organ in the human body. It is a biological network of around 86 billion neurons [1], these nerve cells are the source of electrical activity that is a biological foundation of learning, memory, behavior, perception, consciousness, and emotions. Revealing how countless electric impulses map into our mind and feelings is the ultimate goal of neuroscience. This electrical activity of the brain may be measured non-invasively using an electroencephalogram (EEG). The greatest advantage of EEG over other non-invasive methods of measuring brain activity (like fMRI, MEG, or fNIRS) is its relatively low cost, portability, and great temporal resolution (the details are given in Section 2.1). However, the EEG signals from tens of electrodes placed on the scalp of the head are usually impossible to decode without advanced computational methods. The algorithms that can measure and understand human emotions are a key milestone on the road to artificial emotional intelligence, and thus, to artificial general intelligence (AGI) [2]. These algorithms are a part of the affective computing field which spans computer science, psychology, and cognitive neuroscience [3]. In recent years, significant progress was made in the field of narrow artificial intelligence (AI), but it does not translate to breakthroughs in affective computing. With the rise of deep learning that enabled prominent achievements like AlphaGo [4] or AlphaFold [5], it seems that we have the tools to recognize human emotions from the electrical brain activity, but despite many published works, this goal is still far from being reached. The main reasons are a lack of consensus in terms of psychological emotion models and their psychophysiological mechanisms (the detailed discussion on this matter is provided in Section 2.4) and a reproducibility crisis in neuroscience [6]. To address these issues, we need standardized emotion recognition datasets, unified research reporting methods [7], and universal hardware and software methods for measuring brain activity in real-world settings. The latter area is where my thesis contributes the most. I focus on the technical aspects of emotion recognition from EEG signals, especially, on improving the analysis of event-related potential (ERP) components correlating with emotional face processing. My thesis is an interdisciplinary study spanning computer science, signal

processing, artificial intelligence, psychology, and cognitive neuroscience. The proposed methods can be applied not only in emotion recognition, but in a countless number of applications using ERP features, e.g., brain-computer interfaces, medical diagnosis, forensics, biometry, neurofeedback, and psychology research (see examples in Section 0).

## 1.1 Purpose and goals

During my neuroscience research conducted under the guidance and cooperation of my supervisor prof. Katarzyna Stapor (having also psychological education) and with the international team of experts in biological face processing through EEG led by prof. Werner Sommer (from Humboldt University Berlin), I gained experience in the analysis of ERP correlates of emotional face processing, and I quickly noticed that neuroscience research is highly dependent on algorithms for brain signal processing. Without proper processing of EEG signals, it would be impossible to draw proper conclusions from EEG experiments. Thus, a primary goal (**G1**) of my work is to provide such an EEG processing pipeline for psychologists and neuroscientists working with emotional face processing.

Despite its significant potential, brain monitoring is still not easily accessible, interpretable, or useable in many real-world and clinical environments. Solving this issue would allow researchers to collect large-scale datasets that can help to understand *how emotions are made and the secret life of the brain* (as stated by Lisa Feldman Barrett [8]). The effects of emotion can be observed in different electrophysiological signals like event-related brain potentials (ERPs), frontal EEG asymmetry, event-related synchronization, and steady-state visually evoked potentials [9], [10]. Although, the majority of papers on EEG emotion correlates find them in ERPs [9]. Thus, the dissertation put a special focus on ERPs, which are thoroughly introduced in Section 0. ERPs are especially difficult to measure (e.g., in comparison to brain waves) as they require special experimental and hardware designs, perfect timing synchronization between devices, and algorithms for extracting, filtering, and averaging. The higher the quality of ERP extraction the easier it is to observe and discover the effects of different stimuli

on neural responses, i.e., recognize different evoked emotions. The high quality of ERP extraction can be reflected in a high signal-to-noise ratio, a low latency jitter between epochs, a low variance of components' amplitudes between epochs, and a small number of artifacts in ERP signals. The second goal (**G2**) of my work is to provide methods for increasing the quality of ERP extraction in all the mentioned aspects.

ERPs are usually measured using expensive stationary research-grade devices in a highly controlled laboratory environment. It ensures a high quality of the recordings and reproducibility of the results between institutions. However, it prevents the research in natural environments which can lead to different conclusions than in the lab [11]. There is a growing interest in mobile EEG devices that can be used outside the laboratory as they will allow a paradigm shift in neuroscience experiments [12], including emotional face processing analysis [13]. Additionally, many research institutions cannot afford research-grade devices and they look for low-cost alternatives, especially in the case of large-scale experimental studies with hundreds of participants and hours of recordings. Hence, the third goal (**G3**) of my thesis is to enable ERP research of emotional face processing using low-cost mobile EEG devices like Emotiv EPOC+.

The ERP correlates of emotion can be evoked using a number of affective materials, like videos, texts, conversations, music, or images (as listed in section 2.4.1). In my thesis, I focus especially on the images of faces that are known to have strong ERP correlates such as N170 or N250 components [14]. More importantly, the emotional expression of the observed face modulates different emotion-sensitive ERP components listed in Section 2.5, i.e., the early posterior negativity (EPN) component which is enhanced by angry and happy faces [15]–[18]. This psychophysiological reaction reflects our important evolutionary adaptation to the complex social environment that requires the perception of faces and emotions [19]. This adaptation includes also the acquisition of face familiarity reflected in the N250 ERP component that is studied as a potential confounding factor of EPN [20]. The fourth goal (**G4**) of my thesis is to provide

methods for better analysis of EPN and N250 components in psychological research.

Summarizing the goals:

- G1)** to provide a proper EEG processing pipeline for psychologists and neuroscientists working with emotional face processing,
- G2)** to provide methods for increasing the quality of ERP extraction,
- G3)** to enable ERP research of emotional face processing using low-cost mobile EEG devices,
- G4)** to provide methods for better analysis of EPN and N250 components in psychological research.

## **1.2 Thesis formulation**

The general outline of the dissertation can be summarized in one sentence:

*Using proper EEG processing, it is possible to extract ERP correlates of emotional face processing in such a way that they can be effectively analyzed by neuroscientists and psychologists, even using a low-cost EEG device.*

More specifically, the thesis consists of two parts and is formulated as follows:

- (1) Proper hardware adaptation and robust weighted averaging enable psychologists to analyze neural processing of angry and happy facial expressions, as reflected in the early posterior negativity (EPN) component of event-related potentials (ERP), using a low-cost EEG device.**
- (2) Proper preprocessing including ocular artifacts filtration allows for single-trial ERP analysis of face learning as reflected in the N250 component which is a confounding factor in emotional face processing.**

### **1.3 Original contribution**

The primary original contributions of this dissertation are listed below. Each contribution is concluded with the references to my relevant publications mentioned in Section 1.4:

- 1) A hardware adaptation of a low-cost Emotiv EPOC+ device for precise ERP measurements (a stimuli marking circuit that decreases the time drift and jitter between epochs) [15]
- 2) An ERP extraction pipeline for detecting markers of emotional face processing using Emotiv EPOC+ (including a new wavelet-based epochs filtration) [15]
- 3) A robust weighted averaging scheme that improves the signal-to-noise ratio of ERP waveforms for both simulated and low-cost EEG recordings [21]
- 4) A semi-automatic pipeline for removing ocular artifacts from ERP, based on independent components analysis (ICA) and EOG [22]
- 5) A replication and single-trial ERP analysis of face learning effects in N250 ERP component [20], [22], [23]
- 6) A new mapping between continuous and discrete emotion models [24]
- 7) A design of the machine-learning-based emotion recognition EEG system for validation of affective picture datasets standardization [24]

### **1.4 Relevant publications**

This dissertation is a summary and culmination of a series of articles published (or yet to be published) in ISI-indexed journals, book chapters, and conference proceedings to which I significantly contributed. Many parts of this dissertation are directly referring to or citing these publications. The list of most important publications is given below. It is ordered chronologically and numbered according to the first occurrence of the publication in the dissertation text. Each journal publication is annotated with its 2-year Impact Factor (IF), the number of points according to the Polish Ministry of Science and Higher Education (MNiSW). All

the publications are commented with the number of citations according to Google Scholar (state for the date 21.09.2022) and my main contributions (not including literature review and manuscript writing in which I was always involved).

[15] **K. Kotowski, K. Stapor, J. Leski, M. Kotas**, “Validation of Emotiv EPOC+ for extracting ERP correlates of emotional face processing,” *Biocybernetics and Biomedical Engineering*, 2018, **IF (2018: 2.159, 2021: 4.314), MNiSW (2018: 15, 2021: 100), 26 citations**

Main contributions: The hardware and software adaptation of the Emotiv EPOC+ EEG device for ERP extraction. Conducting experiments and data collection. EEG preprocessing and analysis.

[21] **K. Kotowski, K. Stapor, J. Leski**, „Improved robust weighted averaging for event-related potentials in EEG”, *Biocybernetics and Biomedical Engineering*, 2019, **IF (2019: 2.537, 2021: 4.314), MNiSW 100, 15 citations**

Main contributions: Proposing and implementing the improvements for the robust weighted ERP averaging method. Simulation studies and statistical analysis. Validation on the real-life dataset.

[25] **K. Kotowski, K. Stapor, J. Ochab**, “Deep Learning Methods in Electroencephalography” in *Machine Learning Paradigms: Advances in Deep Learning-based Technological Applications*, Springer, 2020, **6 citations**

Main contributions: A review of the deep learning method in EEG analysis. The practical application of EEGNet [26] for classifying single-trial ERPs evoked by correct and incorrect responses in the Eriksen flanker task [27].

[28] **K. Kotowski, P. Fabian, K. Stapor**, “Machine learning approach to automatic recognition of emotions based on bioelectrical brain activity” in

*Simulations in Medicine. Computer-aided diagnostics and therapy, De Gruyter, 2020, 1 citation*

Main contributions: The review of machine learning techniques of automatic emotion recognition from EEG in the medical context. The summary of psychological models of emotion.

[24] **K. Kotowski**, K. Stapor, “Machine Learning and EEG for Emotional State Estimation” in *The Science of Emotional Intelligence, IntechOpen, 2021, 1 citation*

Main contributions: The review of psychological models of emotion and datasets of affective images. The new mapping between continuous and discrete emotion models. The idea of a machine-learning-based emotion recognition EEG system for validation of affective picture datasets standardization.

[20] W. Sommer, K. Stapor, G. Kończak, **K. Kotowski**, P. Fabian, J. Ochab, A. Bereś, G. Ślusarczyk, „The N250 event-related potential as an index of face familiarity: a replication study”, *Royal Society Open Science, 2021, IF 2.963, MNiSW 100, 3 citations*

Main contributions: Designing and conducting experiments. EEG preprocessing and ERP extraction and analysis. Behavioral results analysis. Statistical analysis.

[29] W. Sommer, K. Stapor, G. Kończak, **K. Kotowski**, P. Fabian, J. Ochab, A. Bereś, G. Ślusarczyk, „Change-point Detection in Noisy Data Using a Novel Residuals Permutation-Based Method (RESPERM): Benchmarking and Application to Single Trial ERPs”, *Brain Sciences. 2022; IF 3.394, MNiSW 100*

Main contributions: A case study about change-points in time series of single-trial N250 ERP amplitudes using the proposed RESPERM method

[22] **K. Kotowski, J. Ochab, K. Stapor, W. Sommer**, “*The importance of ocular artifact removal in single-trial ERP analysis: the case of the N250 in face learning*”, *Biomedical Signal Processing and Control*, 2022; **IF 5.076, MNiSW 140**

Main contributions: Designing a complete pipeline for end-to-end EEG preprocessing and single-trial ERP extraction. The implementation of the semi-automatic ocular artifact filtration method. The single-trial ERP analysis.

## **1.5 Structure of the dissertation**

In Section 2, I present the theoretical introduction to all subjects relevant to my thesis. It includes the comparison of different techniques of measuring brain activity with a special focus on EEG. It describes the functional brain areas with a special focus on the neural sources of emotions. It introduces the topic of event-related potentials (ERPs) which are the main topic of the thesis. It elaborates on different psychological models of emotion that have been proposed in the literature and discusses the differences and mappings between these models. It lists several affective materials that can be used to induce emotions and datasets for emotion recognition from EEG. Finally, it summarizes the known EEG correlates of emotion.

Section 3 is the main part of the dissertation. It presents a series of my original contributions that increase the quality and robustness of ERP measurements using different EEG systems. It includes the adaptation of a low-cost Emotiv EPOC+ EEG device for ERP measurements, the improved robust weighted ERP averaging scheme increasing the signal-to-noise ratio of ERPs, and the semi-automatic ocular artifacts filtration using independent component analysis (ICA) that improves the single-trial ERP analysis. All the contributions are supported by the results from extensive simulation and/or experimental studies published in peer-review journals.

Section 4 concludes and discusses the findings. It summarizes the thesis and its contributions. It highlights the limitations and future research directions of the proposed methods and the whole domain.

## **2 THEORETICAL BASIS**

This section is a thorough introduction to all the topics relevant to my thesis, from the sources of brain activity to the detailed description of psychological emotion models and event-related potentials in EEG.

### **2.1 Measuring brain activity**

The human brain is active all time, from the first months after conception [30] till the end of life. It is driven by the oxygen and glucose transported via blood vessels. They provide energy to around 86 billion brain cells [1], so they can communicate using electrical impulses. This neural network accounts for 20% of the energy budget of the resting human body [31]. Thus, we can measure brain activity by measuring the intensity of the blood flow, glucose metabolism, or small electrical and magnetic fields generated by neurons.

Table 2-1 presents different techniques and devices for measuring brain activity, together with their characteristics in terms of invasiveness, spatial resolution (the precision of locating the signal source), temporal resolution (the sampling frequency of measurement), cost, portability, sensitivity to movement, and potential contraindications. It was compiled using my personal experience and information from multiple sources referenced in the content of Table 2-1.

The most invasive techniques include electrocorticography (ECoG), multi-electrodes arrays (MEA), and local field potential (LFP) measurements. They involve opening the skull of the patient in order to implant measurement electrodes. They are usually used in brain-computer interfaces for people affected by neurologic diseases [32]. In practice, they cannot be used in healthy people for safety and ethical reasons. However, there are some efforts to promote them as the future of brain-computer interfaces (Neuralink) [33]. This is because they are the only techniques that can reliably provide both great temporal and spatial resolution (at least locally).

The only techniques that allow simultaneous measurements of the whole brain volume with a high spatial resolution ( $< 10$  mm) are functional magnetic resonance imaging (fMRI) and positron emission tomography (PET). They are very popular in the research on functional areas of the brain [34] presented in Section 2.2. However, the temporal resolution of these methods is limited by hemodynamic response time and is much too low to capture the dynamics of evoked brain responses. Both fMRI and PET machines are big and very expensive (millions of dollars [35]) and only a few institutions can afford them. Additionally, this type of measurement cannot be applied to several groups of patients (children, claustrophobic, with ferromagnetic implants).

The only non-invasive methods characterized by a high temporal resolution are EEG, magnetoencephalography (MEG), and functional near-infrared spectroscopy (fNIRS). The EEG is one of the most commonly used methods, it is the main area of interest in my thesis and is extensively described in Section 2.3. The MEG gives a similar amount of information to EEG but is extremely expensive and not portable [36]. The fNIRS is a relatively new method that is based on detectors of a specific region of the electromagnetic spectrum to measure the hemodynamic response (similarly to fMRI). It is much cheaper than fMRI but offers much worse spatial resolution and is limited to the regions near the cortical surface. The latest fNIRS systems like Kernel Flow [37] are as portable as EEG. However, besides lower sensitivity to the movement of the patient, they have no significant advantages over EEG.

**Table 2-1. Characteristics of techniques for brain activity measurement.**

	EEG	fMRI [38]	PET	MEG [36]	fNIRS [39]	ECoG [40]	MEA/LFP
Invasiveness	None	None	Low [41]	None	None	High	Very high
Spatial resolution	Low (> 20 mm)	Very high (0.5 – 4 mm)	High (< 10 mm)	Low (> 20 mm)	Medium (10 - 20 mm)	High (< 10 mm)	Very high (< 1 mm)
Temporal resolution	High (< 1 ms)	Low (0.1 – 6 s)	Very low (> 1 min)	High (< 1 ms)	Medium (>10 ms)	High (< 1 ms)	High (< 1 ms)
Device cost	Low [42]	High	Very high	Very high	Medium	Medium	Medium
Portability	High	Low	Low	Medium [43]	High [37]	Very high	Very high
Sensitivity to movement	Medium	High	High	High	Low	Low	Low
Contraindications	None	Few	Few	None	None	Many	Many
Measured activity type [44]	Electrical potentials	Blood flow	Metabolic response	Magnetic field	Blood flow	Electrical potentials	Electrical potentials

## 2.2 Functional brain areas

There are two leading theories about the functional regions of the brain: the theory of modularity and the theory of distributive processing. The first one claims that the brain is divided into modules specialized in different cognitive processes [45]. It assumes that there exists some cognitive architecture of the brain evolved in natural selection. There is strong empirical evidence for that theory in lesion case studies where the patients show specific cognitive disabilities when a specific part of the brain is damaged [46]. Also, the experimental studies using PET and fMRI prove the functional specialization of some brain areas like the fusiform face area (activated during face processing), the visual cortex (perception of color and vision motion), the motor cortex (activated during voluntary body movements), or the somatosensory cortex (processing sensory information). The recent studies list 180 separate brain modules bounded by sharp changes in cortical architecture, function, or connectivity [47]. The indicative locations of selected functional areas are presented in Figure 2-1 together with the division into 4 main anatomical lobes of the brain. The frontal lobe is known to be involved in higher-level cognitive processes [48] and the occipital lobe aggregates many areas connected with vision.

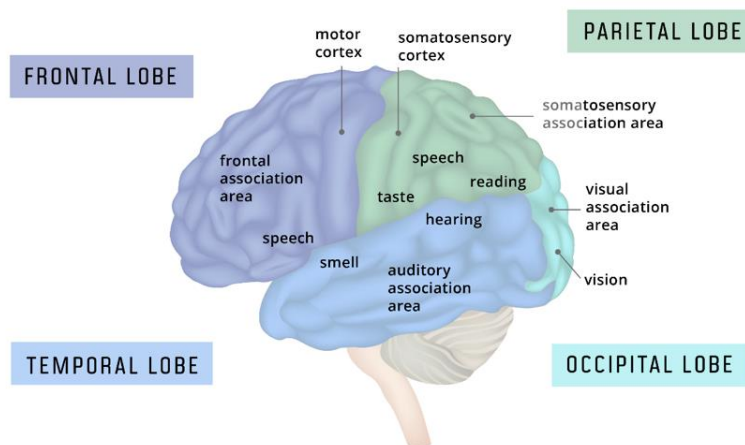


**Figure 2-1. Main brain lobes and examples of functional areas of the brain (source: [tinyurl.com/brainareas](https://tinyurl.com/brainareas)).**

The second theory of distributive processing claims that only some basic parts of the brain may be modular (e.g., sensory or motor cortex), but the other parts are highly interconnected and cannot be considered separate modules [49]. This theory criticizes the assumptions of localization on which the modular theory is dependent. For example, studies are proving that auditory stimuli alone can generate activity in the visual cortex [50]. The distributed theory explains the limits of localizing some cognitive processes by their fuzzy and interconnected nature.

### **2.2.1 Emotion-related brain areas**

It is not yet fully discovered which parts of the human brain “produce” emotions [51], [52]. The main problem lies in the lack of consensus about the theory of emotions (which is discussed in detail in Section 2.4). Just like there are two theories of functional brain regions, there are two theories about the brain basis of emotion: the locationist and constructionist approaches. The older locationist hypothesis suggests that discrete emotion categories correspond to specific functional brain regions [53]. The newer constructionist approach rejects this concept and offers an explanation that emotions are generated by some general brain networks not specific to any emotion categories [8]. However, there is an agreement that emotions in adulthood have a very complex nature and are dependent on many factors, subjective experience, and cognitive processes [54]. The main question remains if we are able to determine a universal emotion-brain correspondence.

Several complementary methods, such as single-cell recordings, functional brain imaging, or neuropsychological investigations of focal brain damage have been used to identify brain structures that are involved in the perception and analysis of emotionally significant information [17]. In the literature, the brain area usually connected with emotion processing is called the limbic system. It consists of regions like the amygdala (activated especially during the processing of fearful facial expressions [55]) and hippocampus (emotion regulation, emotional memory, response to positive stimuli [56], [57]). The higher cognitive processes in the prefrontal cortex and cingulate cortex can regulate emotions through a

psychological reappraisal strategy [58]. Frequently, the lateralization of emotion processing is observed where the right hemisphere is much more active [59] or where the hemispheres are involved depending on the valence of the emotion – the left hemisphere for positively valenced and the right hemisphere for negatively valenced [60].

## 2.3 EEG measurements

As mentioned in Section 2, EEG is one of the most common ways of measuring bioelectrical brain activity. It is completely non-invasive and the cheapest method of all. Currently, only the EEG-based solutions are portable and cheap enough to enable brain reading in practical applications like brain-computer interfaces (BCI). The word electroencephalography originates from the ancient Greek word *encephalo* which stands for “within the head”. This method was introduced in 1924 by German neurologist Hans Berger [61]. The EEG system consists of a cap with a set of electrodes (as presented in Figure 2-2), a signal amplifier, and a recorder (usually a PC). Their prices span from a few hundred dollars for low-cost, wireless, personal devices like Emotiv EPOC+ used in my first studies [15] to tens of thousands of dollars for research-grade systems like BrainProducts actiChamp used in my recent studies [20]. The more expensive systems allow for recording the signal from hundreds of electrodes with higher digital, spatial, and temporal resolution and much lower noise (see the comparison in Table 2-2). They are able to capture the dynamics of sophisticated cognitive processes.

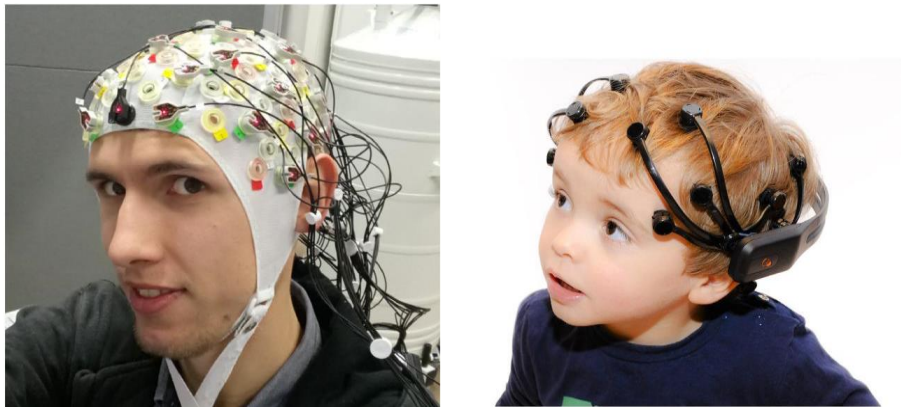


**Figure 2-2. On the left: the BrainProducts actiCAP EEG cap with 64 electrodes (source: [25]). On the right: the Emotiv EPOC+ wireless headset with 14 electrodes (source: [flic.kr/p/diA5hh](https://flic.kr/p/diA5hh)).**

**Table 2-2. Basic technical characteristics of low-cost and research-grade EEG systems.**

	Emotiv EPOC+ (v1.0) <sup>1</sup>	BrainProducts actiChamp <sup>2</sup>
Number of electrodes	14	up to 160
Sampling rate	128 Hz	up to 100 000 Hz
Frequency bandwidth	0.2 – 45 Hz	0 – 7 500 Hz
Digital resolution	14 bits Single converter	24 bits One converter per channel
Connectivity	Wireless, 2.4 GHz band	USB 2.0

Measuring brain activity using a set of electrodes placed on the scalp is an example of the so-called “cocktail party problem” [62] - it is impossible to precisely locate the source of the signal. There are methods like low-resolution electromagnetic tomography (LORETA) [63] and its further modifications that can effectively resolve the EEG inverse problem (converting measurement into information about the physical location of the signal source). However, even for a large number of electrodes, they have limited precision and spatial resolution.

A typical EEG signal sample from a single electrode is a real-valued time series of potentials measured at the specific electrode location on the scalp of the head. The locations of the electrodes on the scalp are usually standardized according to international systems called 10-5, 10-10 (Figure 2-3), and 10-20 [64]. These systems assign standardized names to the electrodes that are directly related to the position of the electrode. The positions are defined at relative distances (5%, 10%, or 20%) between the cranial landmarks (from nasion toinion and from left to right preauricular point). The names consist of up to two letters and one number. The letters denote the brain lobe over which the electrode is placed (F

<sup>1</sup> [https://emotiv.gitbook.io/epoc-user-manual/introduction-1/technical\\_specifications](https://emotiv.gitbook.io/epoc-user-manual/introduction-1/technical_specifications) (13.01.22)

<sup>2</sup> [http://sites.bu.edu/reinhartlab/files/2017/06/actiCHamp\\_OI.pdf](http://sites.bu.edu/reinhartlab/files/2017/06/actiCHamp_OI.pdf) (13.01.22)

for frontal, T for temporal, P for parietal, and O for occipital) and the numbers denote a specific position on the lobe (odd/even numbers denote left/right hemisphere). Another alternative is the numbering of the electrodes according to the geodesic sensor net [65].

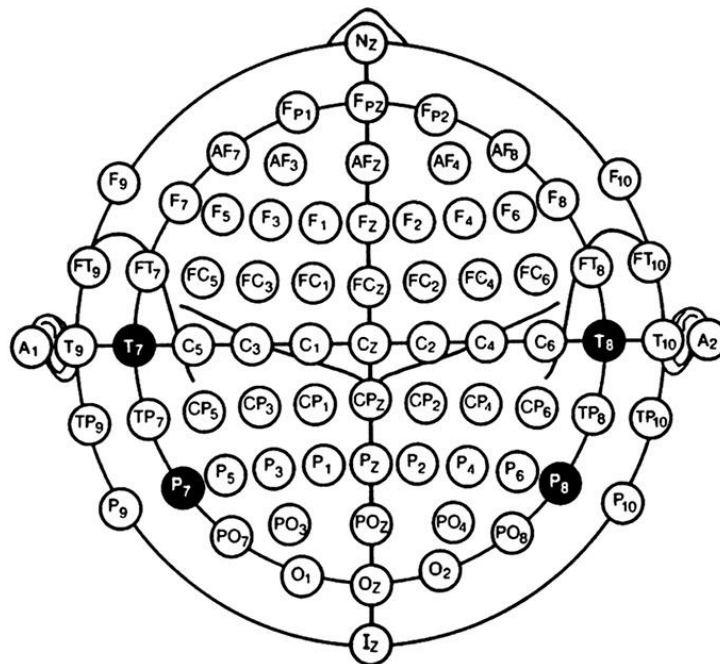


**Figure 2-3. Modified combinatorial nomenclature for the 10-10 system of EEG electrode placement (source: [64]).**

A signal sample of resting-state brain activity from 14 Emotiv EPOC+ electrodes is visualized in Figure 2-4. EEG recordings, especially from low-cost devices, have a problem with the low signal-to-noise ratio (SNR). While the variability of the underlying “true” signal is from several to tens of microvolts ( $\mu\text{V}$ ), the noise is usually at the level of a few  $\mu\text{V}$  and the artifacts may reach several hundreds of  $\mu\text{V}$  (e.g., eye blinks, muscle motions, electrode pops). The artifacts from eye blinks can be observed in Figure 2-4 as sharp peaks affecting all electrodes. The artifacts need to be rejected from analysis or filtered from the signal (i.e., using the method proposed in Section 3.3).

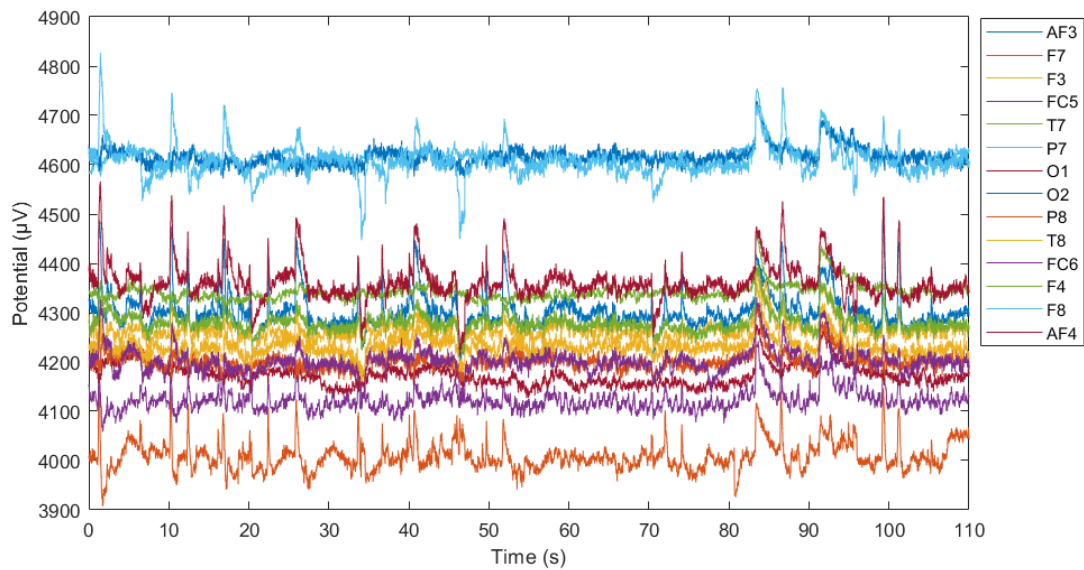


**Figure 2-4. A recording of resting-state brain activity from Emotiv EPOC+.**

The manual analysis of the EEG time series is challenging even for experts in the domain. Computational methods are usually necessary to extract relevant information from the data. One of the most common methods is to reduce the dimensionality by computing the power spectral density (PSD) like the one presented in Figure 2-5. The spectrum of the signal represents specific frequency ranges called delta (0.5-4 Hz), theta (4-8 Hz), alpha (8-12 Hz), beta (12-35 Hz), and gamma (>35 Hz) brain waves [66]. The magnitude of neural oscillations in each band was shown to be the indicator of the specific states of mind, e.g., alpha waves are usually connected with engagement and alertness [67]. Brain waves analysis is usually applied in studies about emotion, stress, fatigue, concentration, sleep disorders, and depth of anesthesia. Brain waves are much easier to interpret than raw EEG signals and are used as an input to simple emotional state classifiers [9].

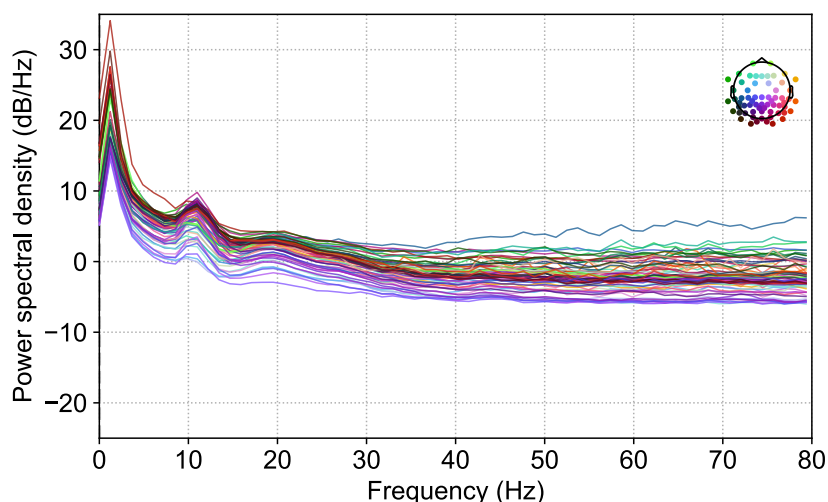


**Figure 2-5. An example of a power spectral density plot for all electrodes of a selected participant from the study [20].**

Besides research purposes, EEG analysis has multiple practical applications listed in Table 2-3. Among them, clinical applications are the most notable and well-described ones (I devoted a separate publication to them [28]). The second broad area consists of brain-computer interfaces (BCIs) in different applications. Other applications span psychology, entertainment, and forensics.

**Table 2-3. Practical applications of EEG in different domains (an extended and updated version of Table 2 from [25]).**

Domain	Practical applications
Medicine	Seizures' detection and prediction. Monitoring the depth of coma, anesthesia, and alertness. Diagnosis of: epilepsy, Alzheimer's disease, dementia, ischemic stroke, brain injury, brain death, schizophrenia, sleep and consciousness disorders, ADHD, and autism spectrum disorders. [28]
Supportive BCI	Text and mouse input. Silent speech decoding [68]. Interface for grasping and lifting using the robotic arm [69]. Controlling an electric wheelchair [70]. Person

	identification, biometry [71]. Monitoring drivers' and pilots' fatigue and drowsiness [72].
Entertainment BCI	Gaming input devices. Monitoring mental states. Sleep scoring [73].
Psychology	Emotion and mood recognition. Neurofeedback and therapies. [74]
Forensics	Lie detectors. Face familiarity [75]

The public datasets of EEG recordings are a crucial factor to increase the reproducibility of the research, benchmarking new methods, and train machine learning models. Table 2-4 lists 15 examples of such datasets in different settings (excluding datasets for emotion recognition which are given separately in Table 2-6).

**Table 2-4. Public datasets for EEG analysis ordered from the newest to the oldest (an extended and updated version of Table 1 from [25]).**

Dataset name (Year) [Ref]	Dataset size	Dataset purpose
Sommer et al. (2021) [20]	16 participants, 864 trials each	Face familiarity research
TUH EEG Artifacts Corpus (2021, v2.0.0) [76]	213 participants, 310 recordings	Automatic EEG artifacts detection
TUH EEG Seizure Corpus (2020, v1.5.2) [76]	692 patients, 6635 recordings (1074 hours)	Epileptic seizure detection
Babayan et al. (2019) [77]	216 participants, 16 minutes each	Resting-state - eyes closed and eyes opened classification

Cao et al. (2018) [78]	27 participants, 62 90-minute recordings	Driver's fatigue level
Nieuwland et al. (2018) [79]	356 participants, 160 trials each, 9 different laboratories	Prediction of the upcoming words
Kaya et al. (2018) [80]	13 participants, 75 recordings (60 hours)	Motor imagery classification
IMAGENET of The Brain (2018) [81]	1 participant, 70'060 3-second trials	Perceived image classification, low-cost devices
Cho et al. (2017) [82]	52 participants, 36 minutes each	Motor imagery classification
MNIST of Brain Digits (2015) [83]	1 participant, 1'207'293 2-second trials	Perceived image classification, low-cost devices
MASS (2014) [84]	200 participants, whole night recording each	Sleep stages analysis
WAY-EEG-GAL (2014) [85]	12 participants, 3936 trials each	Decoding sensation, intention, and action
CHB-MIT (2009) [86]	23 participants, 664 recordings (844 hours)	Epileptic seizure detection
BCI2000 Motor Movement/Imagery (2004) [87]	109 participants, 1500 one- and two-minute recordings each	Motor movements/imagery classification
The CAP Sleep Database (2001) [88]	108 participants, whole night recording each	Sleep disorders scoring

### 2.3.1 Event-related potentials

Event-related potentials (ERPs) are stereotypical brain responses evoked by specific types of events, stimuli, or actions. They can be effectively measured using a single EEG electrode or a group of electrodes. A single ERP trial (called an *epoch*) is just a time window of the EEG signal which starts at the time of the event and ends up to 2 seconds later (depending on the analyzed components). ERP epochs are usually corrected by subtracting the mean potential of a *baseline* (a small fragment of EEG signal right before the event), so the epoch starts from zero potential. In practice, a single epoch reflects thousands of simultaneously ongoing brain processes, so the evoked activity connected with a particular event may be indistinguishable from this noise. Sometimes the analysis of single epochs is possible [89], but usually it is necessary to collect multiple epochs for each type of event and average them to attenuate irrelevant activity and enhance the repeatable ERP waveform. When using a classic arithmetic mean, the signal-to-noise ratio (SNR) of the ERP waveform increases as a function of the square root of the number of trials [90]. Thus, the number of trials is the most basic parameter in ERP experiments. It should be selected to provide the largest possible SNR without fatiguing the participant too much. It is worth adding that there are other averaging schemes, i.e., the improved robust averaging scheme proposed in this dissertation (Section 3.2). In ERP research, it is common to present the grand-average waveform which is the ERP averaged over all the participants.

ERP waveforms are composed of many latent components of different latency and amplitudes (Figure 2-6). These components represent activations of specific brain regions in response to the event and its manipulation. However, a reliable method of inferring the components of interest from an ERP waveform does not exist. According to the Fourier analysis, any waveform can be decomposed into infinitely many sets of such components. Hence, the key to the proper interpretation of changes in ERP components is the proper experimental design. The ERP experiment should focus on manipulating a single component in a maximally controlled environment with a minimum number of confounding variables.

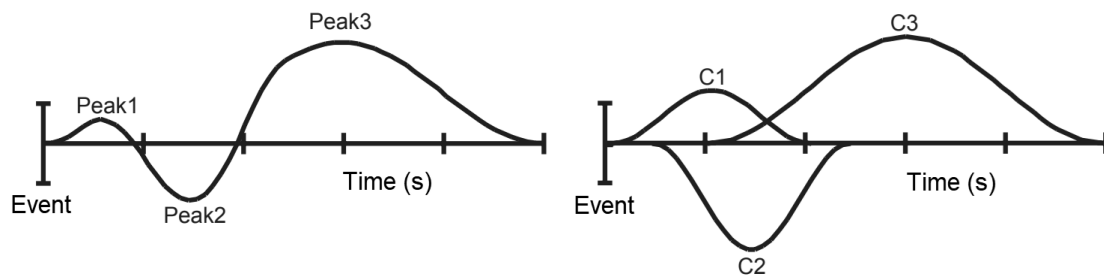


**Figure 2-6** On the left: the example of an ERP waveform with marked peaks. On the right: components (C1, C2, C3) underlying this ERP waveform (example adapted from: [25])

Around 100 different ERP components described in more than 20'000 publications were identified in EEG [91] since the first studies in the 1960s [92]. The number of articles is rapidly growing in recent years (Figure 2-7). The standard naming convention of ERP components is based on their polarity (P for positive, N for negative) and peak latency after the event (post-stimulus) in milliseconds, e.g., N170 denoting a component with negative (N) potential and 170 ms peak latency. However, some components do not fit into this convention like EPN (early posterior negativity) or LPP (late positive potential). There is certainly a need for developing a clear ontology and consistent naming of the components [91].

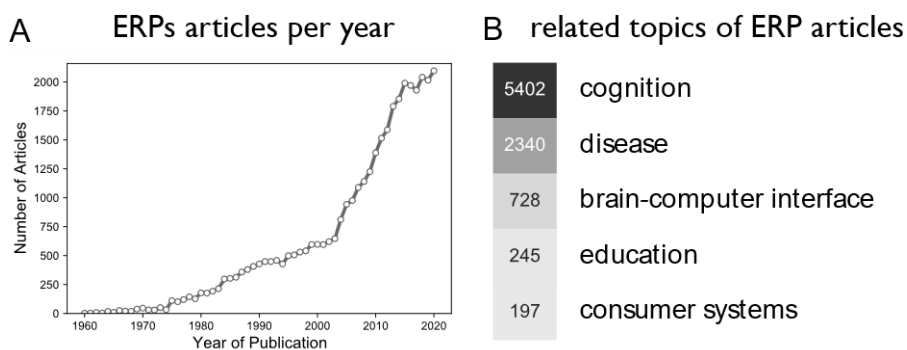


**Figure 2-7.** The prevalence of ERP research. **A)** The number of articles on the topic of ERPs per year. **B)** The number of ERP articles related to different topics (source: [91]).

The ERPs are used to study the neural dynamics of a wide range of cognitive processes. The earliest components (latencies shorter than 100 ms post-stimulus) are connected with basic sensory processing, e.g., the first responses of the visual, somatosensory, or auditory cortex [93]. During the first 100 ms, the brain collects the data needed for higher cognitive processes, so the early components are usually sensitive to the physical parameters of the stimulus. The more complex the event or experimental task the longer the latency. Later components relate to face processing (e.g., N170), object recognition (e.g., N250), body movement (e.g., movement-related cortical potential), semantic processing (e.g., N400), memory (e.g., contralateral delay activity), emotion (components thoroughly described in Section 0), and language (e.g., P600). The recent systematic meta-analysis of ERP components can be found under the link <https://erpscanr.github.io/ERPscanr/> [91]. The descriptions of ERP components of particular interest in my dissertation are given in Section 2.5.

## **2.4 Psychological models of emotion**

The emotion recognition must be preceded by the definition of the model according to which the emotions are measured. Despite a lot of significant studies, there is no universal emotion theory in cognitive psychology [94]. The main reason is that human emotions are mental states that are usually hard to grasp. In the early psychological research, the only methods of measuring perceived emotional states were self-assessment forms or interviews with participants. The information they give is sometimes useful but very subjective and dependent on many confounding factors, e.g., the construction of the form, the experimenter effect, and the level of emotional intelligence of the participant [95]. Moreover, the same stimuli may induce different emotional states in two similar people while the same people may respond similarly to very different stimuli. Emotions are subjective and non-deterministic phenomena that may depend on age, time of the day, mood, experience, and fatigue of the person. The psychophysiological measurements opened new paths for understanding emotions. They were a foundation for creating several new hypothetical models of emotion. In general, they divide into discrete (or categorical) and dimensional (or continuous) models. Discrete emotion models define different numbers of independent emotion categories or classes. Continuous models present emotions as points in multi-dimensional space of valence, arousal, and sometimes some other affective measures.

### **Discrete models**

For a long time, the theory of discrete emotions has been dominant in neuroscience research. This theory was initially suggested by Charles Darwin and was derived from the observations of universal facial expressions across different races and species [96]. The theory assumes that discrete emotions are evolutionarily encoded into our brains, and we are born with the ability to experience, display and recognize them. In his famous research about facial expressions across different cultures and isolated tribes, Paul Ekman described six universal basic emotions of anger, disgust, fear, happiness, sadness, and

surprise [53]. They are presented in Figure 2-8. The paper describing this discrete emotions model was cited, discussed, replicated, and revisited by hundreds of researchers but the existence of basic emotions is still being undermined by many researchers, like Lisa Barrett, promoting the theory of constructed emotion and dimensional models [8], [97]–[99].

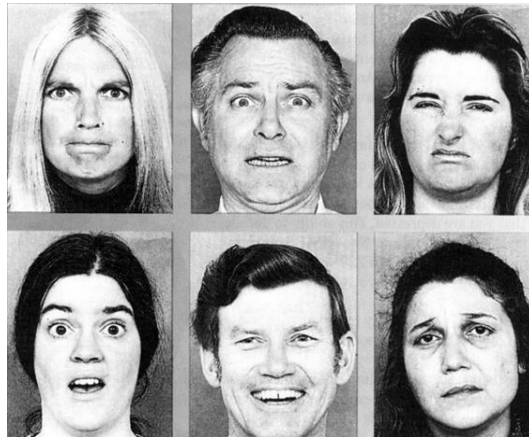


**Figure 2-8. Facial expressions of 6 basic Ekman’s emotions. Top row: anger, fear, disgust. Bottom row: surprise, happiness, sadness (source: [100]).**

Another discrete model was proposed by Plutchik with 8 core bipolar emotions: joy and sadness; anger and fear; surprise and anticipation; and trust and disgust [101]. But, unlike Ekman’s model, Plutchik’s “wheel of emotions” in Figure 2-9 describes relationships between the pairs of emotions and their intensities using the circumplex model and additional emotional terms. Recently, another discrete model consisting of as many as 27 classes bridged by continuous gradients was proposed [102].

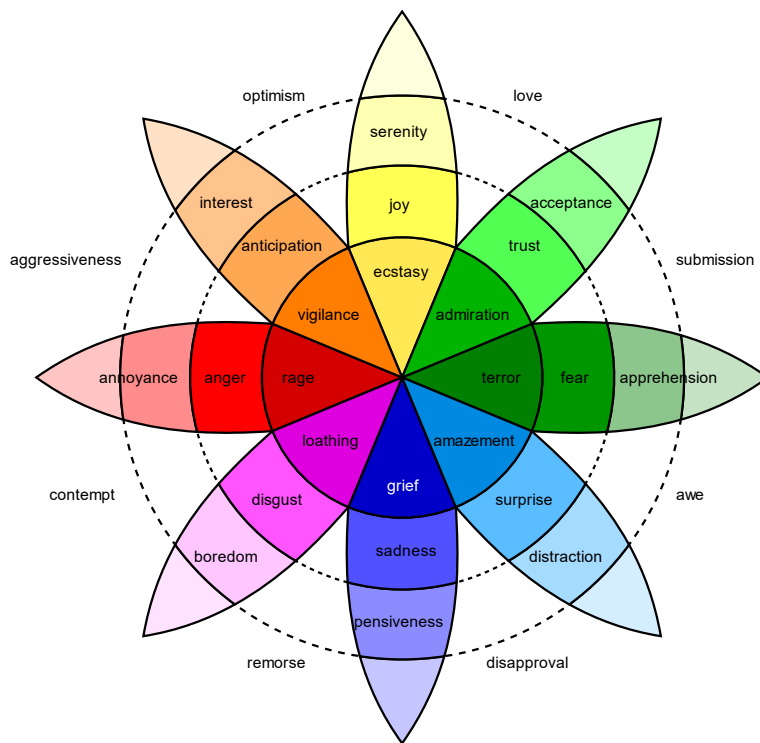


**Figure 2-9. Plutchik's wheel of emotions (source: Wikimedia Commons).**

### Dimensional models

The circumplex approach was utilized also in the most popular continuous model defined by Mehrabian and Russell using dimensions of pleasure, arousal, and dominance (PAD model) [103]. The first dimension is frequently called valence in the literature, it describes how pleasant (or unpleasant) is the stimuli for the participant. The arousal dimension defines the intensity of emotion. Dominance is described as a level of control over the situation [104]. Instead of dominance, some researchers suggest dimensions of control, utility [105], or approach/avoidance [106]. The model that includes only valence and arousal levels is presented in Figure 2-10 and is called a circumplex model of affect [107]. It is one of the most commonly used in literature to describe the emotions elicited by different stimuli. Currently, this model is facing some criticism, because many complex emotions are hard to define within only these two general dimensions.

For example, only the dominance dimension enables allows distinguishing anger from anxiety, alertness from surprise, or relaxation from protection. The newest research findings on the global meaning structure of the emotion domain pointed out that more than two dimensions are needed to describe the nature of the human emotional experience sufficiently [108], [109].

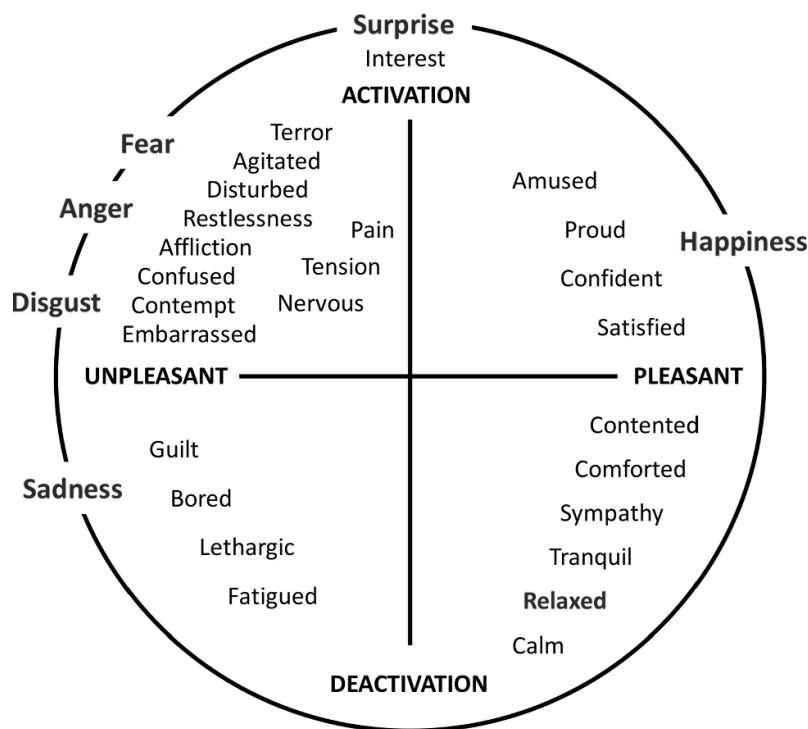


**Figure 2-10. The circumplex model of emotions with primary and secondary emotions marked (source: [110]).**

### **Mappings between models**

However, discrete and dimensional models are not contradictory. Instead, they can both give unique value that can assist in understanding the functions of emotions [111]. The discrete and continuous models are frequently mapped onto each other in order to assess different stimuli from both points of view. An example of such mapping is presented in Figure 2-10 where 6 basic Ekman's emotions and 26 secondary discrete emotions are mapped onto the circumplex model of affect. These secondary emotions are discrete categories described using the continuous scales of arousal and valence. Another example is the

Russell and Mehrabian lexicon which localizes affective words in the PAD model [104].

I discussed the topic of mappings between emotion models in more detail in the publication [24]. There, I proposed a new mapping from the continuous 3-dimensional valence-arousal-approach/avoidance model to 9 discrete emotions from the CAP-D dataset [112] based on the self-assessments provided by the large group of participants for the NAPS affective images set [106]. This mapping is presented in Figure 2-11. We can observe the discrete emotion of disgust in the corner with the lowest valence, lowest approach, and highest arousal. As the opposite emotion, we can consider love or peacefulness.

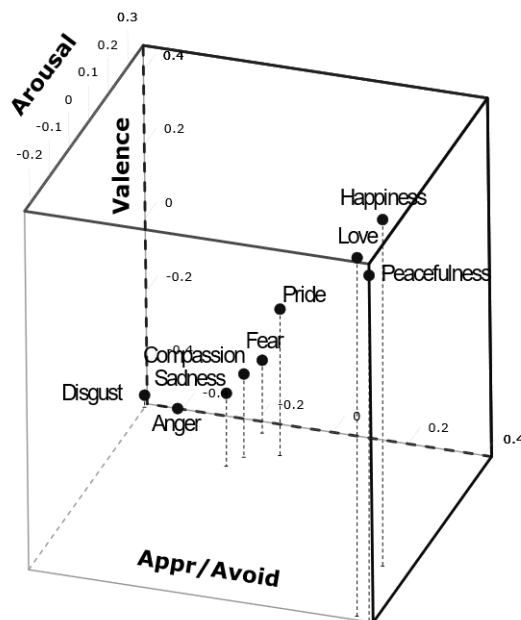


**Figure 2-11. My proposed mapping from the valence-arousal-approach/avoidance model to 9 discrete emotions from the CAP-D dataset (source: [24]).**

### **2.4.1 Affective stimuli**

Different stimuli may be used to induce specific emotions. Typically, the normative sets of videos, images, faces, music, and/or odors are used. They are

annotated using emotional ratings collected from experts or large populations of participants using self-assessment forms. Formerly, the questionnaires to assess the affective stimuli in dimensional emotion models were usually based on Self-Assessment Manikins (SAMs) [113] or Likert scales with 5, 7, or 9 points (like in IAPS [114] or OASIS [115] datasets). The new trend is to use more fine-grained continuous scales like selecting a point on the 10 cm line [105] or Affective Slider [108]. The most common stimuli in the literature about emotion recognition are images and videos [9]. There are many standardized datasets of affective images. I collected and listed the most popular ones in Table 2-5. They contain hundreds of images with curated emotional labels, usually in dimensional models.

**Table 2-5. The affective picture sets ordered from the newest to the oldest (the extended and updated version of Table 2 from [24]).**

Set name (Year) [Ref]	Number of pictures and participants	Assessment method	Emotion models used
CAP-D (2018) [112]	513 pictures, 133 participants (73 women), 15 clinical psychologists	Describing the picture with 1 of 10 emotional words	10 discrete emotions, arousal, and intensity dimensions
OASIS (2017) [115]	900 pictures, 822 participants (420 women)	7-point Likert scale	Dimensional model: valence, arousal
SFIP (2017) [116]	288 pictures, 1671 participants	5-point Likert scale for fear, 9-point Self-Assessment Manikin for valence	Valence and the intensity of fear
NAPS (2014) [106]	1356 pictures, 204 participants (119 women)	9-point sliding scale	Dimensional model: valence, arousal, approach/avoidance  6 basic emotions (only for a subset of 510 images) [117]

GAPED (2011) [118]	730 pictures, 60 participants (no gender given)	100-points rating scale	Dimensional model: valence, arousal, congruence with moral and legal norms
IAPS (2005) [114]	956 pictures, 100 participants (50 women)	5-point Self-Assessment Manikin (SAM)	Dimensional model: valence, arousal, dominance/control

There are many public datasets of EEG recordings of people watching emotionally engaging video clips (usually fragments of movies or music videos). I summarized them in Table 2-6. They are collected with EEG devices of different quality, and they usually contain emotion labels in dimensional models. They contain from 15 to 58 participants. One of the most frequently used datasets is DEAP [119], many researchers benchmark their emotion recognition results against it. However, the main problem with videos as stimuli in terms of this dissertation is that it is impossible to extract ERP from such EEG recordings. There are no clearly defined repeatable “events”, so the researchers are usually limited to frequency features or the raw EEG signal.

**Table 2-6. Public EEG datasets for emotion recognition ordered from the newest to the oldest (the extended and updated version of Table 2.1 from [28]).**

Database name (Year) [Ref]	EEG recording details	Stimuli used	Emotion models used
DEAR-MULSEMEDIA (2021) [120]	18 participants, MUSE EEG, 5 channels, 256 Hz	4 video clips, sensorial effects	Valence and arousal levels
SEED (2018) [121]	15 participants, ESI NeuroScan System, 62 channels, 1000 Hz	72 video clips	Valence and arousal levels, 4 discrete emotion classes: happiness, sadness, neutral, fear
DREAMER (2018) [122]	23 participants, Emotiv EPOC	18 video clips	PAD model levels and 9 discrete

	low-cost EEG, 16 channels, 128 Hz		emotion classes: amusement, excitement, happiness, calmness, anger, disgust, fear, sadness, and surprise
ASCERTAIN (2016) [123]	58 participants, NeuroSky MindWave, 1 channel, 512 Hz	36 video clips	Valence, arousal, engagement, liking, and familiarity levels
USTC-ERVS (2014) [124]	28 participants, Neuroscan Synamps2, 32 channels, 500 Hz	92 video clips	Valence and arousal levels
DEAP (2012) [119]	32 participants, BioSemi ActiveTwo, 32 channels, 512 Hz	40 video clips	Valence and arousal levels divided into 4 classes HAHV, LAHV, HALV, LALV
MAHNOB-HCI (2012) [125]	27 participants, BioSemi ActiveTwo, 32 channels, 1024 Hz	20 video clips	Valence and arousal levels, 9 discrete emotion classes: neutral, anxiety, amusement, sadness, joy, disgust, anger, surprise, and fear
eINTERFACE06_EMOBRAIN (2006) [126]	16 participants, BioSemi ActiveTwo, 54 channels, 1024 Hz	327 images from IAPS	3 discrete emotion classes: calm, exciting positive and exciting negative

#### 2.4.2 EEG correlates of emotion

The relation between EEG data and the emotional state may be considered in the context of two main approaches: the locationist and the constructionist paradigm. The locationist approach is closely related to the theory of basic emotions described in previous Section 2.4. It assumes that each emotion is generated by a unique neural pathway and has a unique footprint on brain signals

[127]. Similar to the theory of basic emotions, the locationist approach is currently being criticized by many researchers in the field [128]. They present the constructionist approach as the alternative where emotions are the result of the interaction between different functional networks of the brain. There is some recent evidence that using dimensional models derived from the constructionist approach (like PAD) reflects the brain activity by means of EEG data more coherently [129]. Also, the majority of recent papers in automatic emotion recognition use dimensional models [9].

Many studies have shown that the effect of emotion can be observed in event-related brain potentials (ERPs), frontal EEG asymmetry, event-related synchronization, and steady-state visually evoked potentials [9], [10]. Although, the majority of papers on EEG emotion correlates (72 out of 130) find them in ERP [9]. The ERP components of latencies up to 300 ms have been shown to correlate more with the valence dimension, e.g., the enhanced N100 and N200 amplitudes for unpleasant stimuli. These effects have been associated with attention orientation at the early stages of processing. The arousal dimension is reflected by later components like P300 and slow waves (550 to 850 ms post-stimulus) with higher amplitudes for more arousing stimuli [130]. Also, it has been shown that unpleasant and highly arousing stimuli evoke greater ERP responses for females relative to males [131]. Basic emotional processing is frequently analyzed by employing ERP correlates of facial expression perception. Here, the EPN component is known to be emotion-sensitive [17]–[19] which was confirmed in Section 3.1 based on the results from my experiments [15].

In terms of brain waves, the power of alpha waves is connected with discrete emotions of happiness, sadness, and fear [132], but also can be treated as an effective index of the cortical arousal level [133]. The asymmetry of the EEG spectrum between frontal parts of different hemispheres of the brain is known as a steady correlate of valence [134]. Studies in the higher frequency gamma band showed a significant interaction between valence and hemisphere, suggesting that the left part of the brain is involved more in positive emotions than the right hemisphere [135]. More complex emotion correlates are defined in terms of

coherence between different areas of the brain, for example, the phase synchronization between frontal and right temporoparietal regions has been connected with higher valence and arousal [136], and the coherence between prefrontal and posterior beta oscillations has been shown to increase while watching highly arousing images [137].

## **2.5 ERP correlates of emotional face processing**

Faces and emotional facial expressions hold paramount nonverbal information in communication with other people. Developmental studies of infants have provided evidence that we are born with the ability to recognize faces [138]. This ability is our important evolutionary adaptation to the complex social environment [19]. Because of the social significance of facial emotions, information about emotional states derived from faces is processed very rapidly, as soon as 100 ms after the face onset [139], to be available for immediate regulation of behavior. The time course of facial expression processing can be divided into three stages [139]: automatic processing (components N100, P100), distinguishing emotional and neutral facial expressions (components VPP, EPN, N250), and differentiation of various emotional facial expressions (components P300, N300, LPP). The studies suggest that some basic facial expressions recognition starts together with the initial processing of face features. However, the structural encoding of faces and the detection of their emotional expression represent parallel and independent processes [17]. Thus, brain signals generated by face recognition and facial expression processing may overlap in ERP components (i.e., face recognition reflected in the N250 component and emotional processing in the EPN component). Many different components were identified in the literature as correlates of emotional face processing. The most important ones are listed in Table 2-7 together with their typical latencies, topographies, short descriptions, and relevant references.

**Table 2-7. Short descriptions of ERP components related to emotional face processing. The bold-faced components are of particular interest to my dissertation.**

Component	Typical latency and topography	Short description
P100	100 – 130 ms Occipital	Initial processing of visual stimuli resembling faces (i.e., in contour or shape) [140]. Initial extraction of fearful face features [139].
N100	60 – 140 ms Temporo-occipital	A concomitant of P100. Processing fearful facial expressions [139].
<b>N170</b>	150 – 200 ms Temporo-occipital	Early processing and detection of face-like objects [141]. No effect of facial expression [20], [142].
VPP	120 – 220 ms Medial fronto-central	A concomitant of the N170. Some studies suggest its association with fearful faces processing [143].
<b>N250</b>	230 – 320 ms Temporo-occipital	Acquiring face representations and face recognition [144].
<b>EPN</b>	240 – 340 ms Temporo-occipital	Increased emotional arousal evoked by facial expressions, especially expressions of anger and happiness [18], [19].
<b>P300</b>	280 – 450 ms Medial fronto-central	Some studies suggest its association with fearful faces processing [143].
N300	250 – 350 ms Temporal	Processing of fearful [139] and angry [145] facial expressions.
N400	300 – 500 ms Medial, occipital and temporal	Retrieval of content from face representations and of its associated verbal-semantic information [138]
LPP	400 – 600 ms Medial central	It reflects the relatively rapid and dynamic allocation of increased attention to emotional stimuli. [146]. Discrimination between fearful and happy and neutral expressions [147].

In the following paragraphs, I provide extended descriptions of ERP components that are particularly important to my thesis: N170, N250, EPN, and P300.

### **N170**

The N170 component reflects the neural processing of faces or highly familiar objects [148]. It is characterized by a sharp negative peak around 170 ms post-stimulus. It is thought to originate from the fusiform gyrus (specifically from the fusiform face area), and thus, it is the strongest at right occipito-temporal electrodes. The N170 is not sensitive to the identity of the face, it rather represents the early processing and detection of face-like objects [141]. Its latency and amplitude can be modulated by the face inversion, especially the Thatcher effect [149], or by the race of the face [150]. Many papers are showing the effect of facial emotional expression on N170, but the latest meta-analytic studies suggest that this effect is small, not robust, and highly dependent on face stimuli [142]. The effect was not observed in our experiments either [20]. The example of the N170-related peak can be found in Figure 3-4 in Section 3.1.

### **N250**

The N250 component is connected with the recognition of faces and objects [151]. It is a relatively short negative deflection that peaks 230 – 320 ms post-stimulus. Like N170, it is generated in the fusiform gyrus, and thus, it is the most apparent occipito-temporal electrode. It can be treated as an index of face familiarity [20] and it is enhanced during the acquisition of face and object familiarity [144], [152]–[154]. Our team confirmed these effects in a number of studies involving face familiarity and a single-trial ERP analysis [20], [22], [23]. The early studies of this component showed that N250 increases when a face image is preceded by the same face as compared to a different face (N250r) [155]. Additionally, this repetition effect is stronger for familiar than unfamiliar faces. The example of an N250-related peak for the target face can be found in Figure 3-22 in Section 3.3.

### **EPN (Early posterior negativity)**

The EPN is an emotion-sensitive component that can be characterized as a negative deflection starting around 150 ms and peaking 240 – 340 ms post-stimulus [19]. The neural sources of this component seem to be located in visual processing areas of the brain, so it is the most apparent at occipito-temporal electrodes. The occurrence of EPN is an indicator of increased emotional arousal evoked by images or facial expressions [156], [16], especially expressions of anger (high arousal and low valence) and happiness (high arousal and high valence) [18]. This was confirmed in one of my studies [15]. It reflects the early stages of emotion discrimination and can be modulated by the level of emotional engagement and the size of the visual stimulus [157]. An example of EPN-related deflection for emotional expression can be found in Figure 3-4 in Section 3.1.

**Important!** The EPN component can be easily confounded with N250 when interpreting the ERP waveforms. It is even impossible to disentangle these two in some experiments [158]. They occur in a similar time range and at similar electrode sites, but they are assumed to reflect different cognitive processes. It was shown that both EPN and N250 components are enhanced for attractive relative to unattractive faces [159], but there is a lack of research on disentangling the face learning and emotional expression processing ERP correlates.

### **P300**

P300 is probably the most popular component in the research literature and practical applications like brain-computer interfaces and mental disorders diagnosis [160]. It is a very strong positive component elicited during decision-making, information processing, and memory operations. It spans a relatively wide time window of the ERP waveform and usually peaks from 300 to 900 ms post-stimulus. It is produced by a pattern of generators in the parietal cortex with contributions from stimulus-specific brain areas. One of the most popular experimental designs to elicit P300 is the *oddball paradigm* where the participant is presented with sequences of repetitive stimuli (visual or auditory) that are

sometimes interrupted by a deviant or target stimulus (called *oddball*) which elicits the P300 response. The participant should be actively engaged in the task (e.g., by counting the oddball presentations) to increase the P300 amplitude. The latency of P300 is usually proportionate to the response time of the participant (or inversely proportionate to the performance of the participant) [161]. Due to its popularity and strength, it is usually used to validate new hardware setups and algorithms for ERP measurement, as I did in [21]. In the context of emotional face processing, some studies suggest its association with fearful faces processing [143]. An example of a P300-related peak can be found in the simulated data in Figure 3-5 in Section 3.2.

### 3 NEW METHODS OF ERP EXTRACTION FOR EMOTIONAL FACE PROCESSING

This section summarizes the original contribution to knowledge that supports the thesis of this dissertation. It focuses on the subject of high-quality ERP extraction from EEG and its impact on emotional face processing analysis. The consecutive subsections are arranged according to the chronological order of my research and publications. The logical order of phases and steps in a typical ERP study is defined in Table 3-1. During my research, I was involved in all the mentioned phases, but my main contributions cover in particular the underlined steps. Table 3-1 itself is a significant contribution as a practical checklist for ERP studies.

**Table 3-1. The order of phases and steps in a typical ERP study. The underlined steps are included in the main contributions of this dissertation.**

Order	Phase	Consecutive steps
1	Experimental design	Defining the goal of the study. <u>Defining hardware and software requirements.</u> Planning the minimum number of participants and trials. Ethical approval. Selection of participants. Programming the experimental procedure.
2	Hardware setup	Preparing the laboratory. <u>Setting up the EEG system and auxiliary devices.</u> Testing the procedures.
3	Preparing participants	Instructing the participants. Obtaining written consent and collecting necessary data from participants. Setting up the EEG cap.
4	EEG acquisition	Initialization of the experiment and recording. Monitoring the status of the participant and the EEG system. Keeping the laboratory notebook.
5	EEG preprocessing	<u>Applying different filters to the raw EEG data, including frequency filtering, re-referencing, cropping, resampling, artifact filtration, etc.</u>

6	ERP extraction	<u>Extracting single-trial epochs.</u> Baseline correction. <u>Rejecting corrupted or non-target epochs.</u> <u>Averaging epochs for each target class.</u>
7	ERP analysis	Visual analysis of ERP waveforms. Statistical analysis of the experimental effects in ERP components. <u>Training ERP classifiers [25]f.</u>

Most of the EEG preprocessing and ERP extraction methods in this dissertation were implemented in Python programming language using mainly NumPy, SciPy, and MNE-Python (MEG + EEG analysis & visualization) packages [162]. The statistical analyses were typically performed in the R programming environment. To support the reproducibility and replicability of the research, I shared all the details of the EEG/ERP methods according to the ARTEM-IS guidelines [7]. Also, I shared the data and code in Open Science Framework (OSF) where necessary.

### 3.1 Adaptation of Emotiv EPOC+

This section summarizes materials from the article “*Validation of Emotiv EPOC+ for extracting ERP correlates of emotional face processing*” [15] published in *Biocybernetics and Biomedical Engineering* journal. It presents my proposed adaptation of the low-cost Emotiv EPOC+ EEG device for ERP experiments by applying an additional stimuli marking circuit to solve problems with the EEG signal transmission delay, time drift (a cumulative desynchronization of clocks in an EEG device and a recording PC), and jitter (unpredictable variability of the timestamps) common to most low-cost wireless systems [163]. The second goal was to check the capabilities of our modification in the ERP experiment on emotional face processing. Results show that the adaptation allows for measuring small differences in the EPN component evoked for neutral and emotional (angry/happy) face expressions consistently with previous works using research-grade EEG systems.

### 3.1.1 Emotional face processing experiment

The goal of the experiment was to check if the low-cost Emotiv EPOC+ device can be used effectively for ERP measurements in evoked emotion recognition. No previous studies offered such analysis. Some of them used Emotiv EPOC+ and brain waves analysis for emotional state recognition [164]–[168], and the others used it for ERP research in different domains, e.g., auditory ERPs [169], N170 [170], or P300 [171]. Hence, we decided to use the experimental design from the psychological study using research-grade EEG for analyzing emotional facial expression processing [19]. As mentioned in Section 2.5, faces with angry and happy expressions generate the face-sensitive N170 and the emotion-sensitive EPN component in ERP waveforms. Thus, we set two goals for our experiment:

- 1) To replicate the detection of the N170 component as presented in [170]
- 2) To verify the possibility of measuring the emotion-sensitive EPN component with Emotiv EPOC+

The exact procedure was (citing from [15]):

*“After signing written informed consent, each participant was seated alone in the same, dimly lit, quiet room. A computer screen was placed on an empty desk at a viewing distance of 70 cm. Participants were instructed to leave any electronic devices away, seat still, keep quiet, limit unnecessary blinking during trials and remain focused on the task. Subjects were also instructed to maintain central eye fixation during the trials. In the task, participants were instructed to monitor the centrally presented faces (the centre of the nose was always in the centre of the screen) and to respond as quickly and accurately as possible with a right-hand button press whenever a male face was displayed and with a left-hand button press whenever a face was female. To control lateral bias in motor response, left- and right-hand responses were counterbalanced across subjects. Each trial began with a 500 ms presentation of the white fixation cross. 750 ms after the offset of the fixation cross, the face was presented for 300 ms (specific timings derived from [19]). In each trial, one face was presented at the fixation covering a 2.5° x 3.5° visual angle. The interval between response and the next stimuli was*

1200 ms. One experimental unit consisted of 32 trials (16 presentations of faces with a neutral expression, 8 presentations of happy faces, and 8 presentations of angry faces, each time in random order). A single experiment consisted of 16 experimental units, it gives 5120 of trials in overall.” [15]

We selected the stimuli from the MUG dataset [172]. They were grayscale face pictures of eight different individuals (four women and four men) displaying angry, happy, and neutral expressions. There were ten participants (students and lecturers of Silesian University of Technology, right-handed, normal vision, 8 males). The experimental procedure was implemented in the OpenVibe software [173].

### 3.1.2 Stimuli marking circuit

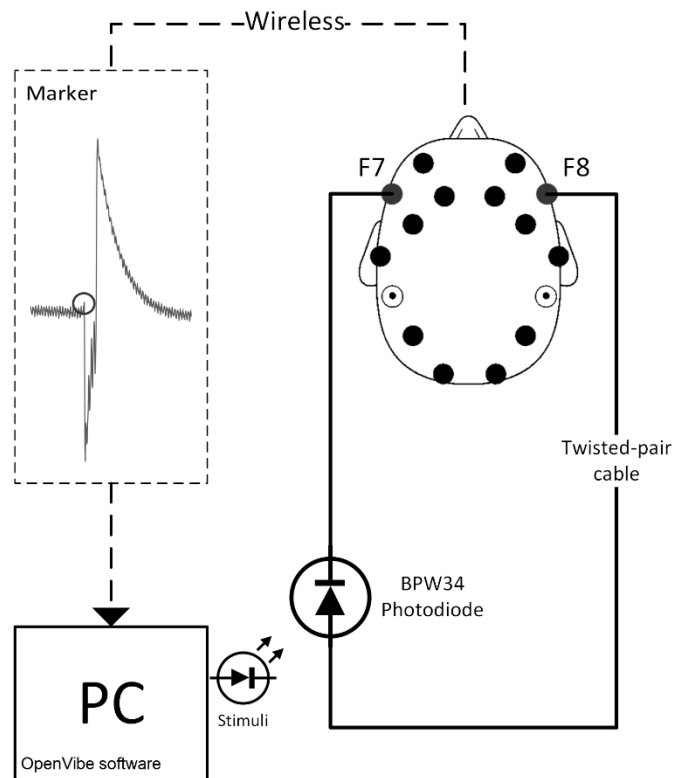


**Figure 3-1. The simplified diagram of my new proposed stimuli marking circuit (source: [15]).**

The design of my stimuli marking circuit is presented in Figure 3-1. The whole module consists of around one meter of a twisted-pair cable soldered to the BPW34 photodiode and two frontal electrodes F7 and F8 isolated from the head by a thick rubber. The circuit may be easily reconnected to any other two electrodes, according to needs. The diode needs to be attached to the part of the screen that changes luminance significantly when a stimulus is displayed. I used a little white square in the right bottom corner of each displayed image. The change of luminance generates a sharp peak of potential between electrodes F7 and F8. Then, a dedicated peak finding algorithm inspired by [174] is used to identify the exact time of stimulus display (the red circle in Figure 3-1). Details about the algorithm can be found in Figure 3-3 and in [15].

The stimuli marking circuit physically connects Emotiv EPOC+ to the PC, which is the main disadvantage of the solution, apart from losing two electrodes. However, the circuit is extremely easy and cheap to build, and most importantly, it offers almost perfect timing synchronization which is crucial for ERP measurements. The effect of using stimuli marking circuit is distinctly visible in the example in Figure 3-2. Without the correction using a marking circuit, epochs are affected by synchronization problems causing amplitude and latency deformations in the averaged signal. After applying the correction, the N170-related peaks are well aligned and have proper latencies close to 170 ms.

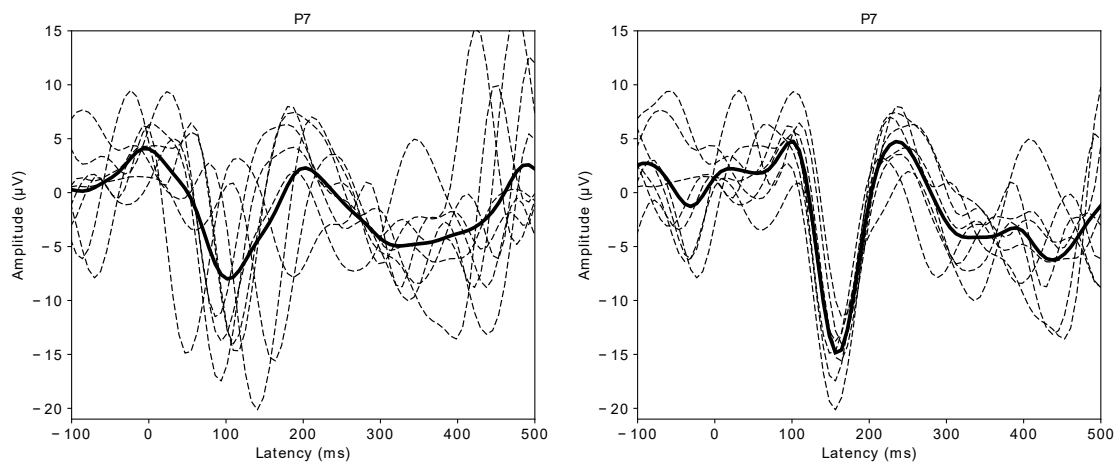


**Figure 3-2. On the left: the original 8 epochs (dotted lines) and their average (solid line). On the right: the same 8 epochs corrected using our stimuli marking circuit (source: [15]).**

### 3.1.3 ERP extraction and results

The complete pipeline for ERP extraction from Emotiv EPOC+ is presented in Figure 3-3. The common average reference (CAR) operation was applied to reduce the environmental noise and enhance a potential emotional effect [156]. Further, to remove a constant offset and irrelevant high frequencies, signals from all electrodes (including stimuli marking electrodes) were band-pass filtered at the range 0.5 – 15 Hz using 3th-order zero-phase forward-backward digital Butterworth filter using Gustafsson's method [175].

A set of 512 epochs was extracted separately for electrodes P7, P8, O1, and O2 for each participant; starting 104 ms before and 512 ms after the stimulus. The epochs for specific electrodes were removed from this set if:

- 1) The participant did not answer or answer wrongly to the task (to avoid samples in which the participant potentially missed the face display)
- 2) The peak-to-peak potential in the epoch was larger than 70 µV (to avoid artifacts from blinks and muscle movements)
- 3) There was no clear N170-related peak detected by the proposed wavelet-based algorithm (to avoid any other problematic or noisy samples)

The algorithm from point 3) is one of the added values of the dissertation. It determines the existence of the N170-related peak by calculating the continuous wavelet transform (CWT) for each epoch using the inverted Ricker wavelet. It detects a peak if the mean value of CWT coefficients over the set of 9 different wavelet widths (1, 1.5, ..., 5) and 5 different shifts (156 ms, 160.8 ms, ..., 180 ms post-stimulus) is larger than zero. The parameters were selected empirically to reject a limited set of clearly corrupted epochs without any peak in the range 156 – 180 ms post-stimulus. The details of the algorithm can be found in [15], I do not focus on them in the dissertation, because in practice this problem can be resolved more effectively by the robust weighted averaging method described in Section 3.2.

After filtering, there were on average 424 out of 512 epochs left per electrode per participant (205 for neutral faces, 219 for emotional faces). All epochs were baseline corrected and averaged for each electrode, each expression, and each participant separately. An example of averaged ERP waveform for the participant with the lowest number of rejected epochs at electrode O1 is presented in Figure 3-4. The more negative values in the EPN component range 240 – 340 ms (marked in grey) can be observed for emotional stimuli.

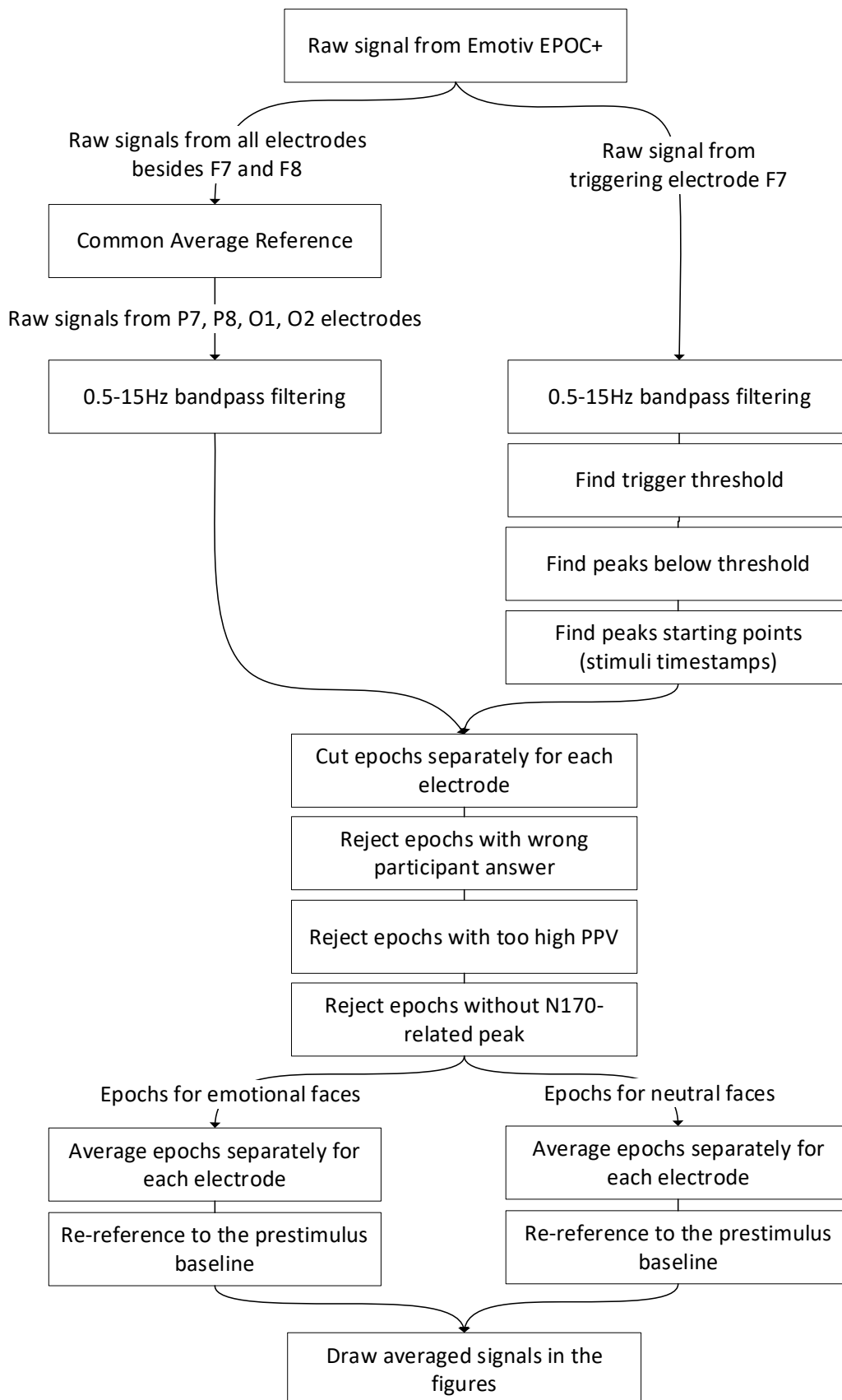
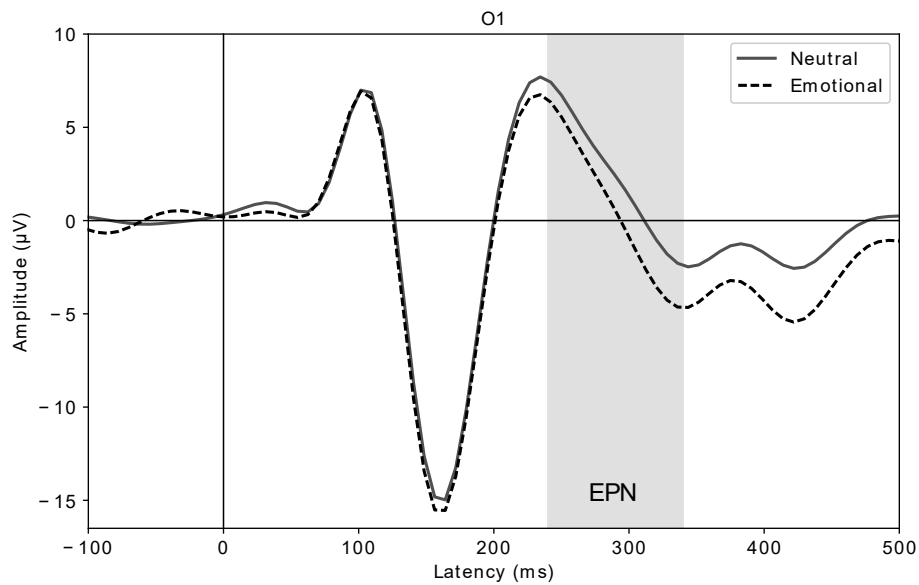


Figure 3-3. The block diagram of the ERP extraction pipeline (source: [15]).



**Figure 3-4. An averaged ERP waveform for emotional and neutral faces for the selected participant at the electrode O1 (source: [15]).**

The differences in EPN amplitudes were analyzed statistically across all 10 participants using a two-tailed paired t-test. The tests confirmed the significance of the effect of emotional expression on the EPN amplitude at  $p < 0.01$  for electrodes O1 (mean:  $-0.92 \mu\text{V}$ ,  $t(9,10) = 3.47$ ,  $p = 0.007$ ) and O2 (mean:  $-0.84 \mu\text{V}$ ,  $t(9,10) = 3.68$ ,  $p = 0.005$ ). The effect was weaker but still present at  $p < 0.05$  at electrodes P7 (mean:  $-0.71 \mu\text{V}$ ,  $t(9,10) = 2.47$ ,  $p = 0.035$ ) and P8 (mean:  $-0.77 \mu\text{V}$ ,  $t(9,10) = 3.17$ ,  $p = 0.011$ ). This is consistent with the results from [156] and [17], and partially consistent with [19] where the main difference is the sign of the derivative of an averaged signal in the time range of 250 – 400 ms. In conclusion, the proposed adaptation of Emotiv EPOC+ allows effective ERP measurements for evoked emotion recognition.

## 3.2 Improved robust weighted averaging

This section summarizes materials from the article “*Improved robust weighted averaging for event-related potentials in EEG*” [21] published in *Biocybernetics and Biomedical Engineering* journal. It presents my proposed ERP-related improvements to the previous work “*Robust weighted averaging for biomedical signals*” [176]. The main reason for this study was to increase the quality of emotional-related ERPs extracted from the adaptation of Emotiv EPOC+ described in the previous Section 3.1. My contribution is fourfold:

- 1) Significantly lower averaging error (higher SNR of ERPs)
- 2) Increased robustness to local minima
- 3) Increased robustness to strong outliers
- 4) Increased robustness to uncorrelated epochs

### 3.2.1 Methods

As mentioned in Section 0, the ERP waveforms are usually a traditional sample-wise arithmetic mean of multiple epochs. This is the simplest method of increasing the SNR in periodical biomedical signals. However, it holds the assumption that the noise is zero mean, stationary and non-correlated with the signal. Most types of noise are not stationary, especially in EEG measurements affected by many types of noise and artifacts. In this case, it is better to use a weighted averaging approach given by Equation (3-1) where  $w_i$  is a weight for the  $i$ -th (out of  $N$ ) epoch  $x_i$  and  $v$  is the averaged ERP.

$$v = \sum_{i=1}^N w_i x_i \quad (3-1)$$

The higher weights should be assigned to more reliable epochs. The main problem is how to find the weights that reflect the amount of the signal in each epoch. In [176], the approach is to iteratively minimize the criterion function  $I_m(\mathbf{w}, v)$  in Equation (3-2) where  $q$  is a dissimilarity measure between the epoch

$x_i$  and the averaged waveform  $\mathbf{v}$ , and  $m$  is an additional weighting exponent larger than 1.

$$I_m(\mathbf{w}, \mathbf{v}) = \sum_{i=1}^N w_i^m \varrho(\mathbf{x}_i - \mathbf{v}) \quad (3-2)$$

The optimal solution is represented by  $\mathbf{v}^*$  that characterizes with the minimal dissimilarity to all epochs  $\mathbf{x}$  by using optimal weights  $\mathbf{w}^*$ . In short, the method iterates over the consecutive estimates of  $\mathbf{w}$  and  $\mathbf{v}$  until the convergence defined by Equation (3-3) where  $l$  is the number of the last iteration and  $\xi$  is a convergence condition set manually.

$$\|\mathbf{w}^l - \mathbf{w}^{l-1}\|_2 < \xi \quad (3-3)$$

The paper [176] points the Vapnik's  $\varepsilon$ -insensitive function [177] as the dissimilarity measure  $\varrho$  providing the best results of the weighted averaging based on criterion minimization (WACFM in short). For simplicity, I focused on improving the special case of WACFM using Vapnik's function with  $\varepsilon$  set to zero (the absolute error function) called later absWACFM. The other parameters were set to  $m = 2$ ,  $\xi = 10^{-5}$ . The selection of these parameters has no impact on the proposed improvements.

### **Increased robustness to local minima**

The problem with the original implementation of the WACFM method is that consecutive iterations are highly biased towards epochs very close to the current estimate  $\mathbf{v}$  of the ERP waveform. For example, if the epoch  $\mathbf{x}_i$  is identical to the current estimate  $\mathbf{v}$  the weight  $w_i$  gets an infinite value and the algorithm runs into a local minimum. This is one of the major flaws of the original algorithm that I encountered when using it for ERP. I proposed a solution significantly minimizing this problem by limiting the maximum weight by adding a small positive constant to the dissimilarity metric  $\varrho$ , so the value of weight  $w_i$  in equation (12) in [176] never reaches infinity. I suggested setting this constant to be equal to the value of the least significant bit of the digital resolution of the EEG amplifier used.

### **Increased robustness to strong outliers**

The EEG data may contain extreme outliers, orders of magnitude larger than the signal itself, e.g., caused by body or electrode movements. Epochs containing such artifacts may affect the waveform estimate  $\nu$  even when they have low weights assigned. I limited this problem by zeroing out the weights smaller than  $1 / (c * N)$  where  $N$  is the number of epochs to average and the specificity constant  $c > 0$  can be adjusted to the needs. The  $c = 1$  means that all epochs with weights less than  $(1 / N)$  will be zeroed out, this is quite a high sensitivity. The larger the value  $c$  the higher the specificity and the fewer weights are zeroed out. The default value of  $c = 100$  is used here and suggested in typical EEG settings but it should be adjusted to the specific task at hand.

After zeroing out the weights it is important to adjust all the other weights, so they sum up to 1 again. I proposed to do it by simply dividing each weight by the sum of weights after the zeroing out operation.

### **Increased robustness to uncorrelated epochs**

This improvement was inspired by the best method from the article [178] about weighted averaging in electrocochleography (called Scheme 5). Scheme 5 updates the weights  $w_i$  using Equation (3-4) where  $S_i$  is a “signal” defined by the Pearson’s correlation between the traditionally averaged ERP waveform and the epoch  $x_i$  in the time window of interest (depending on the task, i.e., the time range of the ERP component of interest),  $N_i$  is a “noise” defined as the standard deviation of samples in the time window representing the noise in the ERP waveform (i.e., the ERP baseline), and  $k$  is just a constant that ensures the weights are unitless.

$$w_i = \frac{S_i}{N_i^2} * k \quad (3-4)$$

In my improvement, I adopted the idea of checking Pearson’s correlation by adding a step to the original WACFM procedure which reinforces or attenuates

weights for specific epochs depending on their correlation with the current ERP waveform estimate. The details are given in steps 4) and 6) in my final procedure called corWACFM (WACFM with correlation-based epochs weighting) summarized in Table 3-2.

**Table 3-2. The proposed corWACFM algorithm for robust weighted averaging of ERP epochs. The proposed improvements to the original WACFM are underlined.**

Step	Operation
1	Initialize the current estimate $\nu$ with the traditionally averaged ERP waveform
2	Update the vector of weights $w$ using equation 12 from [176] with <u>improvements for local minima and strong outliers</u>
3	Update $\nu$ using equation 14 from [176]
4	<u>Calculate the vector <math>u</math> of Pearson's correlations between <math>\nu</math> and each epoch <math>x_i</math>. Rescale <math>u</math> to range (0, 1) where 0 is no correlation and 1 is a perfect correlation</u>
5	Update $w$ using the equation 12 from [176] with the <u>improvement for local minima</u>
6	<u>Update <math>w</math> by multiplying it sample-wise by <math>u</math></u>
7	<u>Divide each weight by the sum of weights, so they sum up to 1</u>
8	<u>Update <math>w</math> using the improvement for strong outliers</u>
9	Update $\nu$ using equation 14 from [176]
10	If the stopping condition from Equation (3-3) is not met, go to step 4. Otherwise, set the current estimate $\nu$ as the optimal solution $\nu^*$ and stop the algorithm

### **3.2.2 Simulation study**

In real-life EEG data, the underlying signal and noise are not known. Thus, to objectively assess the quality of averaging I generated a simulated ERP dataset of 260 epochs from 64-electrodes and 128 Hz sampling frequency using the SEREEGA Matlab toolbox for mimicking the brain activity [179]. The details and code for generating this dataset are accessible as supplementary material to [21].

To generate 200 epochs, I used a combination of simulated N70, P100, N135, and P300 components. Each epoch includes the natural variability of these components. The arithmetic average of these 200 epochs is considered the deterministic component of the ERP waveform as presented in Figure 3-5. To examine the robustness of averaging the pink noise was added to the first 30 epochs, the Bernoulli-Gaussian impulsive noise was added to the first 170 epochs, the Bernoulli impulsive noise was added to epochs 140-170, 30 randomly picked epochs were duplicated, and added to the dataset in inverted versions, and 30 epochs of white noise were added to the dataset. All 260 distorted epochs at the electrode POz are presented in Figure 3-6. They were used for benchmarking the new averaging algorithm.

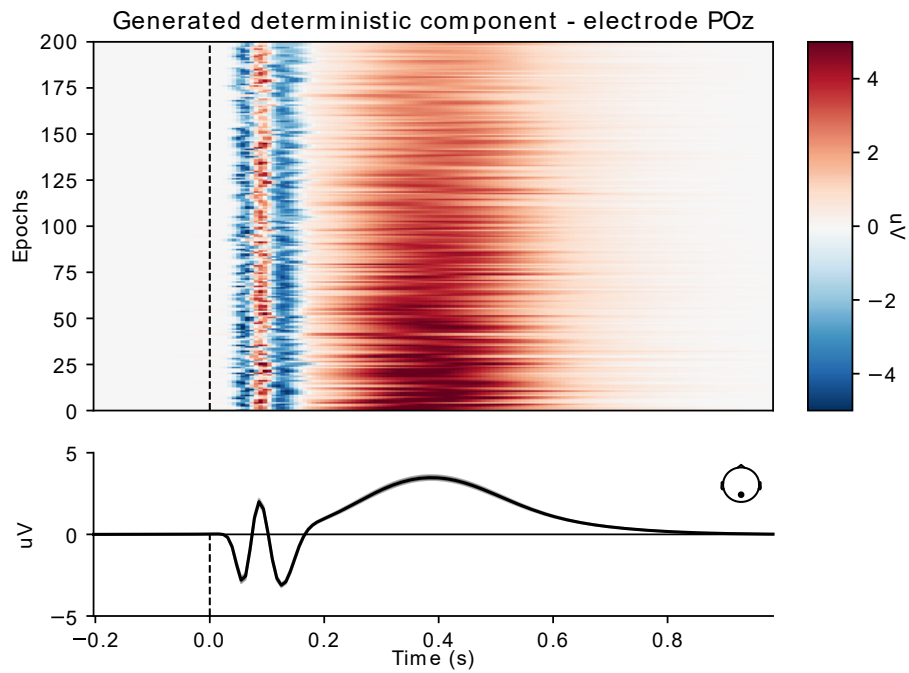


**Figure 3-5. 200 raw generated epochs and their average (the deterministic component) at the POz electrode (source: [21]).**

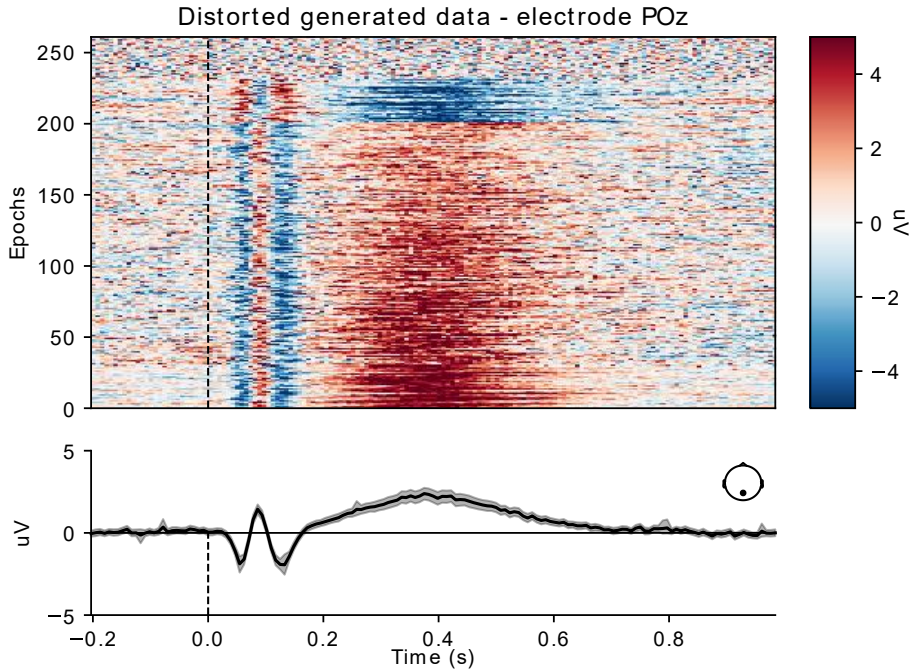


**Figure 3-6. 260 distorted generated epochs at the POz electrode and their average (source: [21]).**

The performance of the proposed corWACFM method was tested using the same metrics as in [176]: the maximal absolute difference between the deterministic component and the averaged signal (MAX) and the root-mean-square error between the deterministic component and the averaged signal (RMSE). The lower the metric the better the algorithm. The corWACFM was compared with traditional averaging, sample-wise median aggregation, the original absWACFM, and Scheme 5 from [178]. The bootstrap testing procedure with a sample size of 130 epochs and 1000 repetitions was used to avoid dependency of results on the data. In practice, the EEG data are usually filtered before extracting ERP epochs, so the results after 0.5 – 24 Hz bandpass filtering are also presented. Below, I present only selected results from my publication [21] which thoroughly compare these methods in different aspects.

The notched boxplots with notches marking the 95% confidence intervals were used to assess the statistical significance of the differences. The boxplots in Figure 3-7 (for RMSE) and Figure 3-8 (for MAX) both show a significant advantage of corWACFM over the traditional averaging and the original absWACFM method. The average improvement over the original method is 45% lower RMSE and 37% lower MAX. Scheme 5 is a bit better than corWACFM when applying bandpass filtering. However, the corWACFM is significantly better for the raw data. Also, Scheme 5 is highly dependent on the initial estimate as presented in figure 13 from [21] and supported by the results on the real-life dataset described in the next Section 3.2.3.

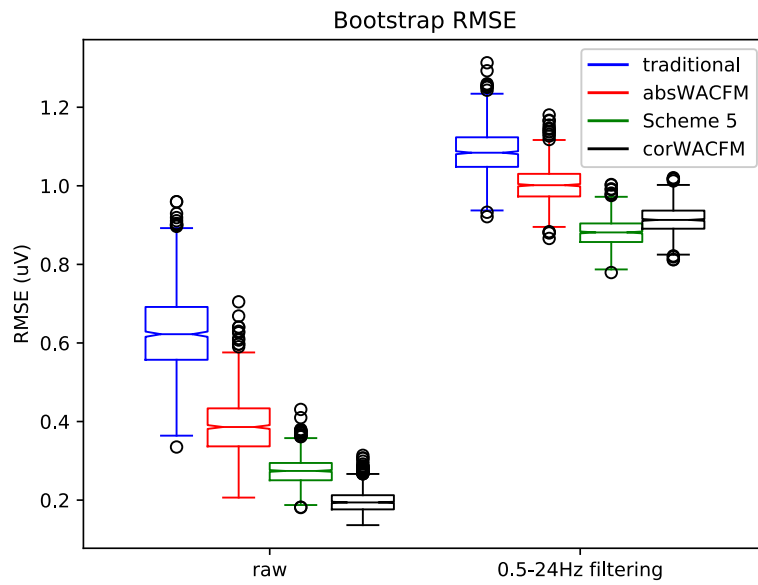


**Figure 3-7. The notched boxplot of bootstrap RMSE for different averaging schemes for the raw simulated dataset and its bandpass filtered version (source: [21]).**

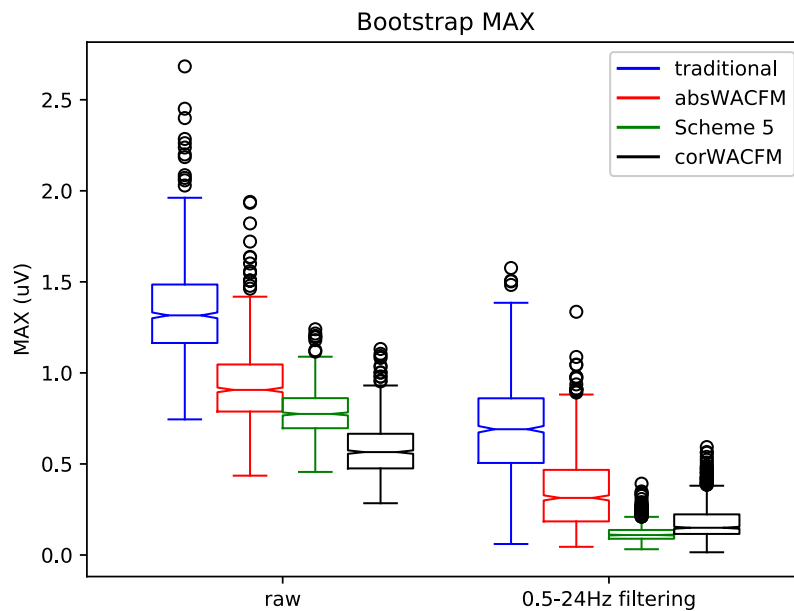


**Figure 3-8. The notched boxplot of bootstrap MAX for different averaging schemes for the raw simulated dataset and its bandpass filtered version (source: [11]).**

The weights calculated by the proposed corWACFM method are visualized in the ERP image in Figure 3-9. This image contains the same epochs as presented in Figure 3-6, but multiplied by weights from corWACFM and multiplied by the number of epochs to keep the same amplitude scale. We can observe how the distorted epochs were attenuated by assigning lower weights.

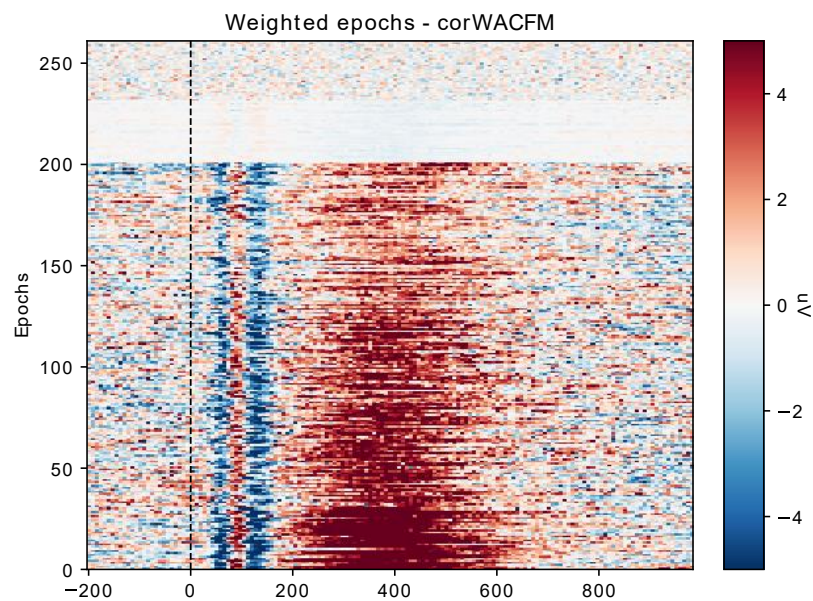


**Figure 3-9. A weighted ERP image of the generated dataset calculated using the new corWACFM method (source: [11]).**

### **3.2.3 Validation on emotional face processing experiment**

To verify the effectiveness of the averaging schemes on challenging real-life data, we used epochs for a selected patient from the experiment described in Section 3.1.1 using our adapted Emotiv EPOC+. To make it particularly challenging, we did not use any additional filtering. The epochs are visualized in Figure 3-10. There are strong outliers in epochs 17 – 20 visible in the traditionally averaged ERP waveform as a sharp peak around 300 ms post-stimulus.

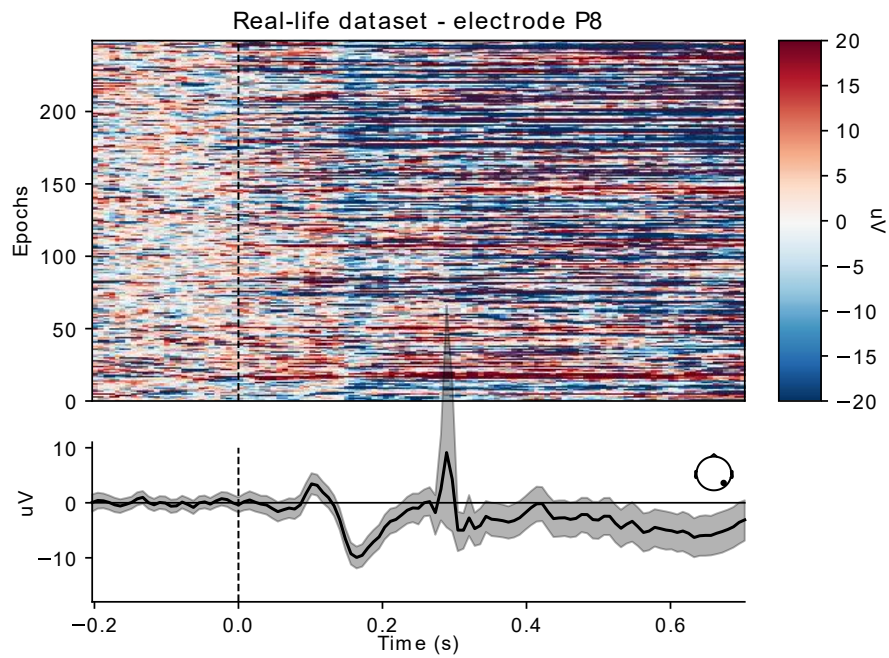


**Figure 3-10. The epochs from the real-life data for the electrode P8 and their average (source: [11]).**

It is impossible to directly compare the RMSE of the methods as the deterministic component is not known, so only the qualitative assessment was performed using the averaged waveforms in Figure 3-11. Scheme 5 achieved the highest N170-related peak, but it failed to remove the strong outliers. The proposed corWACFM has the second-highest N170-related peak method but is robust to outliers.

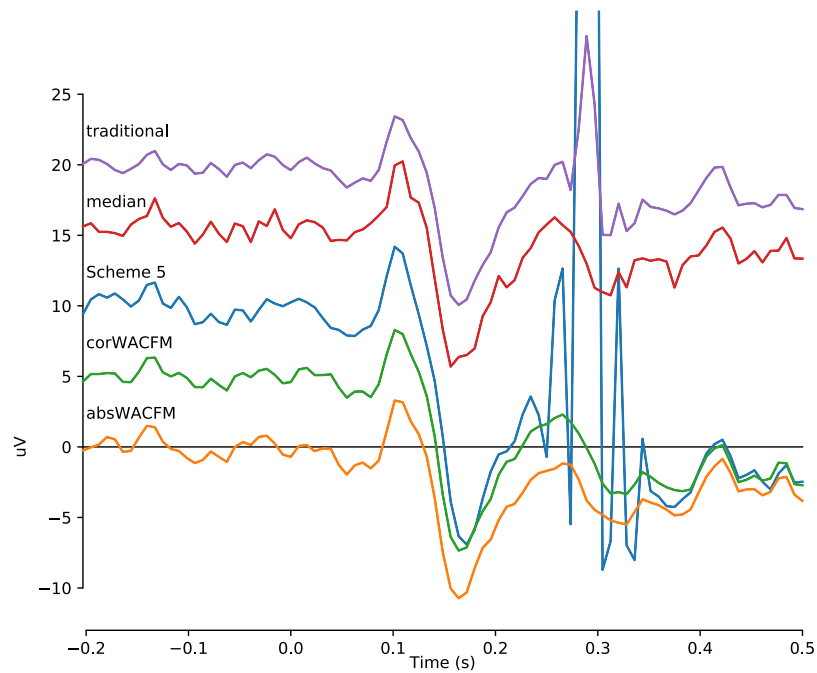


**Figure 3-11. Comparison of the averaged ERP waveforms for the real-life dataset using different averaging schemes (source: [11]).**

The parametrization of the corWACFM method was adjusted to EEG signals but it can be easily incorporated into other repetitive electrophysiological measurements. The robust methods based on epochs weighting do not modify the data, unlike other filtering methods, i.e., the ICA-based ocular artifact removal described in the next Section 0, so there is a lower risk of removing relevant information. However, it should be noted that robust weighting has several assumptions that can prevent us from using it in specific cases. The most important one is that it does not account for the effects of changing latencies or amplitudes of the components during the experiment, i.e., the effect of face learning in the N250 component [20]. The future work includes implementing robust averaging as a function in the MNE-Python package.

### **3.3 Semi-automatic ocular artifacts filtration**

As introduced in Section 0, the familiarity-sensitive N250 component (a negative deflection peaking 230 – 320 ms post-stimulus) and the emotion-sensitive EPN component (a negative deflection peaking 240 – 340 ms post-stimulus) can be easily confounded with each other [158]. It complicates the interpretation of N250 and EPN effects. Thus, to analyze the emotion-related EPN better, we need to understand also the N250 component. This section summarizes and extends a series of articles to which I significantly contributed [20], [22], [23], focused on the fine-grained analysis of the N250 component in face familiarity and face learning. The series of articles starts with the replication study [20] which confirmed the face familiarity effects previously described in [144]. Based on the collected data, I performed the first known single-trial analyses of face learning processes using single-trial ERPs [23]. To improve the quality of the analysis, I designed a complete pipeline optimized for precise ERP extraction, including the ocular artifact filtration method based on independent component analysis (ICA) and EOG [22]. This pipeline and its impact on the quality of ERP analysis of N250 are presented in this section.

#### **3.3.1 Materials**

The presented EOG artifacts rejection method was validated using both simulated and real-life datasets described in this section.

##### **Simulated dataset**

In the simulation study, I used a semi-simulated dataset from [180] in a version from April 2019. It contains 54 data samples obtained from 27 participants. Samples have a duration of 27 to 42 s and each one consists of uncontaminated EEG recording from 19 electrodes (FP1, FP2, F3, F4, C3, C4, P3, P4, O1, O2, F7, F8, T3, T4, T5, T6, Fz, Cz, Pz), vertical and horizontal EOG (VEOG and HEOG), and the EEG artificially contaminated with ocular artifacts according to the model from [181]. The dataset has a sampling rate of 200 Hz and is already band-pass filtered (0.5 – 40 Hz for EEG, 0.5 – 5 Hz for EOG).

## Real-life dataset

In the study [20], our team designed and conducted a close replication of the Joe/noJoe experiment described in “*Activation of Preexisting and Acquired Face Representations: The N250 Event-related Potential as an Index of Face Familiarity*” by Tanaka et al. [144]. The experiments were conducted in an electrically-shielded, quiet, dimly-lit room. Each of 16 participants (12 females; mean age = 21.5 years; range: 19–23) was asked to monitor the centrally presented faces from FACES Lifespan Database for Facial Expression [182] and indicate whether the face was the target (Joe) or not (noJoe) by pressing a right or left button. Each participant performed 36 experimental blocks per 24 trials (864 trials overall) with self-paced breaks between blocks. In each block, there were 2 target faces (Joe), 2 participant’s faces (Own), and 2 presentations of each of 10 other faces. The faces were presented in a pseudo-random order in each block, but the same faces were never immediately presented one after another to avoid repetition effects [183].

The EEG recordings during the experiment were collected using the research-grade BrainProducts actiChamp amplifier and actiCap EEG cap with 64 electrodes and a 2500 Hz sampling rate. The EOG was recorded from a passive electrode located at the outer canthus of the left eye. A Chronos multifunctional device was used to collect responses from participants and record the precise stimulus display times using a photodiode mounted on the screen (the idea similar to our adaptation of Emotiv EPOC+ described in Section 3.1). The diagram of the hardware setup is presented in Figure 3-12. More details about the experimental procedure and data collection can be found in our original paper [20]. The raw EEG recordings were made publicly available at <https://osf.io/7x6w5>.

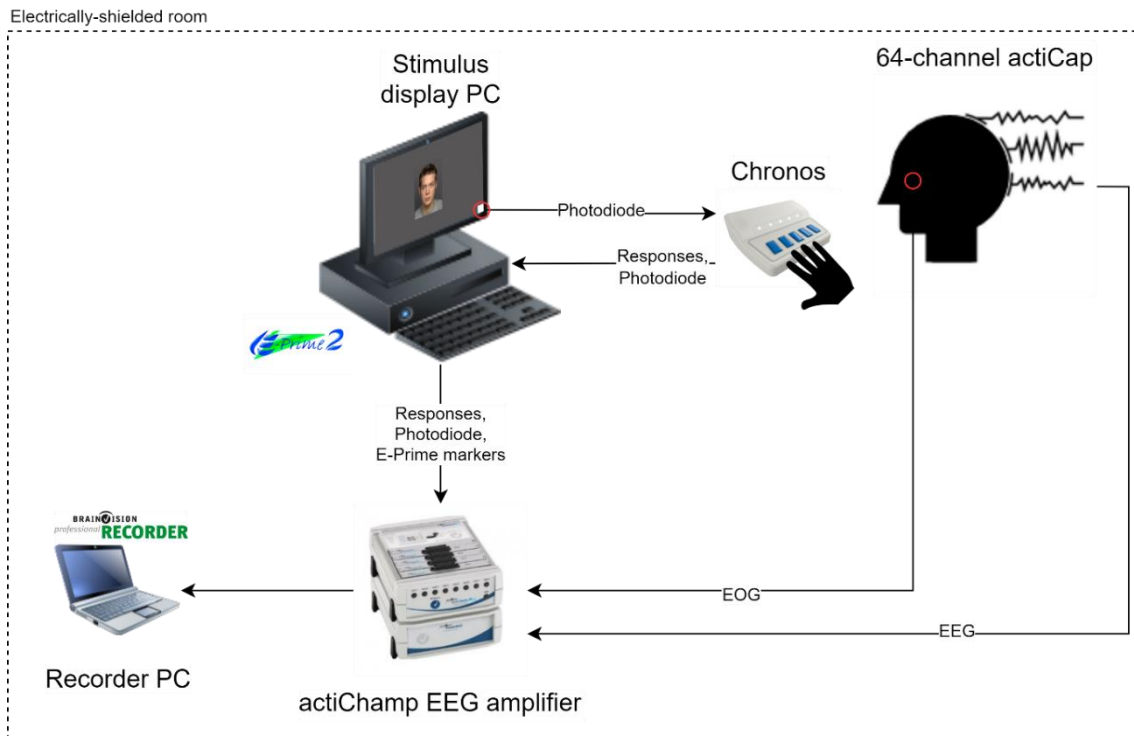


**Figure 3-12. The diagram of a research-grade hardware setup used in N250 experiments (source: [22]).**

### 3.3.2 Methods

The methods presented in this section were published in the article “*The importance of ocular artifact removal in single-trial ERP analysis: the case of the N250 in face learning*” [22] in the *Biomedical Signal Processing and Control* journal. The code and results of the method are publicly available at <https://osf.io/aqhmh> to support the reproducibility of the research.

There are multiple techniques for ocular artifact removal (see [184] for a systematic review), including regression, frequency filtering, wavelet transform [185], blind source separation, empirical mode decomposition, filter banks, deep learning, and hybrid methods. One of the most acknowledged EEG artifact elimination algorithms is blind source separation using independent components analysis (ICA) [186] used for ocular artifacts filtering in many recent studies [187]–[190]. ICA-based filtering was previously analyzed in the context of single-trial ERPs mainly for the detection of the P300 component [187]. The single-trial N250

ERPs with ocular artifacts removed using semi-automatic BESA software (BESA GmbH, Germany) were recently utilized by [75] for the classification of the viewer’s familiarity with a face.

ICA can be calculated using many different algorithms, like Infomax [191], FastICA [192], or SOBI [193], to name just a few. Infomax is held to give the most stable results in ocular artifacts filtration [194], [195]. I’ve decided to use the latest Picard algorithm – a fast and accurate approximation of Infomax that shows superior performance, especially on real data [196]. The first step of ICA-based filtration is a spatial decomposition of EEG signals into a set of statistically independent components. The next step is to select and reject artifact-related components (i.e., blinks) and reconstruct the filtered signal as presented in Figure 3-13.

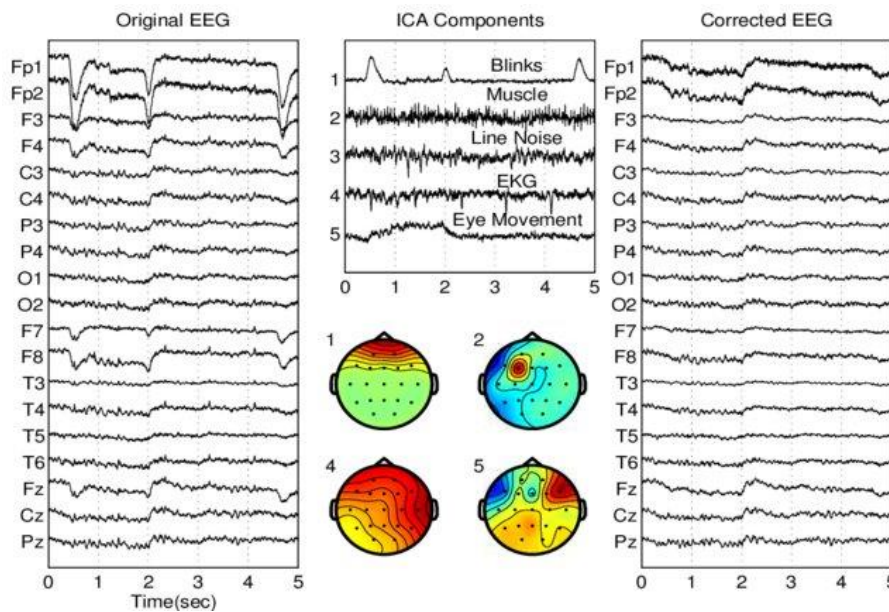


**Figure 3-13. EEG signal decomposition and filtration using ICA (source: [197]).**

The key advantage of ICA-based filtration is that ERP trials are just modified instead of being completely rejected. Minimizing data loss is extremely important in fine-grained single-trial analysis. The artifactual components can be selected

manually by visual inspection of their topographies, power spectra, and time-courses, or automatically, e.g., by calculating artifact-specific features [198] or by machine-learning-based classification [199]. However, if EOG measurements are accessible (like in our case), the proper ICA components can be selected much easier and more reliably by simply comparing them with EOG. I proposed a semi-automatic approach for selecting such components using only one hyperparameter – the level of correlation between components and EOG.

### The initial EEG preprocessing

The raw EEG signal was first cropped to the relevant time range between 2 s before the first stimulus and 2 s after the last stimulus display. Manually identified corrupted channels were interpolated using a spherical spline interpolation [200]. I applied common average reference and band-pass filtering in the range  $<2, 40>$  Hz using a third-order zero-phase forward-backward digital Butterworth filter [175]. The high-pass limit of 2 Hz was selected as suggested in [201] to improve the signal-to-noise ratio for artifact removal using ICA. The low-pass limit of 40 Hz was selected as in [144] to decrease the irrelevant high-frequency noise.

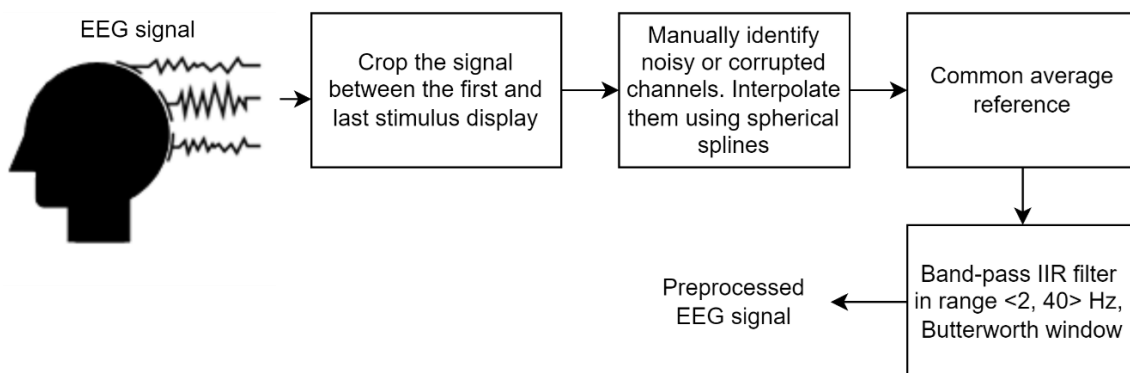


Figure 3-14. The initial EEG preprocessing procedures (source: [22]).

### Automatic blinks detection in EOG

The significant blink-related peaks were detected in the EOG signal using a noise-tolerant fast peak-finding algorithm [202]. The EOG signal was band-pass filtered to range  $<1, 10>$  Hz using FIR filter with Hann window, so it is easier to detect peaks. I used the default peak threshold of  $(\max(\text{EOG}) - \min(\text{EOG})) / 4$ , however, I rejected the upper and lower percentile of values from the  $\max(\text{EOG})$  and  $\min(\text{EOG})$  calculation to increase robustness to extensive outliers observed for a couple of participants. The blinks were defined as EOG signal fragments of  $<-500, 500>$  ms around the peaks. I utilized them to select the blink-correlated independent components later. The average number of detected blinks per minute for a participant was  $22 \pm 10$  which lies in the range of conversational spontaneous eyeblink rate of normal adults (10.5 to 32.5) according to [203].

### **The proposed method of ocular artifacts filtration**

The ERP epochs of  $<-100, 500>$  ms were extracted from EEG around correctly recognized face display markers (both target and non-target). The baseline correction was not used at that stage to avoid altering the original signal before ICA. I calculated the Picard ICA to extract a set of independent components that explains 99.9999% variance (mainly to reject zero-variance components) in the EEG epochs (on average  $61 \pm 2$  components per participant, min. 56, max. 62). I rejected ICA components (on average  $3 \pm 2$  components, min. 1, max. 8) highly correlated with blinks automatically identified in the previous paragraph. The correlation analysis uses an iterative Z-scoring to find ICA components with Pearson's correlation higher by more than 2 standard deviations than others. Such ICA components are considered blink-related, they are rejected, and the procedure is repeated until no more blink-related components are identified. The threshold of 2 standard deviations (the default in `find_bads_eog` is 3) is the only hyperparameter of the algorithm that needed to be manually adjusted to the specific dataset in such a way that blinks for all participants were successfully removed. I adjusted it using a qualitative assessment of topographic maps of the components (Figure 3-15) and by comparing blink-related EEG epochs before and after filtration (Figure 3-16).

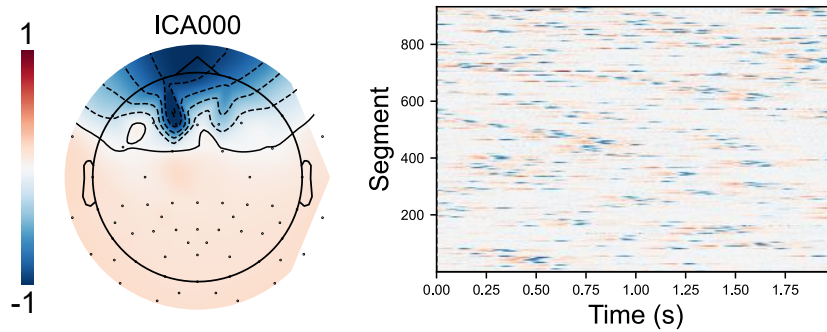


**Figure 3-15.** A topographic map (on the left) of the blink-related independent component for participant 15 and its amplitude in consecutive EEG segments (on the right). The amplitude is given in arbitrary units (source: [22]).

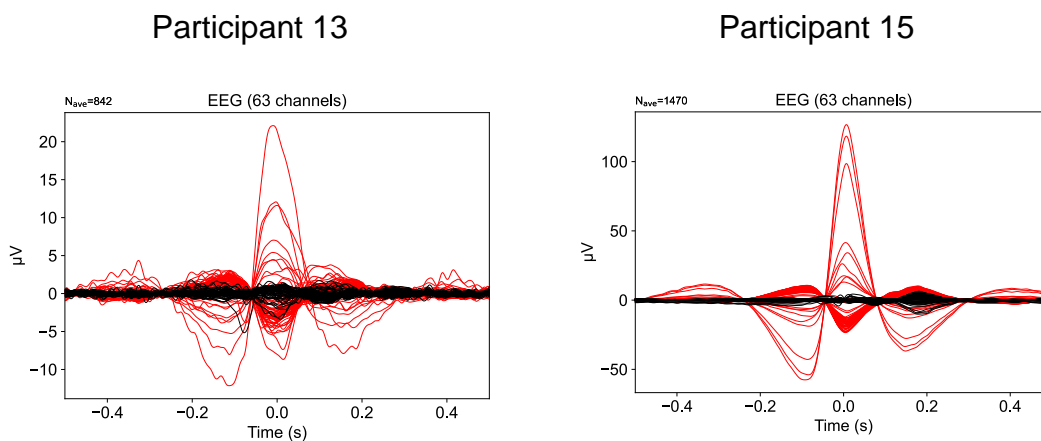


**Figure 3-16.** The averaged blink-evoked EEG signals before (red plot) and after (black plot) ocular artifacts filtration for selected participants. The  $N_{ave}$  is the number of detected blinks (source: [22]).

A topographic map and a time course of the blink-related component for participant 15 are presented in Figure 3-15. The absolute amplitude and polarity of the component activations are meaningless, so I used arbitrary units. There are many blinks visible in the EEG segments and the topography of the component matches the typical template for blink components [204]. In Figure 3-16, we can observe that strong blinks were successfully filtered from the EEG signal. The visualizations of all the other components identified and filtered by our

procedures for all participants are available in our OSF repository. The ocular artifacts were successfully removed for all of them. The described qualitative assessment process could be automated by using, e.g., a template-matching approach described by [204]. The proposed method is summarized in Figure 3-17 together with ERP extraction steps described in the next section.

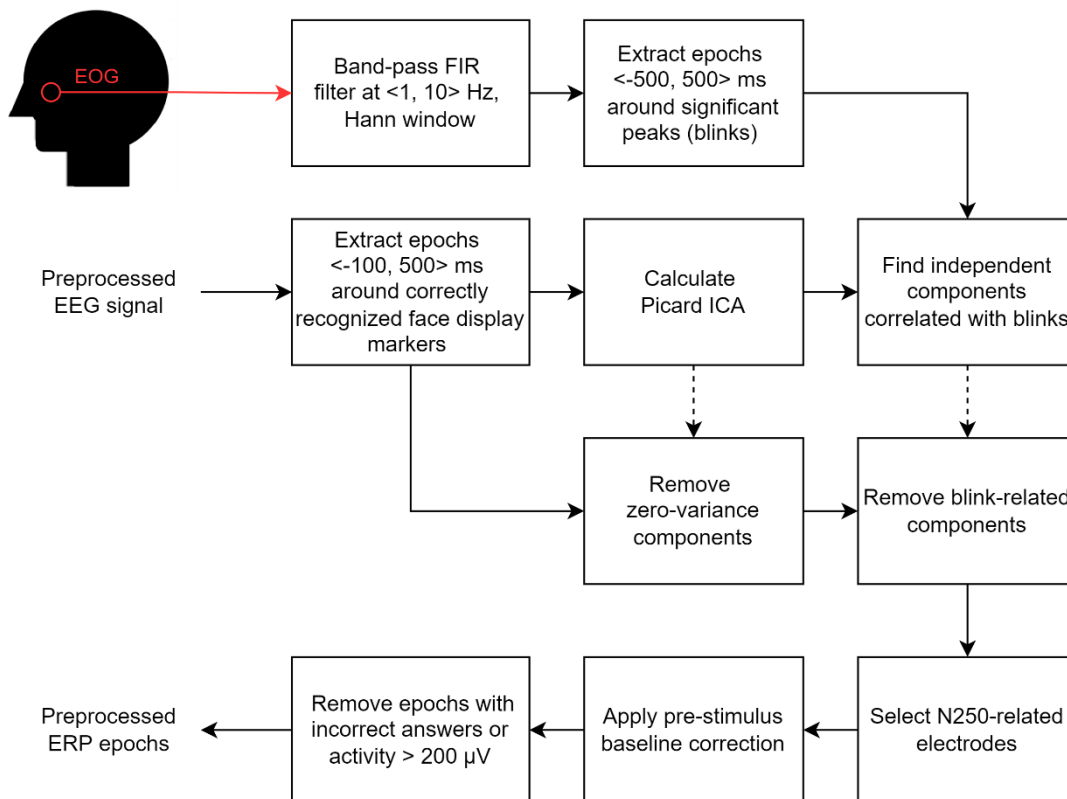


**Figure 3-17. The proposed method of ocular artifacts removal and ERP epochs extraction (source: [22]).**

### 3.3.3 Simulation study and comparison with other methods

The main goal of the simulation study was to assess the performance of our ocular artifact filtration procedure. I assessed the quality of filtering using RMSE between pure and filtered data (the closer to 0 the better) as given by Equation (3-5) where  $N$  is the number of samples times the number of electrodes in the signal sample.

$$RMSE = \sqrt{\frac{1}{N} \sum_{n=1}^N (filtered(n) - pure(n))^2} \quad (3-5)$$

Also, I measured the change of signal-to-noise ratio ( $\Delta SNR$ ) between contaminated and filtered data (the higher the better) as given by Equation (3-6) where  $\sigma_{pure}^2$  is the variance of pure EEG signal, and  $\sigma_{contam}^2$ ,  $\sigma_{filtered}^2$  are variances of the errors between contaminated and filtered signals and the pure EEG signal.

$$\Delta SNR = 10 \log_{10}\left(\frac{\sigma_{pure}^2}{\sigma_{filtered}^2}\right) - 10 \log_{10}\left(\frac{\sigma_{pure}^2}{\sigma_{contam}^2}\right) \quad (3-6)$$

The simulated data are already preprocessed, so the band-pass filtering was omitted. To make the data similar to our real-life dataset, each sample was divided into 600 ms non-overlapping fragments (so they have the same length as epochs in our real-life data). It results in 45 to 70 fragments per data sample. The proposed filtration algorithm was used to find and reject components correlated with either VEOG or HEOG.

In the first step, we assessed the impact of our ocular artifact filtration on the RMSE metric. The average results and p-values from the two-sided signed-rank Wilcoxon test are given in Table 3-3 and they show that filtration statistically significantly decreased RMSE nearly by half when taking the average over all channels. The effect is strongest for the frontal channels which are usually affected the most by the ocular artifacts. The effectiveness of the filtration can be observed in Figure 3-18 where RMSE for the electrode Fp1 for sample 12 before filtration is 27.74 and after filtration is 8.40 (more than 3 times lower). All extensive blink artifacts were removed. For channel Cz in the center of the head, the decrease of RMSE is much smaller but still statistically significant. For channel Pz in the back of the head, the RMSE is even slightly increased after filtration but the change is not statistically significant. It suggests that the ocular artifacts filtration has a smaller effect on electrodes farther from the eyes.

**Table 3-3. The average effect of ocular artifact filtering on the RMSE for different channels in the simulated data. The boldfaced font denotes smaller RMSE. The p-values from two-sided signed-rank Wilcoxon are underlined if  $p < 0.01$  (source: [22]).**

	Without filtration	With filtration	Wilcoxon
Channels	RMSE	RMSE	p-value
All	12.62	<b>6.73</b>	<u>1.14e-9</u>
Fp1	31.38	<b>14.39</b>	<u>2.21e-10</u>
Fp2	31.38	<b>14.46</b>	<u>3.09e-10</u>
Cz	5.64	<b>4.01</b>	<u>1.22e-5</u>
Pz	<b>3.21</b>	3.44	0.667

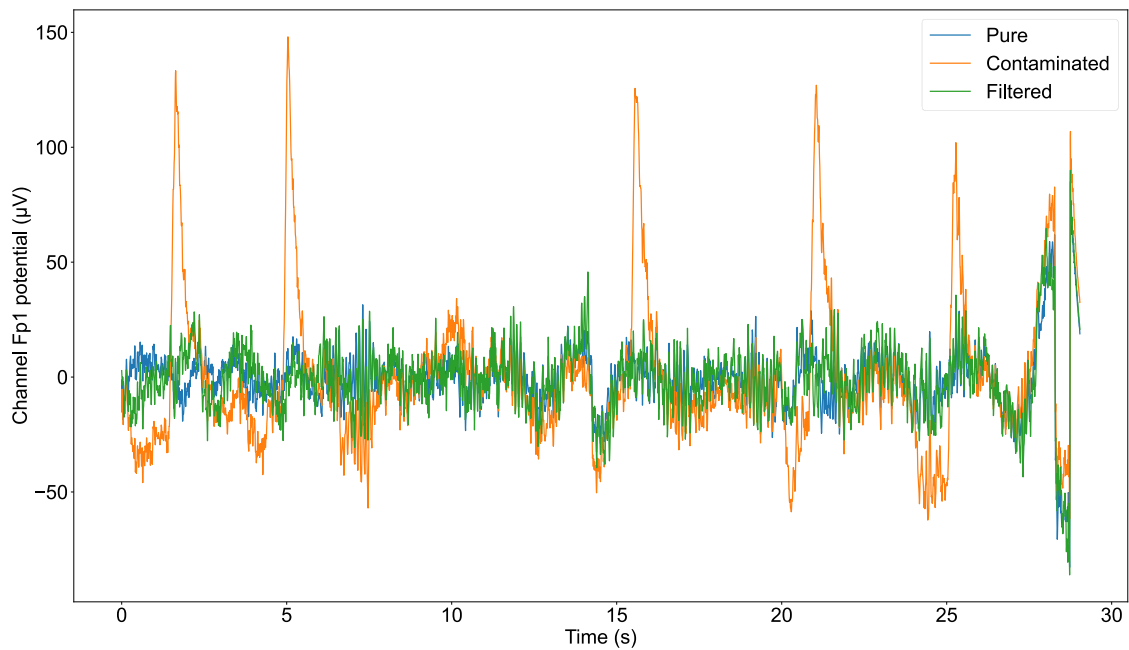


**Figure 3-18. The comparison of pure, contaminated, and filtered signals for electrode Fp1 for sample 12 with the smallest RMSE after filtration (source: [22]).**

In the second step, we compared our method with 4 different ICA-based algorithms for ocular artifacts filtration: ADJUST [198], MARA [201], SASICA [205], and the method from (Trigui et al.) [206]. The RMSE and  $\Delta$ SNR distributions for all the methods on the simulated dataset are presented in Figure 3-19 and Figure 3-20. Our method achieved the highest median  $\Delta$ SNR with median RMSE comparable to the best-performing methods MARA and [206]. We were unable to run statistical tests because the authors of [206] did not share the code or the detailed results for each sample. However, the boxplots confirm that our method has relatively high effectiveness in comparison to other methods.

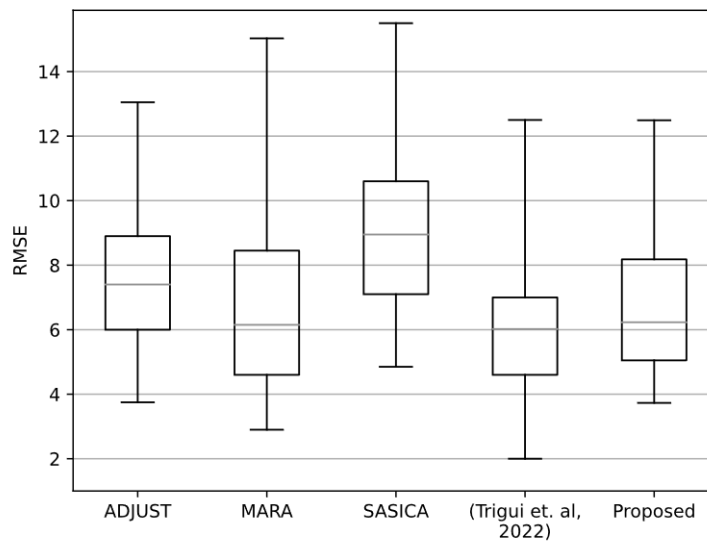


**Figure 3-19. Distributions of RMSE values across all samples in the simulated dataset (source: [22]).**

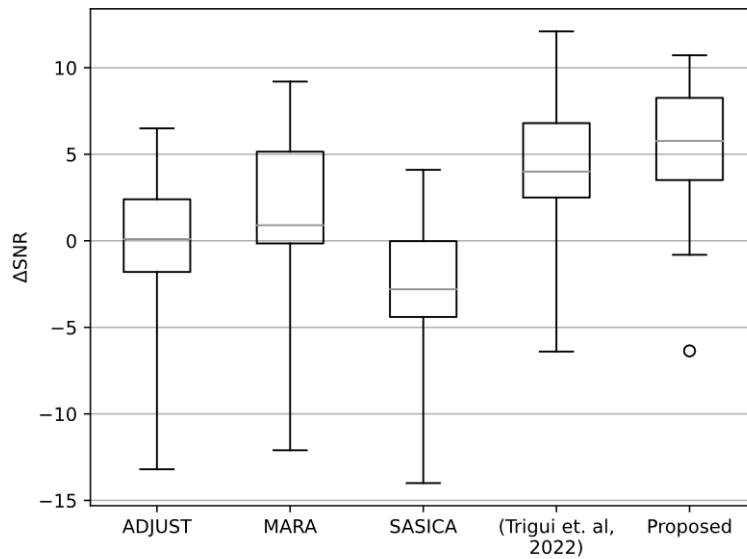


**Figure 3-20. Distributions of  $\Delta$ SNR values across all samples in the simulated dataset (source: [22]).**

### 3.3.4 ERP extraction and results on real-life data

After removing ocular artifacts, the ERP epochs were corrected with respect to the 100 ms pre-stimulus baseline. As in [144], the N250 amplitude for a single trial was defined as the mean signal value in the time range of 230 to 320 ms post-stimulus at the set of 12 relevant electrodes (left hemisphere: TP10, P8, P10, PO8, PO10, O2; right hemisphere: TP9, P7, P9, PO7, PO9, O1). Trials with an activity range greater than 200  $\mu$ V within any channel or with incorrect participant responses were discarded from further analyses (as described in Figure 3-17).

In the replication study [20], using the basic ERP extraction pipeline (limited sampling rate, less strict frequency filtering, ICA calculated on the whole signal, manual ocular artifact filtration), our team concluded that there is no statistically significant difference in N250 amplitudes for Joe between experiment halves, however, the significance is reached when using the division into the first 1/3 of the experiment (when the target face is not yet familiar) and the last 2/3 of the

experiment (the familiarity acquired). In this section, I revisit that analysis using the new preprocessing pipeline to verify the impact of the proposed ocular artifacts filtration on the results. Additionally, I improved two aspects of the analysis in accordance with Rule #8 from [90] which suggests avoiding different numbers of trials between conditions: 1) I used the division into the first and the second 1/3 (instead of the last 2/3) of the experiment, 2) I selected trials for only one Other face instead of all 10 of them. Also, I omit the quantitative analysis of ERP waveforms for the Own face as they were shown to present a non-specific appearance in the original study.

### Division into halves

In the first step, I checked if the significance of the difference in N250 amplitudes for Joe between experiment halves can be reached using the new pipeline. The grand-average ERPs for both halves and all types of faces using the new pipeline with ocular artifacts filtration are presented in Figure 3-21. The opaque regions around waveforms denote 95% confidence intervals of the averaging.

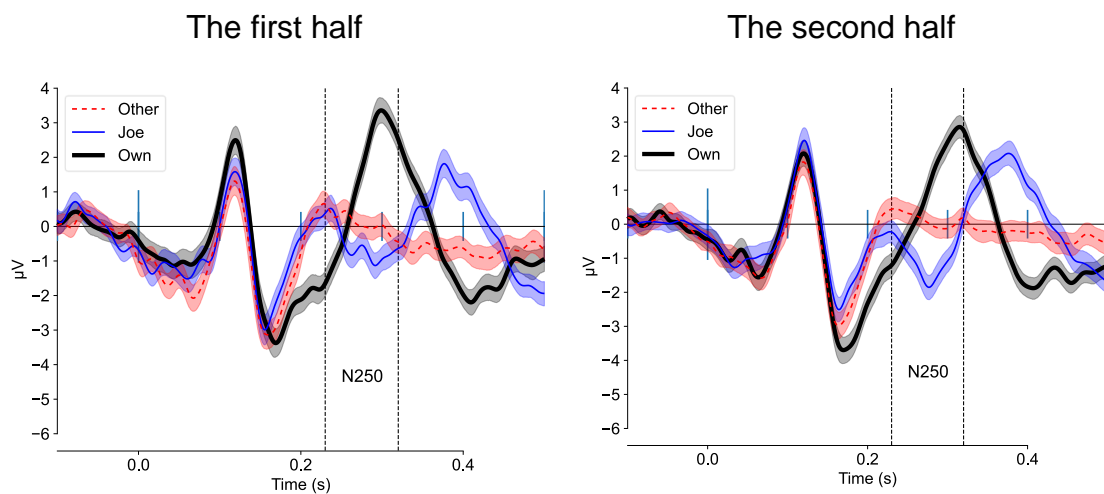


**Figure 3-21. Grand-average ERPs for the first (on the left) and the second half (on the right) of the experiment using the proposed filtering with ocular artifact filtration.**

Like in the original study, the analysis of variance (ANOVA) did not reveal any significant interaction between the face type and the experiment part ( $F(2,15) = 2.00$ ,  $MSE = 0.46$ ,  $p = 0.16$ ). However, the test statistic value was higher than for the original study ( $F(2,15) = 0.91$ ,  $MSE = 1.89$ ,  $p = 0.38$ ) and the N250-related peak is visible in the second half in Figure 3-21.

### The division into the first and the second 1/3

In the second step, I checked the significance of the alternative division into the first and the second 1/3 of the trials. The grand-average ERPs for this case are presented in Figure 3-22. The analysis of variance (ANOVA) revealed a significant interaction of the face type and the experiment part,  $F(2,15) = 7.10$ ,  $MSE = 1.64$ ,  $p = 0.003$ . The test statistic value was higher than for the original study ( $F(2,15) = 5.73$ ,  $MSE = 1.56$ ,  $p = 0.014$ ). Post-hoc pairwise Wilcoxon signed-rank tests revealed that N250 values for Joe were significantly more negative in the second 1/3 than in the first 1/3 of trials ( $M = -1.23$  vs.  $-0.15 \mu V$ ,  $p = 0.005$ ). The strip plots of linked observations in Figure 3-23 show the detailed interaction of condition and experiment part per individual participant. The effect of increased negativity of the N250 component for Joe is visible for 13 out of 16 participants.

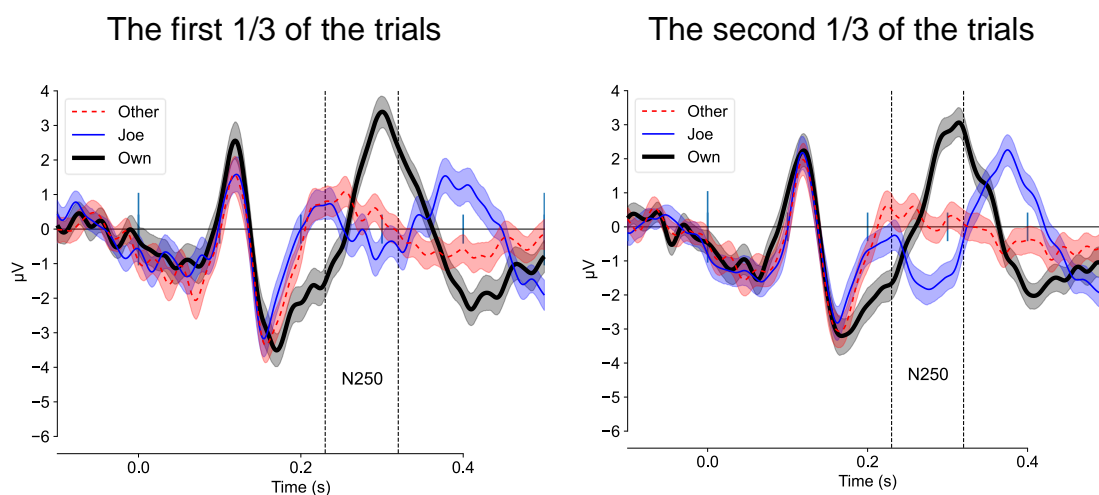


**Figure 3-22. Grand-average ERPs for the first 1/3 (on the left) and the second 1/3 (on the right) of trials using the proposed filtering with ocular artifact filtration.**

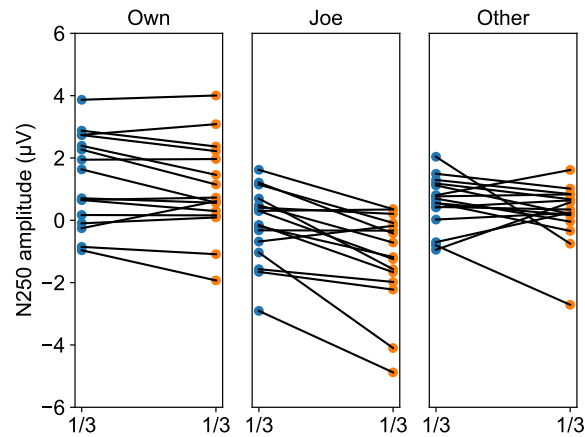


**Figure 3-23. Strip plots of linked N250 amplitudes between the first 1/3 and the second 1/3 of trials for different types of faces.**

### **The impact of ocular artifact filtration on single-trial analysis**

After confirming the face learning effect from the replication study, I analyzed the fine-grained dynamics of the face learning process using single-trial amplitudes. For each participant, a time series of up to 72 single-trial N250 amplitudes ( $67 \pm 9$ , min. 35, max. 72) was extracted for correctly recognized target faces. I applied the broken-line regression modeling using a popular *segmented* R package [207] to determine a hypothetical changepoint (*chp*) in the time series of N250 amplitudes, demarcating the transition point between memory trace acquisition (increasing N250 amplitudes) and maintenance (stable N250 amplitudes). The *segmented* package uses the residual sum of squares (RSS) to find the optimal changepoint location for the regression model, so I assessed the impact of ocular artifact filtration on this metric. Additionally, I measured if the filtration successfully decreased the standard deviation (SD) among the N250 amplitudes. The results are presented in Table 3-4.

**Table 3-4. Changepoint locations (*chp*) detected by the *segmented* method with corresponding RSS and SD of the N250 amplitude series without and with the proposed ocular artifact filtration (source: [22]).**

Participant #	Without filtration			With filtration		
	<i>chp</i>	RSS	SD	<i>chp</i>	RSS	SD
2	314	1.880	1.887	302	<b>1.717</b>	<b>1.744</b>
3	122	2.437	2.495	122	<b>2.072</b>	<b>2.110</b>
4	206	1.844	2.105	206	<b>1.540</b>	<b>1.704</b>
5	296	2.780	2.977	268	<b>1.959</b>	<b>2.197</b>
6	127	2.864	3.138	112	<b>2.252</b>	<b>2.535</b>
7	440	2.937	3.223	389	<b>2.411</b>	<b>2.675</b>
9	220	2.777	2.815	235	<b>2.018</b>	<b>2.047</b>
11	63	3.613	4.033	177	<b>1.866</b>	<b>1.922</b>
12	-	-	2.786	-	-	<b>1.503</b>
13	678	1.942	1.992	572	<b>1.775</b>	<b>1.817</b>
14	714	2.236	2.241	724	<b>1.995</b>	<b>2.016</b>
15	678	6.151	6.136	413	<b>2.285</b>	<b>2.352</b>
17	301	2.159	2.298	297	<b>1.724</b>	<b>1.835</b>
18	114	3.525	3.492	49	<b>2.680</b>	<b>2.706</b>
19	92	4.656	4.878	116	<b>2.067</b>	<b>2.594</b>
20	202	1.501	1.549	209	<b>1.442</b>	<b>1.513</b>

\*The boldfaced font denotes smaller RSS or SD. The dash means that no changepoint was found.

The mean absolute difference between changepoints before and after the filtration was  $48 \pm 68$  trials (median 15, IQR 58, min. 0, max. 265). This translates to  $6\% \pm 8\%$  (median 2%, IQR 7%, min. 0%, max. 31%) mean absolute change relative to the full experiment length (864 trials). The filtration changed locations of changepoints for 13 out of 15 participants, 8 changepoints were found earlier and 5 later (the difference in median changepoint location was not statistically significant according to the two-sided signed-rank Wilcoxon test,  $p = 0.26$ ). The filtration decreased the RSS of the broken-line regression model and SD of single-trial N250 amplitudes for all participants. RSS is lower by  $25\% \pm 17\%$  (min. 4%, max. 63%), and SD is lower by  $25\% \pm 17\%$  (min. 2%, max. 62%). The changes in RSS and SD are both statistically significant ( $p < 0.001$  according to the two-sided signed-rank Wilcoxon test) and highly correlated (Pearson's  $r = 0.99$ ). Thus, there was a significant positive impact of ocular filtration on the single-trial ERP analysis.

### **Significance for emotional face processing**

The results from the single-trial ERP analysis of the N250 component will be used by our team to study the relationship between the face representation acquisition process reflected in the N250 component and facial expression discrimination reflected in the EPN component. Disentangling the time courses of these two components would be a major step forward in understanding the differences in the structural encoding of faces and the detection of their emotional expression.

## 4 GENERAL DISCUSSION AND CONCLUSIONS

In my dissertation, I presented a series of methods for improving different aspects of the ERP extraction quality. My adaptation of Emotiv EPOC+ helped to limit the problem of time drift and jitter between epochs. Additional wavelet-based filtration helped to remove distorted and noisy epochs. The improved robust weighted averaging increased the signal-to-noise ratio of grand-average ERP waveforms by 45%. The proposed ocular artifact filtration based on ICA and EOG helped to remove blink-related components and to decrease the variance in single-trial ERP epochs by 25%. All methods were thoroughly tested, compared with others using simulated and/or real-life EEG data, and published in ISI-indexed journals. This fulfills the second (**G2**) and third goal (**G3**) of my work.

To fulfill the primary goal (**G1**) of my work, I proposed complete pipelines for EEG and ERP preprocessing including, e.g., initial filtering, re-referencing procedures, or epochs filtration. These pipelines are publicly available and can be used by neuroscientists and psychologists working on emotional face processing [22]. The higher the quality of ERP extraction the easier it is to observe and discover the effects of different stimuli on neural responses. The ERPs are commonly used in the recognition of event-evoked emotions from EEG. Thus, the quality of ERPs has a direct impact on the results from psychological experiments on emotional face processing. The presented methods helped to achieve better extraction of two overlapping and related ERP components: the emotion-sensitive EPN and the face-sensitive N250.

**To support my thesis**, I designed and conducted two separate ERP experiments to verify the effectiveness of the proposed methods and to support my thesis. In the first study, **I presented how EPN can be measured using a low-cost EEG system and robust weighted averaging to distinguish the neural responses evoked by angry and happy expressions from neutral faces. The results were consistent with the psychological study by Wronka & Walentowska [19] supporting the (1) part of the thesis.** In the second study, I replicated the results from the psychophysiological study of face learning by Tanaka et al. [144], and **using proper EEG processing and ocular artifacts filtration, I extended**

**it to detailed single-trial ERP analysis [22]. The results fulfill the fourth goal of my thesis (G4), support the (2) part of the thesis**, and will help to reduce the confounding effects of N250 when designing future psychological experiments about emotional face processing.

I targeted a specific problem of emotions evoked by facial expressions but there are other emotion recognition applications in which similar ERPs are frequently used, e.g., emotions evoked by affective images or sounds. However, the lack of consensus according to the universal psychological emotion model and the lack of standardized emotion-related datasets in the literature limit the current diversity and development of large-scale computational emotion recognition models. Fortunately, the proposed methods were designed for a wide range of ERP settings, not only emotion recognition. The methods were tested also on N70, P100, N135, N170, and P300 components [21], and are potentially useful for many other components. They can be used in countless applications using ERP features, e.g., brain-computer interfaces, medical diagnosis, and psychology research. They can be used to improve the quality of input to machine learning workflows as presented in my publications [25], [208]. In particular, the proposed methods are extremely useful in the fine-grained analysis of the neural processes of learning where the quality of every single consecutive epoch is crucial, i.e., I presented the importance of ocular artifact filtration on single-trial N250 analysis in Section 3.3 and publication [22].

The proposed methods have several limitations that should be addressed in future research. The adaptation of Emotiv EPOC+ makes it no longer wireless. However, it would be possible to design a wireless version of our stimuli marking circuit by using the emitter on the screen (like in a remote controller) and a small receiver mounted on the head. Also, there is an example in the literature where stimuli are time-stamped using a loud sound that appears in an EEG signal due to the user's response to it [167]. The improved robust weighted averaging has several assumptions that can prevent it from using in specific cases where components are not stable across time. It could be potentially improved by tracking the components of interest using ICA decomposition as described in

[209]. Our ocular artifacts filtration approach requires adjustment of the correlation threshold between ICA and EOG depending on the specific dataset. Such an approach could be laborious for larger datasets, so it could be improved by an automatic selection of the correlation threshold based on template matching [204] or a machine learning approach [199]. Our future work includes also the collection of a larger dataset and the development of a more robust changepoint detection procedure as an alternative to the *segmented* method [29]. Then, we plan to finalize our single-trial analysis and prepare an experiment to disentangle ERP components of face learning and emotional face processing.

The recent development of smaller, cheaper, and reliable methods of measuring brain activity (like Neuralink [33], Kernel Flow [37], Emotiv EPOC+ and its successors EPOC<sup>X</sup>, and EPOC<sup>Flex</sup>, etc.) prepares a foundation for easily-accessible, consumer-grade brain-computer interfaces. The methods proposed in this dissertation may be a building block of this foundation. One of the main future challenges is the large-scale EEG/ERP data collection, experimental design, and analysis in real-life scenarios, e.g., 24-hour monitoring of medical conditions, supporting the drivers and pilots, measuring emotions in everyday situations, or more generally, conducting cognitive psychological research out of the laboratory. Such new opportunities may engage new groups of researchers and users who will kick off the massive data collection.

However, in the first place, the recent reproducibility and replicability crisis must be addressed in neuroscience research [6] by preparing standardized guidelines for EEG/ERP research (like proposed by the ARTEM-IS initiative [7]), developing reliable large-scale datasets, and most importantly, by sharing the code of the solutions. Only then, the neuroscience field could benefit from artificial intelligence techniques at the level observed currently for computer vision [210] or protein structure prediction [5]. I described and applied some of these techniques in my “*Deep Learning in Electroencephalography*” chapter [25] and subsequently presented the effectiveness of U-Net convolutional architecture in image segmentation [211], [212], and protein secondary structure prediction [213], [214], but for the mentioned reasons I was unable to repeat the same in

EEG and emotion recognition domain. Addressing the issue of a lack of consensus in psychological emotion models is out of the scope of this dissertation, but may be approached in the computer science domain by mappings between emotional models as proposed in [24].

## 5 BIBLIOGRAPHY

- [1] F. A. C. Azevedo *et al.*, 'Equal numbers of neuronal and nonneuronal cells make the human brain an isometrically scaled-up primate brain', *Journal of Comparative Neurology*, vol. 513, no. 5, pp. 532–541, Feb. 2009, doi: 10.1002/cne.21974.
- [2] B. Goertzel, 'Artificial General Intelligence: Concept, State of the Art, and Future Prospects', *Journal of Artificial General Intelligence*, vol. 5, no. 1, pp. 1–48, Dec. 2014, doi: 10.2478/jagi-2014-0001.
- [3] R. W. Picard, *Affective Computing*. Cambridge, MA, USA: MIT Press, 1997.
- [4] D. Silver *et al.*, 'Mastering the game of Go with deep neural networks and tree search', *Nature*, vol. 529, no. 7587, pp. 484–489, Jan. 2016, doi: 10.1038/nature16961.
- [5] J. Jumper *et al.*, 'Highly accurate protein structure prediction with AlphaFold', *Nature*, vol. 596, no. 7873, pp. 583–589, Aug. 2021, doi: 10.1038/s41586-021-03819-2.
- [6] R. A. Poldrack *et al.*, 'Scanning the horizon: towards transparent and reproducible neuroimaging research', *Nat Rev Neurosci*, vol. 18, no. 2, pp. 115–126, Feb. 2017, doi: 10.1038/nrn.2016.167.
- [7] S. J. Styles, V. Ković, H. Ke, and A. Šoškić, 'Towards ARTEM-IS: Design guidelines for evidence-based EEG methodology reporting tools', *NeuroImage*, vol. 245, p. 118721, Dec. 2021, doi: 10.1016/j.neuroimage.2021.118721.
- [8] L. F. Barrett, *How Emotions Are Made: The Secret Life of the Brain*. Pan Macmillan, 2017.
- [9] A. Al-Nafjan, M. Hosny, Y. Al-Ohali, and A. Al-Wabil, 'Review and Classification of Emotion Recognition Based on EEG Brain-Computer Interface System Research: A Systematic Review', 2017.
- [10] M.-K. Kim, M. Kim, E. Oh, and S.-P. Kim, 'A Review on the Computational Methods for Emotional State Estimation from the Human EEG', *Computational and Mathematical Methods in Medicine*, vol. 2013, pp. 1–13, 2013, doi: 10.1155/2013/573734.
- [11] A. L. Gert, B. V. Ehinger, S. Timm, T. C. Kietzmann, and P. König, 'Wild lab: A naturalistic free viewing experiment reveals previously unknown EEG signatures of face processing'. bioRxiv, p. 2021.07.02.450779, Sep. 14, 2021. doi: 10.1101/2021.07.02.450779.
- [12] A. Alreja *et al.*, 'A new paradigm for investigating real-world social behavior and its neural underpinnings', *Behav Res*, Jul. 2022, doi: 10.3758/s13428-022-01882-9.

- [13] V. Soto *et al.*, 'Brain Responses to Emotional Faces in Natural Settings: A Wireless Mobile EEG Recording Study', *Frontiers in Psychology*, vol. 9, 2018, Accessed: Sep. 16, 2022. [Online]. Available: <https://www.frontiersin.org/articles/10.3389/fpsyg.2018.02003>
- [14] B. Rossion, C. A. Joyce, G. W. Cottrell, and M. J. Tarr, 'Early lateralization and orientation tuning for face, word, and object processing in the visual cortex', *NeuroImage*, vol. 20, no. 3, pp. 1609–1624, Nov. 2003, doi: 10.1016/j.neuroimage.2003.07.010.
- [15] K. Kotowski, K. Stapor, J. Leski, and M. Kotas, 'Validation of Emotiv EPOC+ for extracting ERP correlates of emotional face processing', *Biocybernetics and Biomedical Engineering*, vol. 38, no. 4, pp. 773–781, Jan. 2018, doi: 10.1016/j.bbe.2018.06.006.
- [16] M. G. Calvo and D. Beltrán, 'Brain lateralization of holistic versus analytic processing of emotional facial expressions', *Neuroimage*, vol. 92, pp. 237–247, May 2014, doi: 10.1016/j.neuroimage.2014.01.048.
- [17] M. Eimer and A. Holmes, 'Event-related brain potential correlates of emotional face processing', *Neuropsychologia*, vol. 45, no. 1, pp. 15–31, 2007, doi: 10.1016/j.neuropsychologia.2006.04.022.
- [18] M. G. Calvo and D. Beltrán, 'Recognition advantage of happy faces: tracing the neurocognitive processes', *Neuropsychologia*, vol. 51, no. 11, pp. 2051–2061, Sep. 2013, doi: 10.1016/j.neuropsychologia.2013.07.010.
- [19] E. Wronka and W. Walentowska, 'Attention modulates emotional expression processing', *Psychophysiology*, vol. 48, no. 8, pp. 1047–1056, 2011, doi: 10.1111/j.1469-8986.2011.01180.x.
- [20] W. Sommer *et al.*, 'The N250 event-related potential as an index of face familiarity: a replication study', *Royal Society Open Science*, vol. 8, no. 6, p. 202356, 2021, doi: 10.1098/rsos.202356.
- [21] K. Kotowski, K. Stapor, and J. Leski, 'Improved robust weighted averaging for event-related potentials in EEG', *Biocybernetics and Biomedical Engineering*, vol. 39, no. 4, pp. 1036–1046, Oct. 2019, doi: 10.1016/j.bbe.2019.09.002.
- [22] K. Kotowski, J. Ochab, K. Stapor, and W. Sommer, 'The importance of ocular artifact removal in single-trial ERP analysis: The case of the N250 in face learning', *Biomedical Signal Processing and Control*, vol. 79, p. 104115, Jan. 2023, doi: 10.1016/j.bspc.2022.104115.
- [23] K. Kotowski, K. Stapor, and W. Sommer, 'Quantitatively analyzing the time course of face learning: an ERP study', presented at the 21st Conference of the European Society for Cognitive Psychology, Tenerife, Sep. 2019. [Online]. Available: <http://escop2019.webs.ull.es/wp-content/uploads/2019/09/ESCoP2019-ABSTRACTS.pdf>

- [24] K. Kotowski and K. Stapor, 'Machine Learning and EEG for Emotional State Estimation', in *The Science of Emotional Intelligence*, IntechOpen, 2021. doi: 10.5772/intechopen.97133.
- [25] K. Kotowski, K. Stapor, and J. Ochab, 'Deep Learning Methods in Electroencephalography', in *Machine Learning Paradigms: Advances in Deep Learning-based Technological Applications*, G. A. Tsihrintzis and L. C. Jain, Eds. Cham: Springer International Publishing, 2020, pp. 191–212. doi: 10.1007/978-3-030-49724-8\_8.
- [26] V. J. Lawhern, A. J. Solon, N. R. Waytowich, S. M. Gordon, C. P. Hung, and B. J. Lance, 'EEGNet: a compact convolutional neural network for EEG-based brain–computer interfaces', *Journal of Neural Engineering*, vol. 15, no. 5, p. 056013, Oct. 2018, doi: 10.1088/1741-2552/aace8c.
- [27] B. A. Eriksen and C. W. Eriksen, 'Effects of noise letters upon the identification of a target letter in a nonsearch task', *Perception & Psychophysics*, vol. 16, no. 1, pp. 143–149, Jan. 1974, doi: 10.3758/BF03203267.
- [28] K. Kotowski, P. Fabian, and K. Stapor, 'Machine learning approach to automatic recognition of emotions based on bioelectrical brain activity', in *Simulations in Medicine. Computer-aided diagnostics and therapy*, DeGruyter, 2020, pp. 15–34.
- [29] W. Sommer *et al.*, 'Changepoint Detection in Noisy Data Using a Novel Residuals Permutation-Based Method (RESPERM): Benchmarking and Application to Single Trial ERPs', *Brain Sciences*, vol. 12, no. 5, Art. no. 5, May 2022, doi: 10.3390/brainsci12050525.
- [30] L. Konkel, 'The Brain before Birth: Using fMRI to Explore the Secrets of Fetal Neurodevelopment', *Environmental Health Perspectives*, vol. 126, no. 11, p. 112001, doi: 10.1289/EHP2268.
- [31] G. J. Siegel, *Basic neurochemistry: molecular, cellular and medical aspects*. 1999.
- [32] A. B. Ajiboye *et al.*, 'Restoration of reaching and grasping movements through brain-controlled muscle stimulation in a person with tetraplegia: a proof-of-concept demonstration', *The Lancet*, vol. 389, no. 10081, pp. 1821–1830, May 2017, doi: 10.1016/S0140-6736(17)30601-3.
- [33] E. Musk and Neuralink, 'An Integrated Brain-Machine Interface Platform With Thousands of Channels', *Journal of Medical Internet Research*, vol. 21, no. 10, p. e16194, Oct. 2019, doi: 10.2196/16194.
- [34] A. L. Cohen *et al.*, 'Defining Functional Areas in Individual Human Brains using Resting Functional Connectivity MRI', *Neuroimage*, vol. 41, no. 1, pp. 45–57, May 2008, doi: 10.1016/j.neuroimage.2008.01.066.

- [35] I. Sample and D. Adam, “‘The brain can’t lie’”, *The Guardian*, Nov. 20, 2003. Accessed: Jan. 11, 2022. [Online]. Available: <https://www.theguardian.com/science/2003/nov/20/neuroscience.science>
- [36] J. Malmivuo, ‘Comparison of the properties of EEG and MEG in detecting the electric activity of the brain’, *Brain Topogr*, vol. 25, no. 1, pp. 1–19, Jan. 2012, doi: 10.1007/s10548-011-0202-1.
- [37] H. Y. Ban *et al.*, ‘Kernel Flow: a high channel count scalable time-domain functional near-infrared spectroscopy system’, *JBO*, vol. 27, no. 7, p. 074710, Jan. 2022, doi: 10.1117/1.JBO.27.7.074710.
- [38] G. H. Glover, ‘Overview of Functional Magnetic Resonance Imaging’, *Neurosurg Clin N Am*, vol. 22, no. 2, pp. 133–139, Apr. 2011, doi: 10.1016/j.nec.2010.11.001.
- [39] T. Liu, M. Pelowski, C. Pang, Y. Zhou, and J. Cai, ‘Near-infrared spectroscopy as a tool for driving research’, *Ergonomics*, vol. 59, no. 3, pp. 368–379, Mar. 2016, doi: 10.1080/00140139.2015.1076057.
- [40] N. J. Hill *et al.*, ‘Recording human electrocorticographic (ECoG) signals for neuroscientific research and real-time functional cortical mapping’, *J Vis Exp*, no. 64, p. 3993, Jun. 2012, doi: 10.3791/3993.
- [41] M. Gaillard, “‘Invasive’ and ‘Non-invasive’ Technologies in Neuroscience Communication”, *BioéthiqueOnline*, vol. 6, 2017, doi: 10.7202/1044618ar.
- [42] ‘EEG Headset Prices – An Overview of 15+ EEG Devices’, *Imotions*, Jul. 17, 2019. <https://imotions.com/blog/eeg-headset-prices/> (accessed Jan. 11, 2022).
- [43] E. Boto *et al.*, ‘Moving magnetoencephalography towards real-world applications with a wearable system’, *Nature*, vol. 555, no. 7698, Art. no. 7698, Mar. 2018, doi: 10.1038/nature26147.
- [44] G. Buzsáki, C. A. Anastassiou, and C. Koch, ‘The origin of extracellular fields and currents — EEG, ECoG, LFP and spikes’, *Nat Rev Neurosci*, vol. 13, no. 6, pp. 407–420, Jun. 2012, doi: 10.1038/nrn3241.
- [45] J. A. Fodor, *The Modularity of Mind*. Cambridge, MA, USA: A Bradford Book, 1983.
- [46] R. Adolphs, ‘Human Lesion Studies in the 21st Century’, *Neuron*, vol. 90, no. 6, pp. 1151–1153, Jun. 2016, doi: 10.1016/j.neuron.2016.05.014.
- [47] M. F. Glasser *et al.*, ‘A multi-modal parcellation of human cerebral cortex’, *Nature*, vol. 536, no. 7615, Art. no. 7615, Aug. 2016, doi: 10.1038/nature18933.
- [48] J. Duncan and A. M. Owen, ‘Common regions of the human frontal lobe recruited by diverse cognitive demands’, *Trends in Neurosciences*, vol. 23, no. 10, pp. 475–483, Oct. 2000, doi: 10.1016/S0166-2236(00)01633-7.

- [49] W. R. Uttal, 'Précis of the new phrenology: The limits of localizing cognitive processes in the brain', *Brain & Mind*, vol. 3, no. 2, pp. 221–228, 2002, doi: 10.1023/A:1019972122144.
- [50] S. Zeki, *A vision of the brain*. Cambridge, MA, US: Blackwell Scientific Publications, 1993, pp. xi, 366.
- [51] K. A. Lindquist, T. D. Wager, H. Kober, E. Bliss-Moreau, and L. F. Barrett, 'The brain basis of emotion: A meta-analytic review', *Behav Brain Sci*, vol. 35, no. 3, pp. 121–143, Jun. 2012, doi: 10.1017/S0140525X11000446.
- [52] N. Palomero-Gallagher and K. Amunts, 'A short review on emotion processing: a lateralized network of neuronal networks', *Brain Struct Funct*, Jul. 2021, doi: 10.1007/s00429-021-02331-7.
- [53] P. Ekman, 'Basic Emotions', in *Handbook of Cognition and Emotion*, Wiley-Blackwell, 2005, pp. 45–60. doi: 10.1002/0470013494.ch3.
- [54] R. R. McCrae and P. T. Costa Jr., *Personality in adulthood: A five-factor theory perspective, 2nd ed.* New York, NY, US: Guilford Press, 2003, pp. xii, 268. doi: 10.4324/9780203428412.
- [55] H. C. Breiter *et al.*, 'Response and habituation of the human amygdala during visual processing of facial expression', *Neuron*, vol. 17, no. 5, pp. 875–887, Nov. 1996, doi: 10.1016/s0896-6273(00)80219-6.
- [56] A. Schumacher, F. R. Villaruel, A. Ussling, S. Riaz, A. C. H. Lee, and R. Ito, 'Ventral Hippocampal CA1 and CA3 Differentially Mediate Learned Approach-Avoidance Conflict Processing', *Curr Biol*, vol. 28, no. 8, pp. 1318-1324.e4, Apr. 2018, doi: 10.1016/j.cub.2018.03.012.
- [57] V. Santangelo *et al.*, 'Enhanced brain activity associated with memory access in highly superior autobiographical memory', *PNAS*, vol. 115, no. 30, pp. 7795–7800, Jul. 2018, doi: 10.1073/pnas.1802730115.
- [58] R. Singh, R. Sharma, V. S. Chauhan, and K. Chatterjee, 'Neurobiological underpinnings of emotions', *Ind Psychiatry J*, vol. 30, no. Suppl 1, pp. S308–S310, Oct. 2021, doi: 10.4103/0972-6748.328838.
- [59] J. C. Borod *et al.*, 'Right hemisphere emotional perception: evidence across multiple channels', *Neuropsychology*, vol. 12, no. 3, pp. 446–458, Jul. 1998, doi: 10.1037//0894-4105.12.3.446.
- [60] R. J. Davidson, 'Affect, cognition, and hemispheric specialization', in *Emotions, cognition, and behavior*, New York, NY, US: Cambridge University Press, 1985, pp. 320–365.
- [61] H. Berger, 'Über das Elektrenkephalogramm des Menschen', *Archiv für Psychiatrie und Nervenkrankheiten*, vol. 87, no. 1, pp. 527–570, Dec. 1929, doi: 10.1007/BF01797193.

- [62] W. A. Yost, 'The cocktail party problem: Forty years later', in *Binaural and spatial hearing in real and virtual environments*, Hillsdale, NJ, US: Lawrence Erlbaum Associates, Inc, 1997, pp. 329–347.
- [63] R. D. Pascual-Marqui, C. M. Michel, and D. Lehmann, 'Low resolution electromagnetic tomography: a new method for localizing electrical activity in the brain', *International Journal of Psychophysiology*, vol. 18, no. 1, pp. 49–65, Oct. 1994, doi: 10.1016/0167-8760(84)90014-X.
- [64] J. N. Acharya, A. Hani, J. Cheek, P. Thirumala, and T. N. Tsuchida, 'American Clinical Neurophysiology Society Guideline 2: Guidelines for Standard Electrode Position Nomenclature', *Journal of Clinical Neurophysiology*, vol. 33, no. 4, 2016, [Online]. Available: [https://journals.lww.com/clinicalneurophys/Fulltext/2016/08000/American\\_Clinical\\_Neurophysiology\\_Society.4.aspx](https://journals.lww.com/clinicalneurophys/Fulltext/2016/08000/American_Clinical_Neurophysiology_Society.4.aspx)
- [65] D. M. Tucker, 'Spatial sampling of head electrical fields: the geodesic sensor net', *Electroencephalogr Clin Neurophysiol*, vol. 87, no. 3, pp. 154–163, Sep. 1993, doi: 10.1016/0013-4694(93)90121-b.
- [66] P. A. Abhang, B. W. Gawali, and S. C. Mehrotra, 'Chapter 2 - Technological Basics of EEG Recording and Operation of Apparatus', in *Introduction to EEG- and Speech-Based Emotion Recognition*, P. A. Abhang, B. W. Gawali, and S. C. Mehrotra, Eds. Academic Press, 2016, pp. 19–50. doi: 10.1016/B978-0-12-804490-2.00002-6.
- [67] J. Moini and P. Piran, 'Chapter 6 - Cerebral cortex', in *Functional and Clinical Neuroanatomy*, J. Moini and P. Piran, Eds. Academic Press, 2020, pp. 177–240. doi: 10.1016/B978-0-12-817424-1.00006-9.
- [68] D. Vorontsova *et al.*, 'Silent EEG-Speech Recognition Using Convolutional and Recurrent Neural Network with 85% Accuracy of 9 Words Classification', *Sensors*, vol. 21, no. 20, Art. no. 20, Jan. 2021, doi: 10.3390/s21206744.
- [69] C. E. Yew and D. T. M. Yung, 'Electroencephalography Robotic Arm Control', in *2018 IEEE 4th International Symposium in Robotics and Manufacturing Automation (ROMA)*, Dec. 2018, pp. 1–5. doi: 10.1109/ROMA46407.2018.8986734.
- [70] Z. T. Al-qaysi, B. B. Zaidan, A. A. Zaidan, and M. S. Suzani, 'A review of disability EEG based wheelchair control system: Coherent taxonomy, open challenges and recommendations', *Computer Methods and Programs in Biomedicine*, vol. 164, pp. 221–237, Oct. 2018, doi: 10.1016/j.cmpb.2018.06.012.
- [71] F. A. Rosli, S. Ardeena, A. A. Abdullah, and M. S. Salim, 'Biometric authentication system using EEG biometric trait – A review', *AIP Conference Proceedings*, vol. 2339, no. 1, p. 020135, May 2021, doi: 10.1063/5.0044955.

- [72] Z. Ren *et al.*, 'EEG-Based Driving Fatigue Detection Using a Two-Level Learning Hierarchy Radial Basis Function', *Frontiers in Neurorobotics*, vol. 15, 2021, Accessed: Jan. 13, 2022. [Online]. Available: <https://www.frontiersin.org/article/10.3389/fnbot.2021.618408>
- [73] P. Pradhapan, U. Großekathöfer, G. Schiavone, B. Grundlehner, and V. Mihajlović, 'Toward Practical BCI Solutions for Entertainment and Art Performance', in *Brain–Computer Interfaces Handbook*, CRC Press, 2018.
- [74] A. Kubik, P. Kubik, M. Stanios, and B. Kraj, '[Clinical and neurophysiological data of neurofeedback therapy in children with ADHD]', *Przegl Lek*, vol. 73, no. 3, pp. 148–151, 2016.
- [75] H. Wiese, D. Anderson, U. Beierholm, S. C. Tüttenberg, A. W. Young, and A. M. Burton, 'Detecting a viewer's familiarity with a face: Evidence from event-related brain potentials and classifier analyses', *Psychophysiology*, vol. 59, no. 1, p. e13950, 2022, doi: 10.1111/psyp.13950.
- [76] V. Shah *et al.*, 'The Temple University Hospital Seizure Detection Corpus', *Frontiers in Neuroinformatics*, vol. 12, Nov. 2018, doi: 10.3389/fninf.2018.00083.
- [77] A. Babayan *et al.*, 'A mind-brain-body dataset of MRI, EEG, cognition, emotion, and peripheral physiology in young and old adults', *Scientific Data*, vol. 6, p. 180308, Feb. 2019.
- [78] Z. Cao, C.-H. Chuang, J.-K. King, and C.-T. Lin, 'Multi-channel EEG recordings during a sustained-attention driving task', *Scientific Data*, vol. 6, no. 1, p. 19, Apr. 2019, doi: 10.1038/s41597-019-0027-4.
- [79] M. S. Nieuwland *et al.*, 'Large-scale replication study reveals a limit on probabilistic prediction in language comprehension', *eLife*, vol. 7, p. e33468, Apr. 2018, doi: 10.7554/eLife.33468.
- [80] M. Kaya, M. K. Binli, E. Ozbay, H. Yanar, and Y. Mishchenko, 'A large electroencephalographic motor imagery dataset for electroencephalographic brain computer interfaces', *Scientific Data*, vol. 5, p. 180211, Oct. 2018.
- [81] D. Vivancos, 'IMAGENET of The Brain', 2018. <http://www.mindbigdata.com/opendb/imagenet.html> (accessed Jul. 08, 2019).
- [82] H. Cho, M. Ahn, S. Ahn, M. Kwon, and S. C. Jun, 'EEG datasets for motor imagery brain–computer interface', *GigaScience*, vol. 6, no. 7, p. gix034, 2017.
- [83] D. Vivancos, 'The MNIST of Brain Digits', 2015. <http://mindbigdata.com/opendb/index.html> (accessed Jul. 08, 2019).
- [84] C. O'Reilly, N. Gosselin, J. Carrier, and T. Nielsen, 'Montreal Archive of Sleep Studies: an open-access resource for instrument benchmarking and

- exploratory research', *Journal of Sleep Research*, vol. 23, no. 6, pp. 628–635, Dec. 2014, doi: 10.1111/jsr.12169.
- [85] M. D. Luciw, E. Jarocka, and B. B. Edin, 'Multi-channel EEG recordings during 3,936 grasp and lift trials with varying weight and friction', *Scientific Data*, vol. 1, p. 140047, Nov. 2014.
- [86] A. H. Shoeb, 'Application of machine learning to epileptic seizure onset detection and treatment', Thesis, Massachusetts Institute of Technology, 2009. Accessed: Jul. 13, 2019. [Online]. Available: <https://dspace.mit.edu/handle/1721.1/54669>
- [87] G. Schalk, D. J. McFarland, T. Hinterberger, N. Birbaumer, and J. R. Wolpaw, 'BCI2000: a general-purpose brain-computer interface (BCI) system', *IEEE Transactions on Biomedical Engineering*, vol. 51, no. 6, pp. 1034–1043, Jun. 2004, doi: 10.1109/TBME.2004.827072.
- [88] M. G. Terzano *et al.*, 'Atlas, rules, and recording techniques for the scoring of cyclic alternating pattern (CAP) in human sleep', *Sleep Medicine*, vol. 2, no. 6, pp. 537–553, Nov. 2001, doi: 10.1016/S1389-9457(01)00149-6.
- [89] B. Blankertz, S. Lemm, M. Treder, S. Haufe, and K.-R. Müller, 'Single-trial analysis and classification of ERP components — A tutorial', *NeuroImage*, vol. 56, no. 2, pp. 814–825, May 2011, doi: 10.1016/j.neuroimage.2010.06.048.
- [90] S. J. Luck, 'Ten Simple Rules for Designing and Interpreting ERP Experiments', in *Event-related Potentials: A Methods Handbook*, The MIT Press, 2004, pp. 17–32.
- [91] T. Donoghue and B. Voytek, 'Automated meta-analysis of the event-related potential (ERP) literature', *Sci Rep*, vol. 12, no. 1, Art. no. 1, Feb. 2022, doi: 10.1038/s41598-022-05939-9.
- [92] W. A. Cobb and G. D. Dawson, 'The latency and form in man of the occipital potentials evoked by bright flashes', *J Physiol*, vol. 152, no. 1, pp. 108–121, Jun. 1960.
- [93] H. Pratt, 'Sensory ERP Components', *The Oxford Handbook of Event-Related Potential Components*, Dec. 15, 2011. <https://www.oxfordhandbooks.com/view/10.1093/oxfordhb/9780195374148.001.0001/oxfordhb-9780195374148-e-004> (accessed Jan. 14, 2022).
- [94] P. Ekman, 'What Scientists Who Study Emotion Agree About', *Perspect Psychol Sci*, vol. 11, no. 1, pp. 31–34, Jan. 2016, doi: 10.1177/1745691615596992.
- [95] J. D. Mayer, R. D. Roberts, and S. G. Barsade, 'Human Abilities: Emotional Intelligence', *Annu. Rev. Psychol.*, vol. 59, no. 1, pp. 507–536, Dec. 2007, doi: 10.1146/annurev.psych.59.103006.093646.

- [96] C. Darwin, *The expression of the emotions in man and animals*. London, England: John Murray, 1872, pp. vi, 374. doi: 10.1037/10001-000.
- [97] M. Gendron, D. Roberson, J. M. van der Vyver, and L. F. Barrett, 'Perceptions of Emotion from Facial Expressions are Not Culturally Universal: Evidence from a Remote Culture', *Emotion*, vol. 14, no. 2, pp. 251–262, Apr. 2014, doi: 10.1037/a0036052.
- [98] J. A. Russell, 'Core affect and the psychological construction of emotion.', *Psychological Review*, vol. 110, no. 1, pp. 145–172, 2003, doi: 10.1037/0033-295X.110.1.145.
- [99] R. E. Jack, O. G. B. Garrod, H. Yu, R. Caldara, and P. G. Schyns, 'Facial expressions of emotion are not culturally universal', *Proc Natl Acad Sci U S A*, vol. 109, no. 19, pp. 7241–7244, May 2012, doi: 10.1073/pnas.1200155109.
- [100] P. Ekman and W. V. Friesen, 'Constants across cultures in the face and emotion.', *Journal of Personality and Social Psychology*, vol. 17, no. 2, pp. 124–129, 1971, doi: 10.1037/h0030377.
- [101] R. Plutchik, 'The Nature of Emotions: Human emotions have deep evolutionary roots, a fact that may explain their complexity and provide tools for clinical practice', *American Scientist*, vol. 89, no. 4, pp. 344–350, 2001.
- [102] A. S. Cowen and D. Keltner, 'Self-report captures 27 distinct categories of emotion bridged by continuous gradients', *Proceedings of the National Academy of Sciences*, vol. 114, no. 38, pp. E7900–E7909, Sep. 2017, doi: 10.1073/pnas.1702247114.
- [103] A. Mehrabian and J. A. Russell, *An approach to environmental psychology*. Cambridge, MA, US: The MIT Press, 1974.
- [104] J. A. Russell and A. Mehrabian, 'Evidence for a three-factor theory of emotions', *Journal of Research in Personality*, vol. 11, no. 3, pp. 273–294, Sep. 1977, doi: 10.1016/0092-6566(77)90037-X.
- [105] R. Trnka, A. Lačev, K. Balcar, M. Kuška, and P. Tavel, 'Modeling Semantic Emotion Space Using a 3D Hypercube-Projection: An Innovative Analytical Approach for the Psychology of Emotions', *Front. Psychol.*, vol. 7, Apr. 2016, doi: 10.3389/fpsyg.2016.00522.
- [106] A. Marchewka, Ł. Żurawski, K. Jednoróg, and A. Grabowska, 'The Nencki Affective Picture System (NAPS): Introduction to a novel, standardized, wide-range, high-quality, realistic picture database', *Behavior Research Methods*, vol. 46, no. 2, pp. 596–610, Jun. 2014, doi: 10.3758/s13428-013-0379-1.
- [107] J. A. Russell, M. Lewicka, and T. Niit, 'A cross-cultural study of a circumplex model of affect.', *Journal of Personality and Social Psychology*, vol. 57, no. 5, pp. 848–856, 1989, doi: 10.1037/0022-3514.57.5.848.

- [108] J. J. R. Fontaine and K. R. Scherer, 'The global meaning structure of the emotion domain: Investigating the complementarity of multiple perspectives on meaning', in *Components of emotional meaning: A sourcebook*, New York, NY, US: Oxford University Press, 2013, pp. 106–125. doi: 10.1093/acprof:oso/9780199592746.003.0008.
- [109] J. R. J. Fontaine, K. R. Scherer, E. B. Roesch, and P. C. Ellsworth, 'The World of Emotions is not Two-Dimensional', *Psychological Science*, vol. 18, no. 12, pp. 1050–1057, Dec. 2007, doi: 10.1111/j.1467-9280.2007.02024.x.
- [110] L. Y. Mano *et al.*, 'An intelligent and generic approach for detecting human emotions: a case study with facial expressions', *Soft Comput*, vol. 24, no. 11, pp. 8467–8479, Jun. 2020, doi: 10.1007/s00500-019-04411-7.
- [111] E. Harmon-Jones, C. Harmon-Jones, and E. Summerell, 'On the Importance of Both Dimensional and Discrete Models of Emotion', *Behavioral Sciences*, vol. 7, no. 4, p. 66, Sep. 2017, doi: 10.3390/bs7040066.
- [112] N. Moyal, A. Henik, and G. E. Anholt, 'Categorized Affective Pictures Database (CAP-D)', *Journal of Cognition*, vol. 1, no. 1, p. 41, Sep. 2018, doi: 10.5334/joc.47.
- [113] P. J. Lang, 'Behavioral treatment and bio-behavioral assessment: Computer applications', in *Technology in mental health care delivery systems*, J. B. Sidowski, J. H. Johnson, and T. A. Williams, Eds. Norwood, NJ: Ablex, 1980, pp. 119–137.
- [114] M. M. Bradley and P. J. Lang, 'The International Affective Picture System (IAPS) in the study of emotion and attention.', in *Handbook of emotion elicitation and assessment.*, New York, NY, US: Oxford University Press, 2007, pp. 29–46.
- [115] B. Kurdi, S. Lozano, and M. R. Banaji, 'Introducing the Open Affective Standardized Image Set (OASIS)', *Behav Res*, vol. 49, no. 2, pp. 457–470, Apr. 2017, doi: 10.3758/s13428-016-0715-3.
- [116] J. M. Michałowski, D. Drożdziel, J. Matuszewski, W. Koziejowski, K. Jednoróg, and A. Marchewka, 'The Set of Fear Inducing Pictures (SFIP): Development and validation in fearful and nonfearful individuals', *Behav Res*, vol. 49, no. 4, pp. 1407–1419, Aug. 2017, doi: 10.3758/s13428-016-0797-y.
- [117] M. Riegel *et al.*, 'Characterization of the Nencki Affective Picture System by discrete emotional categories (NAPS BE)', *Behavior Research Methods*, vol. 48, no. 2, pp. 600–612, Jun. 2016, doi: 10.3758/s13428-015-0620-1.
- [118] E. S. Dan-Glauser and K. R. Scherer, 'The Geneva affective picture database (GAPED): a new 730-picture database focusing on valence and normative significance', *Behavior Research Methods*, vol. 43, no. 2, pp. 468–477, Jun. 2011, doi: 10.3758/s13428-011-0064-1.

- [119] S. Koelstra *et al.*, 'DEAP: A Database for Emotion Analysis; Using Physiological Signals', *IEEE Transactions on Affective Computing*, vol. 3, no. 1, pp. 18–31, Jan. 2012, doi: 10.1109/T-AFFC.2011.15.
- [120] A. Raheel, M. Majid, and S. M. Anwar, 'DEAR-MULSEMEDIA: Dataset for emotion analysis and recognition in response to multiple sensorial media', *Information Fusion*, vol. 65, pp. 37–49, 2021, doi: 10.1016/j.inffus.2020.08.007.
- [121] W. Zheng, W. Liu, Y. Lu, B. Lu, and A. Cichocki, 'EmotionMeter: A Multimodal Framework for Recognizing Human Emotions', *IEEE Transactions on Cybernetics*, pp. 1–13, 2018, doi: 10.1109/TCYB.2018.2797176.
- [122] S. Katsigiannis and N. Ramzan, 'DREAMER: A Database for Emotion Recognition Through EEG and ECG Signals From Wireless Low-cost Off-the-Shelf Devices', *IEEE Journal of Biomedical and Health Informatics*, vol. 22, no. 1, pp. 98–107, Jan. 2018, doi: 10.1109/JBHI.2017.2688239.
- [123] R. Subramanian, J. Wache, M. K. Abadi, R. L. Vieriu, S. Winkler, and N. Sebe, 'ASCERTAIN: Emotion and Personality Recognition Using Commercial Sensors', *IEEE Transactions on Affective Computing*, vol. 9, no. 2, pp. 147–160, Apr. 2018, doi: 10.1109/T-AFFC.2016.2625250.
- [124] S. Wang, Y. Zhu, G. Wu, and Q. Ji, 'Hybrid video emotional tagging using users' EEG and video content', *Multimedia Tools and Applications*, vol. 72, no. 2, pp. 1257–1283, Sep. 2014, doi: 10.1007/s11042-013-1450-8.
- [125] M. Soleymani, J. Lichtenauer, T. Pun, and M. Pantic, 'A Multimodal Database for Affect Recognition and Implicit Tagging', *IEEE Transactions on Affective Computing*, vol. 3, no. 1, pp. 42–55, Mar. 2012, doi: 10.1109/T-AFFC.2011.25.
- [126] A. Savran *et al.*, 'Emotion Detection in the Loop from Brain Signals and Facial Images', in *Proceedings of the eNTERFACE 2006 Workshop*, 2006. [Online]. Available: <https://archive-ouverte.unige.ch/unige:47926>
- [127] P. Ekman, 'An argument for basic emotions', *Cognition & emotion*, vol. 6, no. 3–4, pp. 169–200, 1992.
- [128] K. A. Lindquist and L. F. Barrett, 'A functional architecture of the human brain: emerging insights from the science of emotion', *Trends in Cognitive Sciences*, vol. 16, no. 11, pp. 533–540, Nov. 2012, doi: 10.1016/j.tics.2012.09.005.
- [129] M. Wyczesany and T. S. Ligeza, 'Towards a constructionist approach to emotions: verification of the three-dimensional model of affect with EEG-independent component analysis', *Experimental Brain Research*, vol. 233, no. 3, pp. 723–733, Mar. 2015, doi: 10.1007/s00221-014-4149-9.

- [130] B. Rozenkrants and J. Polich, 'Affective ERP processing in a visual oddball task: Arousal, valence, and gender', *Clinical Neurophysiology*, vol. 119, no. 10, pp. 2260–2265, Oct. 2008, doi: 10.1016/j.clinph.2008.07.213.
- [131] C. Lithari *et al.*, 'Are Females More Responsive to Emotional Stimuli? A Neurophysiological Study Across Arousal and Valence Dimensions', *Brain Topogr*, vol. 23, no. 1, pp. 27–40, Mar. 2010, doi: 10.1007/s10548-009-0130-5.
- [132] M. Balconi and C. Lucchiari, 'EEG correlates (event-related desynchronization) of emotional face elaboration: A temporal analysis', *Neuroscience Letters*, vol. 392, no. 1, pp. 118–123, Jan. 2006, doi: 10.1016/j.neulet.2005.09.004.
- [133] X. Hu *et al.*, 'EEG Correlates of Ten Positive Emotions', *Frontiers in Human Neuroscience*, vol. 11, 2017, Accessed: Sep. 12, 2022. [Online]. Available: <https://www.frontiersin.org/articles/10.3389/fnhum.2017.00026>
- [134] M. Balconi and G. Mazza, 'Brain oscillations and BIS/BAS (behavioral inhibition/activation system) effects on processing masked emotional cues.: ERS/ERD and coherence measures of alpha band', *International Journal of Psychophysiology*, vol. 74, no. 2, pp. 158–165, Nov. 2009, doi: 10.1016/j.ijpsycho.2009.08.006.
- [135] M. M. Müller, A. Keil, T. Gruber, and T. Elbert, 'Processing of affective pictures modulates right-hemispheric gamma band EEG activity', *Clinical Neurophysiology*, vol. 110, no. 11, pp. 1913–1920, Nov. 1999, doi: 10.1016/S1388-2457(99)00151-0.
- [136] M. Wyczesany, S. Grzybowski, R. Barry, J. Kaiser, A. M. Coenen, and A. Potoczek, 'Covariation of EEG Synchronization and Emotional State as Modified by Anxiolytics', *Journal of Clinical Neurophysiology*, vol. 28, no. 3, pp. 289–296, Jun. 2011, doi: 10.1097/WNP.0b013e31821c34f7.
- [137] V. Miskovic and L. A. Schmidt, 'Cross-regional cortical synchronization during affective image viewing', *Brain Research*, vol. 1362, pp. 102–111, Nov. 2010, doi: 10.1016/j.brainres.2010.09.102.
- [138] Y. Otsuka, 'Face recognition in infants: A review of behavioral and near-infrared spectroscopic studies', *Japanese Psychological Research*, vol. 56, no. 1, pp. 76–90, 2014, doi: 10.1111/jpr.12024.
- [139] W. Luo, W. Feng, W. He, N.-Y. Wang, and Y.-J. Luo, 'Three stages of facial expression processing: ERP study with rapid serial visual presentation', *NeuroImage*, vol. 49, no. 2, pp. 1857–1867, Jan. 2010, doi: 10.1016/j.neuroimage.2009.09.018.
- [140] E. I. Olivares, J. Iglesias, C. Saavedra, N. J. Trujillo-Barreto, and M. Valdés-Sosa, 'Brain Signals of Face Processing as Revealed by Event-Related Potentials', *Behavioural Neurology*, vol. 2015, pp. 1–16, 2015, doi: 10.1155/2015/514361.

- [141] A. S. Ghuman *et al.*, 'Dynamic encoding of face information in the human fusiform gyrus', *Nat Commun*, vol. 5, no. 1, p. 5672, Dec. 2014, doi: 10.1038/ncomms6672.
- [142] J. A. Hinojosa, F. Mercado, and L. Carretié, 'N170 sensitivity to facial expression: A meta-analysis', *Neurosci Biobehav Rev*, vol. 55, pp. 498–509, Aug. 2015, doi: 10.1016/j.neubiorev.2015.06.002.
- [143] L. M. Williams, D. Palmer, B. J. Liddell, L. Song, and E. Gordon, 'The "when" and "where" of perceiving signals of threat versus non-threat', *NeuroImage*, vol. 31, no. 1, pp. 458–467, May 2006, doi: 10.1016/j.neuroimage.2005.12.009.
- [144] J. W. Tanaka, T. Curran, A. L. Porterfield, and D. Collins, 'Activation of Preexisting and Acquired Face Representations: The N250 Event-related Potential as an Index of Face Familiarity', *Journal of Cognitive Neuroscience*, vol. 18, no. 9, pp. 1488–1497, Sep. 2006, doi: 10.1162/jocn.2006.18.9.1488.
- [145] D. J. L. G. Schutter, E. H. F. de Haan, and J. van Honk, 'Functionally dissociated aspects in anterior and posterior electrocortical processing of facial threat', *International Journal of Psychophysiology*, vol. 53, no. 1, pp. 29–36, Jun. 2004, doi: 10.1016/j.ijpsycho.2004.01.003.
- [146] G. Hajcak, A. MacNamara, and D. M. Olvet, 'Event-Related Potentials, Emotion, and Emotion Regulation: An Integrative Review', *Developmental Neuropsychology*, vol. 35, no. 2, pp. 129–155, Feb. 2010, doi: 10.1080/87565640903526504.
- [147] L. Sun, J. Ren, and W. He, 'Neural correlates of facial expression processing during a detection task: An ERP study', *PLOS ONE*, vol. 12, no. 3, p. e0174016, Mar. 2017, doi: 10.1371/journal.pone.0174016.
- [148] G. Rhodes, A. Calder, M. Johnson, J. V. Haxby, and M. Eimer, 'The Face-Sensitive N170 Component of the Event-Related Brain Potential', in *Oxford Handbook of Face Perception*, Oxford University Press, 2012. [Online]. Available: <http://www.oxfordhandbooks.com/view/10.1093/oxfordhb/9780199559053.001.0001/oxfordhb-9780199559053-e-017>
- [149] N. Mestry, T. Menneer, M. J. Wenger, N. Benikos, R. A. McCarthy, and N. Donnelly, 'The Role of Configurality in the Thatcher Illusion: An ERP Study', *Psychon Bull Rev*, vol. 22, no. 2, pp. 445–452, Apr. 2015, doi: 10.3758/s13423-014-0705-3.
- [150] R. H. Ofan, N. Rubin, and D. M. Amodio, 'Seeing race: N170 responses to race and their relation to automatic racial attitudes and controlled processing', *J Cogn Neurosci*, vol. 23, no. 10, pp. 3153–3161, Oct. 2011, doi: 10.1162/jocn\_a\_00014.
- [151] L. J. Pierce, L. Scott, S. Boddington, D. Droucker, T. Curran, and J. Tanaka, 'The N250 Brain Potential to Personally Familiar and Newly Learned Faces

- and Objects', *Front. Hum. Neurosci.*, vol. 5, 2011, doi: 10.3389/fnhum.2011.00111.
- [152] M. Miyakoshi, M. Nomura, and H. Ohira, 'An ERP study on self-relevant object recognition', *Brain and Cognition*, vol. 63, no. 2, pp. 182–189, Mar. 2007, doi: 10.1016/j.bandc.2006.12.001.
- [153] J. M. Kaufmann, S. R. Schweinberger, and A. M. Burton, 'N250 ERP correlates of the acquisition of face representations across different images', *Journal of Cognitive Neuroscience*, vol. 21, no. 4, pp. 625–641, 2009, doi: 10.1162/jocn.2009.21080.
- [154] O. E. Krigolson, L. J. Pierce, C. B. Holroyd, and J. W. Tanaka, 'Learning to Become an Expert: Reinforcement Learning and the Acquisition of Perceptual Expertise', *Journal of Cognitive Neuroscience*, vol. 21, no. 9, pp. 1833–1840, Sep. 2008, doi: 10.1162/jocn.2009.21128.
- [155] S. R. Schweinberger, E.-M. Pfütze, and W. Sommer, 'Repetition priming and associative priming of face recognition: Evidence from event-related potentials', *Journal of Experimental Psychology: Learning, Memory, and Cognition*, vol. 21, no. 3, pp. 722–736, 1995, doi: 10.1037/0278-7393.21.3.722.
- [156] J. Rellecke, W. Sommer, and A. Schacht, 'Emotion Effects on the N170: A Question of Reference?', *Brain Topography*, vol. 26, no. 1, pp. 62–71, Jan. 2013, doi: 10.1007/s10548-012-0261-y.
- [157] A. De Cesare and M. Codispoti, 'When does size not matter? Effects of stimulus size on affective modulation', *Psychophysiology*, vol. 43, no. 2, pp. 207–215, Mar. 2006, doi: 10.1111/j.1469-8986.2006.00392.x.
- [158] J. Hagemann, T. Straube, and C. Schulz, 'Too bad: Bias for angry faces in social anxiety interferes with identity processing', *Neuropsychologia*, vol. 84, pp. 136–149, 2016, doi: 10.1016/j.neuropsychologia.2016.02.005.
- [159] H. Wiese, C. S. Altmann, and S. R. Schweinberger, 'Effects of attractiveness on face memory separated from distinctiveness: Evidence from event-related brain potentials', *Neuropsychologia*, vol. 56, pp. 26–36, Apr. 2014, doi: 10.1016/j.neuropsychologia.2013.12.023.
- [160] D. E. J. Linden, 'The P300: Where in the Brain Is It Produced and What Does It Tell Us?', *Neuroscientist*, vol. 11, no. 6, pp. 563–576, Dec. 2005, doi: 10.1177/1073858405280524.
- [161] C. C. Duncan-Johnson and E. Donchin, 'The P300 component of the event-related brain potential as an index of information processing', *Biol Psychol*, vol. 14, no. 1–2, pp. 1–52, Mar. 1982, doi: 10.1016/0301-0511(82)90016-3.
- [162] A. Gramfort *et al.*, 'MEG and EEG data analysis with MNE-Python', *Frontiers in Neuroscience*, vol. 7, p. 267, 2013, doi: 10.3389/fnins.2013.00267.

- [163] W. D. Hairston, 'Accounting For Timing Drift And Variability In Contemporary Electroencephalography (EEG) Systems', *Army Research Laboratory*, no. ARL-TR-5945, Mar. 2012, doi: 10.21236/ADA561715.
- [164] I. Carrillo, V. Meza-Kubo, A. L. Morán, G. Galindo, and E. García-Canseco, 'Emotions Identification to Measure User Experience Using Brain Biometric Signals', in *Human Aspects of IT for the Aged Population. Design for Aging*, 2015, pp. 15–25.
- [165] R. Ramirez and Z. Vamvakousis, 'Detecting Emotion from EEG Signals Using the Emotive EPOC Device', in *Brain Informatics*, 2012, pp. 175–184.
- [166] T. D. Pham and D. Tran, 'Emotion Recognition Using the Emotiv EPOC Device', in *Neural Information Processing*, 2012, pp. 394–399.
- [167] J.-M. Lopez-Gil *et al.*, 'Method for Improving EEG Based Emotion Recognition by Combining It with Synchronized Biometric and Eye Tracking Technologies in a Non-invasive and Low Cost Way', *Frontiers in Computational Neuroscience*, vol. 10, p. 85, 2016, doi: 10.3389/fncom.2016.00085.
- [168] V. Meza-Kubo, A. L. Moran, I. Carrillo, G. Galindo, and E. Garcia-Canseco, 'Assessing the user experience of older adults using a neural network trained to recognize emotions from brain signals', *Journal of Biomedical Informatics*, vol. 62, pp. 202–209, Aug. 2016, doi: 10.1016/j.jbi.2016.07.004.
- [169] N. A. Badcock *et al.*, 'Validation of the Emotiv EPOC EEG system for research quality auditory event-related potentials in children', *PeerJ*, vol. 3, p. e907, Apr. 2015, doi: 10.7717/peerj.907.
- [170] P. de Lissa, S. Sörensen, N. Badcock, J. Thie, and G. McArthur, 'Measuring the face-sensitive N170 with a gaming EEG system: A validation study', *Journal of Neuroscience Methods*, vol. 253, pp. 47–54, 2015, doi: <https://doi.org/10.1016/j.jneumeth.2015.05.025>.
- [171] M. Duvinage, T. Castermans, M. Petieau, T. Hoellinger, G. Cheron, and T. Dutoit, 'Performance of the Emotiv EPOC headset for P300-based applications', *BioMedical Engineering OnLine*, vol. 12, pp. 56–56, 2013, doi: 10.1186/1475-925X-12-56.
- [172] N. Aifanti, C. Papachristou, and A. Delopoulos, 'The MUG facial expression database', in *11th International Workshop on Image Analysis for Multimedia Interactive Services WIAMIS 10*, Apr. 2010, pp. 1–4.
- [173] Y. Renard *et al.*, 'OpenViBE: An Open-Source Software Platform to Design, Test, and Use Brain-Computer Interfaces in Real and Virtual Environments', *Presence: Teleoperators and Virtual Environments*, vol. 19, no. 1, pp. 35–53, 2010, doi: 10.1162/pres.19.1.35.

- [174] Z. Frankiewicz and J. Leski, 'Adaptive fiducial point detector for ECG stress testing systems.', *Int J Biomed Comput*, vol. 28, no. 1–2, pp. 127–135, Jun. 1991.
- [175] F. Gustafsson, 'Determining the initial states in forward-backward filtering', *IEEE Transactions on Signal Processing*, vol. 44, no. 4, pp. 988–992, Apr. 1996, doi: 10.1109/78.492552.
- [176] J. Leski, 'Robust weighted averaging [of biomedical signals]', *IEEE Transactions on Biomedical Engineering*, vol. 49, no. 8, pp. 796–804, Aug. 2002, doi: 10.1109/TBME.2002.800757.
- [177] V. N. Vapnik, 'Methods of Function Estimation', in *The Nature of Statistical Learning Theory*, V. N. Vapnik, Ed. New York, NY: Springer, 2000, pp. 181–224. doi: 10.1007/978-1-4757-3264-1\_7.
- [178] C. L. Kumaragamage, B. J. Lithgow, and Z. K. Moussavi, 'Investigation of a New Weighted Averaging Method to Improve SNR of Electrocochleography Recordings', *IEEE Transactions on Biomedical Engineering*, vol. 63, no. 2, pp. 340–347, Feb. 2016, doi: 10.1109/TBME.2015.2457412.
- [179] L. R. Krol, J. Pawlitzki, F. Lotte, K. Gramann, and T. O. Zander, 'SEREEGA: Simulating event-related EEG activity', *Journal of Neuroscience Methods*, vol. 309, pp. 13–24, Nov. 2018, doi: 10.1016/j.jneumeth.2018.08.001.
- [180] M. A. Klados and P. D. Bamidis, 'A semi-simulated EEG/EOG dataset for the comparison of EOG artifact rejection techniques', *Data in Brief*, vol. 8, pp. 1004–1006, Wrzesie 2016, doi: 10.1016/j.dib.2016.06.032.
- [181] T. Elbert, W. Lutzenberger, B. Rockstroh, and N. Birbaumer, 'Removal of ocular artifacts from the EEG — A biophysical approach to the EOG', *Electroencephalography and Clinical Neurophysiology*, vol. 60, no. 5, pp. 455–463, Maj 1985, doi: 10.1016/0013-4694(85)91020-X.
- [182] N. C. Ebner, M. Riediger, and U. Lindenberger, 'FACES—A database of facial expressions in young, middle-aged, and older women and men: Development and validation', *Behavior Research Methods*, vol. 42, no. 1, pp. 351–362, Feb. 2010, doi: 10.3758/BRM.42.1.351.
- [183] P. Tacikowski, K. Jednoróg, A. Marchewka, and A. Nowicka, 'How multiple repetitions influence the processing of self-, famous and unknown names and faces: An ERP study', *International Journal of Psychophysiology*, vol. 79, no. 2, pp. 219–230, Feb. 2011, doi: 10.1016/j.ijpsycho.2010.10.010.
- [184] R. Ranjan, B. Chandra Sahana, and A. Kumar Bhandari, 'Ocular artifact elimination from electroencephalography signals: A systematic review', *Biocybernetics and Biomedical Engineering*, vol. 41, no. 3, pp. 960–996, Jul. 2021, doi: 10.1016/j.bbe.2021.06.007.
- [185] M. Shahbakhti *et al.*, 'VME-DWT: An Efficient Algorithm for Detection and Elimination of Eye Blink From Short Segments of Single EEG Channel',

*IEEE Transactions on Neural Systems and Rehabilitation Engineering*, vol. 29, pp. 408–417, 2021, doi: 10.1109/TNSRE.2021.3054733.

- [186] S. Makeig, A. J. Bell, T.-P. Jung, and T. J. Sejnowski, 'Independent Component Analysis of Electroencephalographic Data', in *Advances in Neural Information Processing Systems 8*, D. S. Touretzky, M. C. Mozer, and M. E. Hasselmo, Eds. MIT Press, 1996, pp. 145–151. [Online]. Available: <http://papers.nips.cc/paper/1091-independent-component-analysis-of-electroencephalographic-data.pdf>
- [187] F. Ghaderi, S. K. Kim, and E. A. Kirchner, 'Effects of eye artifact removal methods on single trial P300 detection, a comparative study', *Journal of Neuroscience Methods*, vol. 221, pp. 41–47, Jan. 2014, doi: 10.1016/j.jneumeth.2013.08.025.
- [188] M. B. Pontifex, V. Miskovic, and S. Laszlo, 'Evaluating the efficacy of fully automated approaches for the selection of eyeblink ICA components', *Psychophysiology*, vol. 54, no. 5, pp. 780–791, 2017, doi: 10.1111/psyp.12827.
- [189] S. Zhang, J. McIntosh, S. M. Shadli, P. S.-H. Neo, Z. Huang, and N. McNaughton, 'Removing eye blink artefacts from EEG—A single-channel physiology-based method', *Journal of Neuroscience Methods*, vol. 291, pp. 213–220, Nov. 2017, doi: 10.1016/j.jneumeth.2017.08.031.
- [190] P. Ablin, J.-F. Cardoso, and A. Gramfort, 'Spectral Independent Component Analysis with noise modeling for M/EEG source separation', *Journal of Neuroscience Methods*, vol. 356, p. 109144, May 2021, doi: 10.1016/j.jneumeth.2021.109144.
- [191] T.-W. Lee, M. Girolami, and T. J. Sejnowski, 'Independent Component Analysis Using an Extended Infomax Algorithm for Mixed Subgaussian and Supergaussian Sources', *Neural Computation*, vol. 11, no. 2, pp. 417–441, Feb. 1999, doi: 10.1162/089976699300016719.
- [192] A. Hyvarinen, 'Fast and robust fixed-point algorithms for independent component analysis', *IEEE Transactions on Neural Networks*, vol. 10, no. 3, pp. 626–634, May 1999, doi: 10.1109/72.761722.
- [193] A. Belouchrani, K. Abed-Meraim, J.-F. Cardoso, and E. Moulines, 'A blind source separation technique using second-order statistics', *IEEE Transactions on Signal Processing*, vol. 45, no. 2, pp. 434–444, Feb. 1997, doi: 10.1109/78.554307.
- [194] M. B. Pontifex, K. L. Gwizdala, A. C. Parks, M. Billinger, and C. Brunner, 'Variability of ICA decomposition may impact EEG signals when used to remove eyeblink artifacts', *Psychophysiology*, vol. 54, no. 3, pp. 386–398, 2017, doi: 10.1111/psyp.12804.
- [195] L. Frølich and I. Dowding, 'Removal of muscular artifacts in EEG signals: a comparison of linear decomposition methods', *Brain Inf.*, vol. 5, no. 1, pp. 13–22, Mar. 2018, doi: 10.1007/s40708-017-0074-6.

- [196] P. Ablin, J.-F. Cardoso, and A. Gramfort, 'Faster Independent Component Analysis by Preconditioning With Hessian Approximations', *IEEE Transactions on Signal Processing*, vol. 66, no. 15, pp. 4040–4049, Aug. 2018, doi: 10.1109/TSP.2018.2844203.
- [197] T.-P. Jung *et al.*, 'Extended ICA removes artifacts from electroencephalographic recordings', in *Proceedings of the 10th International Conference on Neural Information Processing Systems*, Cambridge, MA, USA, Dec. 1997, pp. 894–900.
- [198] A. Mognon, J. Jovicich, L. Bruzzone, and M. Buiatti, 'ADJUST: An automatic EEG artifact detector based on the joint use of spatial and temporal features', *Psychophysiology*, vol. 48, no. 2, pp. 229–240, Feb. 2011, doi: 10.1111/j.1469-8986.2010.01061.x.
- [199] L. Pion-Tonachini, K. Kreutz-Delgado, and S. Makeig, 'ICLabel: An automated electroencephalographic independent component classifier, dataset, and website', *NeuroImage*, vol. 198, pp. 181–197, Sep. 2019, doi: 10.1016/j.neuroimage.2019.05.026.
- [200] F. Perrin, J. Pernier, O. Bertrand, and J. F. Echallier, 'Spherical splines for scalp potential and current density mapping', *Electroencephalography and Clinical Neurophysiology*, vol. 72, no. 2, pp. 184–187, Feb. 1989, doi: 10.1016/0013-4694(89)90180-6.
- [201] I. Winkler, S. Debener, K.-R. Müller, and M. Tangermann, 'On the influence of high-pass filtering on ICA-based artifact reduction in EEG-ERP', in *2015 37th Annual International Conference of the IEEE Engineering in Medicine and Biology Society (EMBC)*, Aug. 2015, pp. 4101–4105. doi: 10.1109/EMBC.2015.7319296.
- [202] N. Yoder, 'PeakFinder', 2021. <https://www.mathworks.com/matlabcentral/fileexchange/25500-peakfinder-x0-sel-thresh-extrema-includeendpoints-interpolate> (accessed Dec. 12, 2021).
- [203] M. J. Doughty, 'Consideration of three types of spontaneous eyeblink activity in normal humans: during reading and video display terminal use, in primary gaze, and while in conversation', *Optom Vis Sci*, vol. 78, no. 10, pp. 712–725, Oct. 2001, doi: 10.1097/00006324-200110000-00011.
- [204] Y. Li, Z. Ma, W. Lu, and Y. Li, 'Automatic removal of the eye blink artifact from EEG using an ICA-based template matching approach', *Physiol. Meas.*, vol. 27, no. 4, pp. 425–436, Mar. 2006, doi: 10.1088/0967-3334/27/4/008.
- [205] M. Chaumon, D. V. M. Bishop, and N. A. Busch, 'A practical guide to the selection of independent components of the electroencephalogram for artifact correction', *Journal of Neuroscience Methods*, vol. 250, pp. 47–63, Lipiec 2015, doi: 10.1016/j.jneumeth.2015.02.025.

- [206] O. Trigui, S. Daoud, M. Ghorbel, M. Dammak, C. Mhiri, and A. Ben Hamida, 'Removal of eye blink artifacts from EEG signal using morphological modeling and orthogonal projection', *SIViP*, vol. 16, no. 1, pp. 19–27, Feb. 2022, doi: 10.1007/s11760-021-01947-w.
- [207] V. M. R. Muggeo, 'Estimating regression models with unknown break-points', *Statistics in Medicine*, vol. 22, no. 19, pp. 3055–3071, 2003, doi: 10.1002/sim.1545.
- [208] K. Kotowski and K. Stapor, 'Deep learning in EEG: Detection of error-related negativity in Eriksen flanker task', in *Proceedings of PP-RAI'2019*, Wrocław, Oct. 2019, pp. 49–52. [Online]. Available: [http://pp-rai.pwr.edu.pl/PPRAI19\\_proceedings.pdf](http://pp-rai.pwr.edu.pl/PPRAI19_proceedings.pdf)
- [209] D. M. Groppe, S. Makeig, and M. Kutas, 'Independent Component Analysis of Event-Related Potentials', *Cognitive Science Online*, no. 6.1, pp. 1–44, 2008.
- [210] J. Nalepa *et al.*, 'Fully-automated deep learning-powered system for DCE-MRI analysis of brain tumors', *Artificial Intelligence in Medicine*, vol. 102, p. 101769, Jan. 2020, doi: 10.1016/j.artmed.2019.101769.
- [211] K. Kotowski, J. Nalepa, and W. Dudzik, 'Detection and Segmentation of Brain Tumors from MRI Using U-Nets', in *Brainlesion: Glioma, Multiple Sclerosis, Stroke and Traumatic Brain Injuries*, Cham, 2020, pp. 179–190. doi: 10.1007/978-3-030-46643-5\_17.
- [212] K. Kotowski, S. Adamski, W. Malara, B. Machura, L. Zarudzki, and J. Nalepa, 'Segmenting Brain Tumors from MRI Using Cascaded 3D U-Nets', in *Brainlesion: Glioma, Multiple Sclerosis, Stroke and Traumatic Brain Injuries*, Cham, 2021, pp. 265–277. doi: 10.1007/978-3-030-72087-2\_23.
- [213] K. Kotowski, T. Smolarczyk, I. Roterman-Konieczna, and K. Stapor, 'ProteinUnet—An efficient alternative to SPIDER3-single for sequence-based prediction of protein secondary structures', *Journal of Computational Chemistry*, vol. 42, no. 1, pp. 50–59, 2021, doi: <https://doi.org/10.1002/jcc.26432>.
- [214] K. Stapor, K. Kotowski, T. Smolarczyk, and I. Roterman, 'Lightweight ProteinUnet2 network for protein secondary structure prediction: a step towards proper evaluation', *BMC Bioinformatics*, vol. 23, no. 1, p. 100, Mar. 2022, doi: 10.1186/s12859-022-04623-z.